91602
new 82-10

LEGAL NOTICE

This report was prepared by Ontario Hydro and, while effort has been made to assure the accuracy and applicability of the material contained herein, neither Ontario Hydro nor any person acting on its behalf:

(a) makes any warranty, express or implied with respect to the use of any information, apparatus, method or process disclosed in this report or that such use may not infringe privately owned rights; or

(b) assumes any liabilities with respect to the use of, or for damages resulting from the use of, any information, apparatus, method or process disclosed in this report.

ontario hydro
research division

COMPLIMENTARY COPY
Please Credit Ontario Hydro Research if
Reproduced in Whole or in Part

EXPERIMENTAL AND THEORETICAL MODELLING OF THE NEAR-FIELD THERMAL REGIME IN A NUCLEAR FUEL WASTE DISPOSAL VAULT

Report No 88-18-K

H.S. Radhakrishna and K.C. Lau
Engineers
Soil Sciences Section
Civil Research Department

ABSTRACT

The near-field thermal regime in a buffer-backfill disposal vault in which the nuclear fuel waste is emplaced in canisters, is studied by a one-eighth scale experimental model. This is Phase 3 of the five-phase experimental and theoretical study program. The experimental data is compared with the predictions made by the computer code TRUCHAM developed by Ontario Hydro for analyzing the transient and coupled heat and moisture flow through unsaturated media. Good comparison between the measured and predicted temperature regimes in the model was obtained. This finding further assures the reliability and capacity of the computer code TRUCHAM for the design of the Underground Research Laboratory experiment. Through this study, substantial instrumentation experience was gained. This experience will be transferred to the scientists involved in the Underground Research Laboratory.

job	file	date	report no.
43-157-461 43-334-061	843.	April 6, 1988	88-18-K

TABLE OF CONTENTS

	Page
1.0 INTRODUCTION	1
2.0 OBJECTIVES AND REVIEW OF PREVIOUS WORK	3
2.1 Objectives	3
2.2 Review of Previous Work	4
3.0 EXPERIMENTAL MODEL	6
3.1 Design Considerations	6
3.2 Description of Model	7
3.3 Construction of Model	9
3.3.1 Formwork for the Concrete Mass	9
3.3.2 Concrete Placement	10
3.3.3 The Buffer Zone	10
3.3.4 The Vault Area	11
3.4 Instrumentation	12
3.4.1 Thermocouples	12
3.4.2 Petur Pressure Cells	12
3.4.3 Psycrometers	12
3.4.4 Flow Meters	13
3.4.5 Data Acquistion System	13
4.0 EXPERIMENT SCHEDULE	13
5.0 EXPERIMENTAL DIFFICULTIES AND REMEDIES	14
6.0 ANALYSIS OF DATA	16
6.1 Experimental Data	16
6.2 Theoretical Analysis	18
7.0 CONCLUSIONS AND RECOMMENDATIONS	20
REFERENCES	23
TABLES I and II	24
FIGURES 1 to 42	26
APPENDIX A to F	68
DISTRIBUTION	last page

ontario hydro
research division

To Mr. H.N. Isaac
Manager
Nuclear Materials Management Department
Design and Development Division

Attn: Dr. J. Freire-Canosa

EXPERIMENTAL AND THEORETICAL MODELLING OF NEAR-FIELD THERMAL REGIME IN A NUCLEAR FUEL WASTE DISPOSAL VAULT

1.0 INTRODUCTION

The safe disposal of nuclear fuel waste requires the isolation of the waste from the biosphere for a sufficient period of time. Depending on the operation procedures of the Candu reactors, two types of nuclear waste can be produced. These are the irradiated fuel and the immobilized recycled waste. The irradiated fuel is the product of the fusion of the uranium bundles. Plutonium in the irradiated fuel can be recovered through chemical processes, and is used in advanced fuel cycles. Through such a recovery process, liquid and gaseous wastes are produced. These wastes are called recycled wastes and are highly radioactive. One method of handling them for subsequent disposal is through their immobilization in highly insoluble glass or ceramic products. Both the spent fuel and immobilized recycled wastes are sources of heat and radiation and pose special problems for the engineering design of a waste disposal facility/1/.

The Canadian concept for nuclear waste disposal is to emplace the waste, packaged in corrosion-resistant containers, in a vault mined deep into plutonic rock of the Canadian shield. It is proposed that the vault will comprise of a number of mined chambers some 500-1000 m below the ground surface. The preliminary layout of the disposal vault consists of a single-level vault, approximately 1700 m by 3600 m. A total of 822 rooms, 195 m long, 7.5 m wide and 5-6.2 m high will be arranged within 16 rectangular panels/2,3/. Based on current forecasts of the growth of electrical energy demand, such a vault would have an operating life of approximately 50 years before being permanently closed.

After closure of the vault, with time, ground water will penetrate the waste, dissolve the radionuclides, and carry them towards the biosphere. A number of protective (or isolation) barriers, each one engineered to a high degree of integrity, will delay and minimize the rate at which the radionuclides migrate/4/. These barriers are 1) the buffer, 2) the backfill in rooms, drifts and shafts, 3) the seals and plugs in the shafts, and 4) the host rock. In case of radionuclide release, radionuclide transport is attenuated by a dilution, dispersion and retention process. The engineered and geotechnical barriers serve to isolate or to prolong the travel times of radionuclides to the biosphere.

Figure 1 shows cross-sections of the two methods which have been proposed for placing the waste in the vault. These are known as in-room emplacement (TEC-1 design) and borehole emplacement (TEC-2 design). For in-room emplacement, the containers or canisters will be placed on a bed of prepared buffer, with additional buffer being packed around and above them. The remaining volume would then be backfilled. In borehole emplacement, the canisters will be surrounded by buffer in a large diameter hole drilled in the floor of the vault. In this case the total volume of the drift will be backfilled.

The functions of the engineered buffer are:

1. To enhance the life of the canisters by minimizing access of ground water to the surface of the canister and controlling ground water chemistry to minimize container corrosion.

2. To retard the migration of the radionuclides from failed canisters.

3. To provide mechanical support to the canisters and absorb any excessive stresses induced by movements of the surrounding rock.

4. To dissipate the heat generated by radionuclide decay to the surrounding rock.

The physical and chemical attributes that the buffer material should possess in order to perform the above functions effectively over a long period of time were discussed in detail by Bird/5/. From the current research work, the candidate materials considered for buffer components include various commercial bentonites from Western Canada, illitic shales from southern Ontario, and crushed quartzite known commercially as "Silica Sand".

Backfill is the material that will be used to fill the emplacement rooms and access drifts and shafts during vault decommissioning. Its main function is to seal openings with a stiff material of very low hydraulic conductivity. The candidate backfill material is a lean mix of clay and crushed rock. The preferred type of clay would have slight swelling properties. At the present time, both commercial bentonite and natural glaciolacustrine clay deposits are being considered.

In order to assess the efficiency of the Canadian nuclear waste disposal concept, a research program was initiated by the Civil Research Department. The research program consists of five phases. Namely:

1. Thermal material properties,
2. 1-1/2 heater model test - drying phase,
3. Multiple heater model test - drying phase
4. Multiple heater model test - wetting phase and,
5. Analytical studies.

Because of the complicated thermal and hydraulic conditions involved, the testing program was specifically designed such that the effects of thermal drying on the buffer-backfill zones with and without a rewetting phase could be studied separately.

Special provisions were made in the experimental model such that the adequacy of the monitoring system and the design of the model for the subsequent phases of the experiment could be evaluated. Such a design concept for the experimental model ensured the success of the testing program.

It is anticipated that with the completion of this research program, the heat and moisture transport properties of the candidate materials will have been determined and the performance of these buffer and backfill materials when subjected to simulated in situ vault conditions, will have been evaluated. The results from the experimental model tests will be used to validate and calibrate the computer code developed for the analysis of transient heat and moisture diffusion in the near-field of the disposal vault.

The experience developed in the research program will be transferred to the scientists who are involved in the design of the in situ field tests at the Underground Research Laboratory (URL). In this report, the work and results of Phase 3 of the research program are presented.

2.0 OBJECTIVES AND REVIEW OF PREVIOUS WORK

2.1 Objectives

The objectives of the research program initiated by the Civil Research Department are:

1. To assess the thermal properties of clay based buffer and backfill materials.

2. To assess the temperatures and temperature gradients which develop in the buffer and backfill zone under simulated thermal loadings.

3. To assess the thermally induced moisture migration and volume changes in the buffer and backfill.

4. To assess the temperature and moisture distributions in the buffer and backfill during the recharge phase (rewetting phase).

5. To provide data for the calibration and validation of the computer code developed for the study of near-field heat and moisture flow in an underground nuclear waste disposal vault.

6. To develop expertise in the instrumentation of the near-field experiments in the URL.

7. To develop experience in predicting the near-field thermal hydraulic behaviour of the underground disposal vault.

A review of the progress of the research program is presented in the next section.

2.2 Review of Previous Work

Phase 1 of the study was completed in 1984. During this phase, the various factors which affect the thermal conductivity of clay based buffers were investigated through laboratory measurements (Appendix A). The transient heat dissipation method was used in the study. In general, the following conclusions were drawn/6/:

1. The thermal conductivity of clay based buffers is highly dependent on the moisture content in the low moisture region and the relationship between thermal conductivity and moisture content is generally non-linear.

2. The density to which a clay based buffer is compacted affects its thermal conductivity. Addition of crushed granite or silica sand improves the thermal conductivity through improved compactability.

3. The ambient temperature has no significant effect on the thermal conductivity of the buffer, provided the buffer moisture is not allowed to vapourize.

Considering a scenario that the disposal vault will be initially maintained for several years in a dry or semi-dry condition, the emplaced buffer and backfill in the disposal rooms will undergo an initial phase of thermal drying. This will be followed by a wetting phase as the disposal vault is sealed and the ground water regime is allowed to re-establish itself. The drying phase will be critical to the overall performance of the engineered barriers. This is so because drying will degrade the thermal properties of the buffer and may also cause the formation of shrinkage cracks in the buffer. The presence of such cracks could alter the integrity of the buffer as a barrier to contaminant migration. In view of the complexity of the phenomenon, a laboratory scale experiment was performed in Phase 2 of the study. The main objectives of Phase 2 was to investigate the thermal drying of the buffer and backfill materials under simulated vault conditions. In addition, the design and performance of the monitoring system were evaluated.

In Phase 2, a one-eighth scale experimental model was built to simulate the near-field thermal environment of a backfilled disposal vault in which the waste is emplaced in boreholes. The model consisted of a concrete block to simulate the thermal mass of rock and electric heaters to simulate the heat production from the waste fuel containers.

Since the waste fuel containers are placed in long rows of boreholes (3 per row in the TEC-2 design) and the disposal vault has several disposal rooms parallel to each other, only one half of a single row of waste containers in a disposal room were studied in this experimental model. This was achieved by emplacing one full round heater and one half round heater in one and a half boreholes. Four adiabatic boundaries were simulated by insulating the vertical faces of the concrete block with 150 mm thick polystyrene insulation.

A total of 80 thermocouples were installed at strategic positions in the heater, buffer, backfill and concrete block. Four moisture sensors (psycrometers) and four thermal conductivity probes were also placed in the buffer, backfill and concrete to monitor the changes in moisture content. The heat input was controlled by a programmable power supply and the thermocouples were monitored by a digital data acquisition system controlled by a desk top computer.

The buffer material used in this experimental program was a mixture of crushed granite (maximum 2 mm size) and Avonlea bentonite in equal proportions by dry weight. The mix material was compacted around the heaters to a dry density of 1500 kg/m^3 at a moisture content of 22.7 per cent.

During the experiment, a constant heat input of 36 watts per heater, one eighth of the heat production by a waste container, was maintained for a period of 40 days. The heater temperature reached steady state at about 18 days after which the near field thermal regime stabilized.

The heater surface temperatures reached a maximum of about 105^{o}C and rather steep thermal gradients were measured in the buffer zone.

After 40 days of heating, followed by cooling to ambient temperature, the condition of the buffer and backfill was examined. Desiccation cracks in the buffer were carefully mapped.

A three dimensional analysis was performed to predict the thermal regime in the system. Three cases were analyzed/7/:

1. Constant thermal properties with no moisture migration,
2. Thermal properties changing with moisture migration and,
3. Thermal properties changing with moisture migration and including the effects of desiccation cracking of the buffer.

A good agreement resulted between the predicted and measured data for the case in which the thermal properties changed with moisture migration and the thermal cracking of the buffer was considered. This suggested that the effects of thermal drying and desiccation cracking of the buffer on its performance as an engineered barrier should be further investigated.

3.0 EXPERIMENTAL MODEL

The conceptual three-dimensional experimental model used in the Phase 3 of the study of the behaviour of buffer and backfill materials under thermal drying conditions is shown in Figure 2. This model was designed as a result of the experience gained from the tests conducted in Phase 2 of this research program. In this improved model, the heat and moisture conditions experienced in an underground vault are properly simulated, including the effects of interaction between the heaters.

Because of the complicated phenomena involved in the rewetting phase (Phase 4) of the research program, a water injection system was provided in the Phase 3 experimental model so that at the end of the thermal drying test, preliminary rewetting conditions could be simulated. From this, the performance of the instrumentation, water injection system and various components of the model would be evaluated. Experience gained during the rewetting conditions would be implemented in the design of the experimental model for Phase 4 of this research program.

3.1 Design Considerations

In Phase 2 of the research program, deficiencies in the design and performance of the 1-1/2 heater model were identified, namely:

1. The insulated boundary at the interface between the 1/2 heater and the atmosphere did not function as a proper adiabatic boundary/7/. The large temperature difference between the 1/2 heater and the atmosphere induced high thermal gradients across the insulation and thus a significant amount of heat and/or moisture loss occurred through this boundary.

2. In the TEC-2 design, the structural boundary condition at the interface between the 1/2 heater and the insulation is one of complete restraint, that is; no horizontal movement can occur. In the 1-1/2 heater model, such a structural boundary condition could not be simulated due to the low stiffness of the insulation material. Such a boundary condition may have had an influence on the formation of buffer shrinkage cracks as were observed after the completion of the test. As shown by numerical analysis, the formation of cracks in the buffer has a significant effect on the hydraulic and thermal integrity of the buffer as an engineered barrier. Such induced structural boundary conditions were eliminated in subsequent experimental models.

3. In the 1-1/2 heater model, because of symmetry along the drift, only one row of heaters was simulated. This was based on the assumption that adiabatic boundaries could be imposed on the lines of symmetry. However, during the test, due to the large surface area of the adiabatic boundaries, heat loss through the insulation became significant, thereby reducing the temperature build up within the model. Thus, the

buffer and backfill zones were not subjected to thermal conditions as critical as those to be expected in the disposal vault.

4. The dimensions of the 1-1/2 heaters experimental model were scaled to model the disposal room (TEC-2 design) to a one-eighth geometric scale. The rate of energy output for each heater was 1/8 of the rate of energy output of the canisters of the TEC-2 design. The consequence of such a geometric scaling effect on the model is that the thermal gradient in the scale model is 8 times higher than that of the prototype. The rate of temperature change in the scale model is 64 times greater than that of the prototype. Such geometric scaling subjected the buffer and backfill zones of the model to a more severe thermal environment than would be applied in the vault.

Based on the deficiencies identified during the 1-1/2 heaters test and on the need for the provision of water injection facilities, a new experimental model was designed.

The new 3-dimensional model consists of 3 heaters per row (TEC-2 design). With such a layout, the structural and thermal boundary conditions created by the 1/2 heater in the previous experimental model were eliminated. In addition, the difficulties involved in the design of a hydraulically impermeable boundary was also eliminated.

Along the drift direction, 3 rows of heaters were included in the new model in order to alleviate possible problems of non-adiabatic boundary conditions. The provision of 3 rows of heaters also provided insight into possible interactions between the heaters and their effect on the performance of the buffer and backfill materials.

The rate of energy output per heater in the present experiment is the same as that of the Phase 2 experiment. Although such a rate of energy output will have a scale effect on the model, it is believed that the higher temperature gradients in the buffer and backfill zones will counteract the possible adverse effects of prolonged heating conditions to which the buffer and backfill material are to be subjected to in the field.

In general, the model consisted of 9 heaters. Between the buffer and concrete interface, a clay tile was embedded. PVC tubings, 3 mm OD in size, were installed between the concrete and clay tile interface to facilitate the injection of water to simulate the effect of water uptake and rewetting of the buffer and backfill zones. The annular gap between the concrete and clay tile interface was cement grouted.

The heaters, a scale model of the TEC-2 design canister, were custom designed and manufactured by Geotherm Inc.

3.2 Description of the Model

The experimental model consists of 9 heaters and was geometrically scaled to one-eighth of the TEC-2 design (Figure 2). Because of the number of instruments and heaters involved in the model, a coordinate system was implemented as shown in Figure 3. In the model, a concrete block of 3660 x

3050 x 1020 mm was used to simulate the rock mass. Electric heaters simulated the canisters which were embedded in the disposal vault. The arrangement of the heaters, buffer and backfill in the X-Y, Y-Z and X-Z planes are shown in Figures 4, 5 and 6 respectively. Clay tile allowed water to be introduced into the buffer area during the resaturation phases of the testing program. Two rubber membranes were provided at the backfill and insulation interface (Figure 5).

The ends of the rubber membranes were embedded in the concrete block with a waterstop to provide a water tight seal. Thermocouples, monitored by an HP computerized data acquisition system, were placed in strategic locations throughout the model. These locations are shown in Figures 4, 5 and 6.

The dimensions and details of the heater-buffer arrangement in the borehole are presented in Figure 7. For each heater, two water injection tubes were embedded in the cement grout to facilitate the introduction of water. The ends of the tubes were connected to a 25.4 mm thick sand layer which lay directly above the buffer zone. The purpose of the sand layer was to accelerate the injection of water by providing access to both the buffer and backfill zones.

The heaters were custom designed and manufactured by Geotherm Inc. The specification of the heaters is given in Appendix B. Each heater comprised of two 9 ohms heating coils connected in series. A common lead was connected between the two heating coils. Such a circuit design provided a combination of 3 operation modes for each heater, namely, two 9 ohms heating coils and one 18 ohms heating coil. Thus, in case of a heating coil failure or a lead burn out, an alternate operating mode can be used as a backup unit.

A concrete plug was provided above the backfill zone. This concrete plug was used to simulate the rock mass above the vault as well as to provide a facility for the placement of the heater's buffer and backfill from the top. The waterstops in the upper ends of the two rubber membranes were embedded in concrete.

Adiabatic boundaries were simulated by insulating the vertical faces of the concrete block with 150 mm thick polystyrene insulation. The infinite extent of rock mass above the disposal room and beneath the disposal boreholes could not be well simulated in this model due to the limitation on its size. Thus, these boundaries were also insulated to simulate the long heat paths in the vertical direction. Plywood panels encased the model in order to support the polystyrene insulation.

The instrumentation system comprised of 273 thermocouples, 3 Petur pneumatic pressure cells, 9 Wescor psycrometers and 18 flow meters.

The pneumatic pressure cells were placed, one on each side of the backfill room and the third one between the backfill and concrete plug. These were intended to measure the backfill compaction pressures, and subsequent change in backfill pressures due to thermal drying and rewetting.

The nine psycrometers installed in the buffer zone above the heaters were intended to record the change in buffer moisture content during the drying and wetting phases.

The flow meters were placed one in each of the water injection line to record the flow rates and rate of water uptake by the buffer-backfill mass.

3.3 Construction of the Model

3.3.1 Formwork for the Concrete Mass

The formwork required for the scale-model was designed and built by Ontario Hydro's Generation Projects Division, Field Design Department. The formwork had to meet the following criteria. The maximum form pressure was 47.88 kPa. The maximum allowable liquid head was 3.05 m. Bulkhead coil ties were restricted to areas at least 0.61 metres from the buffer/backfill areas. The concrete mass total dimensions were 3660 mm x 3050 mm x 1020 mm. The base of the concrete mass consisted of 19 mm plywood top and bottom and a core of 150 mm of polystyrene insulation.

A slide-in centre form was fabricated to form the nine canister holes, the vault area and the tapered temporary access shaft. The tapered access shaft was later filled with concrete.

This was done after all the buffer and backfill areas were filled, compacted and instrumented. The details of the slide-in centre form are shown in Figure 8.

Due to the difficulty of instrumentation after the pouring of the concrete mass, as much instrumentation as possible was installed prior to the pour. Ninety-eight thermocouples were installed on the X-Z plane (Figure 6). The thermocouples were attached to non-conductive nylon line. These nylon lines were run into the inside of the canister holes and tightened using small turnbuckles. This tightening of the lines, minimized the sag and movement of the thermocouples during the concrete pour. The thermocouple wires were allowed to fan out for approximately 0.6 m before they were bundled and run through a 36 mm diameter plastic conduit pipe out the bottom of the concrete block. This fanning out of the wires was intended to prevent the possibility of having water exit through the wire bundle.

Water injection lines were also installed before the concrete was poured. Two water lines were installed into each canister cylinder. These lines each consisted of an inner and outer line. This double line allowed the end of the 6.3 mm line to be adjusted to the required position in the canister cylinder after the concrete was poured. The two lines in each cylinder provided backup water intake lines for each cylinder (Figure 9).

An impervious water membrane was also installed on each side wall of the concrete mass. This rubber membrane consisted of a rectangular shaped tub-like container. The side walls were fabricated from a solid rubber waterstop which was joined together.

The rubberstop, originally 152.4 mm wide, was sliced through its centre to make 76.2 mm high side walls. A 3.2 mm rubber membrane was then glued to the side walls. This completed the rectangular shaped tub-like impervious membrane. The rubber membrane sealed off the total backfill and buffer areas. This membrane restricted the movement of water within the vault area. It also allowed the water to escape only through the concrete mass. Details of the membrane location and the membrane structures are shown in Figure 9.

The Petur pressure cells were also installed prior to the concrete pour. These pressure cells were located at the mid point of the vertical concrete side walls of the backfill area. The plywood slide-in centre form was cut out to allow the pressure cell to protrude into the backfill area. This allowed for a good backfill/cell contact.

3.3.2 Concrete Placement

The Concrete Technology Section of the Civil Research Department designed a concrete mix and coordinated the concrete placement and laboratory testing program. The mix criteria was as follows:

- 35 MPa strength
- 25% fly ash replacement
- Type 10 cement, 322 kg/m^3
- Fly ash 108 kg/m^3
- Water 180 kg/m^3
- Sand 745 kg/m^3
- 10 mm stone 1070 kg/m^3
- Water reducer 140.8 g/50 kg of the mix.

A concrete pump system was used for the placement of the concrete. The pump was used because of the height restrictions within the building, for ease of placement and to minimize the damage to the installed instrumentation (Figure 10). A grout mixture was used to lubricate the pump system prior to the concrete placement.

The concrete mix allowed for a high slump, good flowability and low shrinkage. No problems were encountered during the concrete placement.

The concrete formwork and slide-in centre section were removed two weeks after the concrete placement (Figure 11). The water intake lines were then extended to the top of the canister hole/backfill interface. The steel coil ties (formwork ties) were removed from their PVC tubes and the PVC tubes were then filled with a cement grout. The concrete model was then ready for the fabrication and installation of the insulated wall panels.

3.3.3 The Buffer Zone

The packing of the buffer material and the installation of the canister-heater mock-ups were done in the laboratory, not within the test model. This stage of the preparation consisted of a number of different steps. They are as follows: the joining of the pervious clay tiles, the packing of the buffer material and embedding within the tiles, the installation of the thermocouples and psycrometers.

The clay tiles were used to provide a pervious membrane around the buffer/heater column, so as to introduce water to the buffer area during the resaturating phases of the test program. The clay tiles were 305 mm high with an outside diameter of 167 mm and an inside diameter of 127 mm. Two clay tiles had to be coupled together to allow for a pervious column 610 mm high. The clay tiles were joined using Epoxy-Patch. A jig was designed to maintain the tiles in a vertical position. Plastic tubing with a diameter of 6.4 mm was installed between the two epoxy faces of the adjoining clay tile. These tubes allowed a water path through the Epoxy-Patch adhesive. The tile columns were saturated before the buffer material was compacted in the tile.

The buffer material was a mixture of graded silica sand and Avonlea bentonite in equal proportions by weight. The materials were first dry mixed. Water was then introduced to the mix using a spray gun. The spraying of the water prevented the bentonite from adsorbing large quantities of water. The buffer material was mixed until a moisture content of 18% dry weight was achieved. The buffer material was allowed to condition in sealed containers for at least 48 hours before compaction. The buffer material was compacted in 38 mm thick layers and to a wet density of 2000 kg/m^3. Dynamic methods were used for compaction. Steel reinforcing rings were placed around the outside of the clay tile columns to prevent them from cracking during the compaction stage. Thermocouples were installed in the mid-plane of the heaters. The thermocouple locations are shown in Figure 6. Cracks developed in the clay tile columns due to the swelling of the buffer material. This swelling occurred because water was drawn out of the saturated clay tile columns.

The heaters (mock-up canisters) were installed using three methods: (1) an oversized hole was augered into the buffer column, the heaters were dropped into place and pure bentonite was packed around the heaters, (2) the heaters were put in place and the buffer was packed around the heaters in layers, (3) a removable steel sleeve of the same diameter as the heater was installed when the buffer layers were packed. This sleeve was removed after the buffer had been packed to the height equivalent to the top of the heater. The heater was then pushed into the hole. A Wescor psycrometer was installed 12 mm above the heater centreline in each hole.

The finished columns containing the clay tile outer sleeve, the buffer material and the heaters were lowered into their respective preformed holes in the concrete mass (Figure 12). The annular space between the tiles and the concrete mass was filled with cement grout.

3.3.4 The Vault Area

The vault area preparation and instrumentation consisted of placing the sand layer, the backfill material, thermocouples and earth pressure cells. A 25 mm thick sand layer was placed at the buffer/backfill interface. This sand layer did not extend beyond the outer perimeter of the heater holes (Figure 13). The sand layer was not continued to the outer walls so as to avoid a direct water path to the side walls of the model. A layer of impervious backfill material was compacted between the sand layer and the outer wall.

The backfill consisted of 75% crushed granite and 25% Avonlea bentonite mixture by weight. The crushed granite gradation was a mixture of 80% AECL granite (18 mm-#8 sieves) and 20% AECL LAKEFIELD passing #10 mix.

The backfill material was hand mixed to a moisture content of 17% by dry weight. The backfill material was packed by hand compaction to a dry density of 1700 kg/m^3. The backfill material was packed in 40 mm layers. Thermocouples were placed at 152, 304 and 457 mm above the buffer/backfill interface, vertically above the centreline of heaters #2, #5 and #8. An earth pressure cell was installed after the top layer of the backfill was compacted. The pressure cell was located at the centre point (Figure 14).

This pressure cell was intended to measure the vertical swelling pressure during the wetting and drying stages of the test program.

The final stage of the test model construction was the pouring of the tapered concrete plug, sealing the temporary access shaft. The concrete mix design was the same as the initial pour. Due to the small quantity of concrete required a concrete dump bucket was used for the placement. Vibrators were used to ensure that there was good contact between the concrete and the waterstop around the perimeter of the temporary shaft. The top insulating panel was installed after the concrete had set. The steel plate and the structural members which were designed to withstand the uplift force were installed. The test model was then complete and ready for testing. The structural steel layout is shown in Figure 14.

3.4 Instrumentation

The behaviour of the buffer and backfill zones when subjected to thermal drying conditions with multiple heaters was monitored by thermocouples, psycrometers and earth pressure cells. In addition, flow meters were installed to evaluate the water injection system subsequent to the thermal drying test. Figure 15 shows the instruments used in the experiments.

3.4.1 Thermocouples

A total of 273 copper constantan type thermocouples were installed in the model. These were located mainly along the X-Y and X-Z planes of the model (Figures 3, 4, 5 and 6) which provided a complete picture of the thermal regime in the 2 mid-planes of the model.

Thermocouples were also located across the adiabatic (insulated) boundaries to monitor the efficiency of the insulated boundaries and to provide information which was required for the analytical study of the test results.

3.4.2 Earth Pressure Cells

Three (Petur) pneumatic pressure cells were installed in the model to monitor the vertical and horizontal swelling pressures of the backfill material. Two of the pressure cells were located vertically at the interface between the concrete block and the backfill zone. A third cell was located at the top of the backfill zone. The specifications supplied by the manufacturer are listed in Appendix C.

3.4.3 Psycrometers

Nine Wescor psycrometers (model PCT-55-30-SF) were installed to monitor the moisture content of the buffer material. One psycrometer was installed per heater buffer column in the buffer zone at 12.5 mm above the heater. Details of the instrument are given in Appendix D.

3.4.4 Flow Meters

The rate of water injection into the buffer-backfill zones was monitored by 18 high accuracy rotameters (model FL-112) manufactured by Omega Engineering Inc. The meters were located at the north panel of the model (Figure 16). The rate of water injection through each PVC tubing connected to the buffer backfill zones was monitored separately by individual rotameters. Data for the rotameter supplied by the manufacturer is provided in Appendix E.

3.4.5 Data Acquisition System

The data acquisition system comprised of an HP Vectra computer, a NEC colour monitor, an HP 3497A data logger and an HP 3498A extender box (Figure 17). The system was protected by an uninterruptible power supply and filters to ensure that no disturbance due to any power failure or power fluctuation could interfere with the data acquisition process.

At specific times, the data logger was set to scan all of the 288 channels and store the data on a floppy diskette. At the same time, the temperatures measured by the thermocouples were plotted and displaced on the monitor. Thus, at any instant throughout the experiment, two graphs of different colours were shown on the monitor. The bottom graph was from the data of the previous scan. Thus, the status of the experiment was determined from a quick reference of the two graphs.

The voltage across heaters #3, #5 and #7 was also shown on the monitor. The data recorded on the floppy diskette was transferred to another computer system for analysis.

4.0 EXPERIMENT SCHEDULE

The multiple heater experiment consisted of two stages. The first stage consisted of examining the behaviour of the buffer-backfill zones when subjected to thermal drying. The second stage consisted of evaluating the water injection system used for simulating rewetting of the vault.

The thermal drying phase which started on June 10, 1986, was completed on October 27, 1986. During this stage of the test, the rate of energy output from each heater was maintained at 36 watts. Initially, the thermocouples were scanned once every minute for the first hour. Subsequently, the scanning interval was extended to once in every 30 minutes for an additional 2 weeks. As the rate of temperature rise in the model decreased with time, the frequency of scanning thermocouples was reduced to once in every 240 minutes and then to once in every 480 minutes.

The psycrometers were read once in every 2 days and the pressure cells were monitored once in every 5 days.

The experiment was interrupted on August 20, 1986 due to the failure of the power supply to the heaters and burnout of the common lead of heater #8. The test was restarted on August 22, 1986 after the replacement of the power supply. A new Kepco power supply was used to supply power independently to heater #8. The current supplied to heater #8 was adjusted such that the rate of energy output from the two heating coils (instead of one) was 36 watts.

On October 23, 1986, the common leads of heaters #7 and #9 burnt out. By changing the power supply and decreasing the amperage, the energy output for the two heaters was kept constant at 36 watts/heater. One of the 9 ohms heating coils in heater #4 also burnt out and the backup heating coil was used to continue the experiment.

With the completion of the thermal drying test, testing of the water injection system and its effect on the performance of the instruments was started on October 27, 1986. Initially, water was injected into the system at a pressure of 35 kPa. Water leakage was observed at the outlet of the 76 mm diameter pipe at the north panel of the model. On November 4, 1986, expansive grout, composed of 45 kg of type 10 cement, 18 kg water and 0.34 kg of Interplast N, was injected into the space between the inner wall of the 76 mm diameter pipe and the outside walls of the water injection tubes and the thermocouple cables going through the 76 mm diameter pipe. The 76 mm diameter pipe extending from the model was then embedded in an epoxy resin block which composed of 1 part of Cappar 204 epoxy and 7 parts of silica sand.

No further water leak was observed until the water pressure was increased to 70 kPa. The leak was evidenced by a thin film of water on part of the top of the epoxy and some slight water stains on the plywood box containing the epoxy.

On November 21, 1986, the power supplied for the heaters was turned off because water was found to be condensing in one of the data acquisition cards in the HP data logger. The condensation of water caused a short circuit of the data acquisition card.

On November 23, 1986, the pressure in the water supply tank was increased to 140 kPa. Water leaks through the insulation boundaries as well as at the epoxy box were observed. The injection test was terminated on November 26, 1986.

5.0 EXPERIMENTAL DIFFICULTIES AND REMEDIES

The experimental difficulties involved in this phase of the research program can be divided into 4 categories. These are:

1. Instrumentation

The instrumentation used in the thermal drying stage of the experiment were thermocouples, Petur pressure cells and psycrometers.

The Petur pressure cells functioned well throughout the thermal drying stage and the rewetting stage.

For the psycrometers, the attempts to measure the moisture content of the buffer with these devices were unsuccessful. The reason for this lack of success in monitoring the moisture content of the buffer may have been due to the high thermal gradients which were set up in the buffer zone. The psycrometers were designed to determine moisture contents in domains with minimum thermal gradients. This observation implies a limitation in the use of psycrometers for monitoring changes in moisture contents. New equipment for the monitoring of moisture content is required.

The performance of the thermocouples during the thermal drying phase of the program was very satisfactory. Throughout the test, only three thermocouples malfunctioned. This indicated the high reliability of these temperature sensors. During the injection of water, water seeped through the plastic sleeves of the thermocouple cables, and most likely caused the short circuit of one of the data acquisition cards in the HP data logger. One method to limit the seepage of water through the sleeves is to apply an impervious epoxy coating at the thermocouple junction so as to seal off the entrance for water into the cable sleeves. In addition, a junction box should be provided to break the continuity of the water seepage paths.

2. Heaters

The performance of the heaters during the thermal drying stage of the test was satisfactory. Throughout the test, only minor servicing was required for four of the heaters.

During the injection of water, three heaters were completely destroyed within one week of the injection period. One possible cause of the heater failure was due to the influx of water through the ceramic epoxy shell into the heaters, thereby causing a short circuit of the heating coils. It is proposed that in the design of heaters for Phase 4 of the research program, the heaters should be fabricated as an impervious system for water penetration.

3. Water Injection System

During the evaluation test of the water injection system, water leaked through the outlet of the 76 mm diameter pipe at the north panel of the model. The leak was sealed off by grouting. At a higher water pressure, 140 kPa, leakage occurred through the insulation boundaries. This indicated that under high pressure, the rubber membrane which was installed to seal the buffer-backfill zones may not have been very effective.

Two extreme conditions may be envisaged in the rewetting of the buffer-backfill zones. If the host rock surrounding the vault has a very low hydraulic conductivity, with the closure of the vault and termination of dewatering of the site the rate of water pressure build up at the vault will be extremely slow. If the hydraulic conductivity of the rock is much lower than that of the buffer material, then water pressure within the buffer will build up slowly and the amount of water available for the rewetting of the buffer-backfill zones will be small. In this case, the water pressure required to simulate the rewetting of the experimental model should be minimal.

On the other hand, when the hydraulic conductivity of the host rock is much larger than that of the buffer material, water pressure build-up in the buffer-backfill zones may be very rapid. To simulate this case, a high water pressure should be applied to the experimental model so as to simulate the in situ water uptake conditions.

It is believed that if the host rock were very pervious it would not be selected as a nuclear waste disposal site. Otherwise, treatment of the rock will be required to correct its hydraulic conductivity characteristics. Thus it is proposed that a low water injection pressure would be sufficient and realistic in Phase 4 of this program.

4. Power Supply

The thermal drying stage of the test was interrupted due to failure of the power supply to the heaters. Thus it is proposed that during the Phase 4 test, which will require a much longer testing period, a backup power supply unit for the heater should be available in the laboratory such that in case of a power failure, the testing program will not be interrupted.

For Phase 4 of the test program all of the above problems have been addressed and remedied. In addition, a 3.2 mm thick rubber membrane has been applied to the inside wall of the backfill room to improve water tightness of the model boundaries.

6.0 ANALYSIS OF DATA

In this section, the measured and predicted thermal regimes in the experimental model are presented. The relationship between the thermal conductivity and moisture content of the buffer material is presented in Figure 18. Comparisons of the measured and predicted thermal distribution along the X-axis and Y-axis are made.

6.1 Experimental Data

For the thermal drying stage, the temperature at the heaters versus time plots provide a complete loading history of the experiment. In Figure 19, the temperature versus the logarithm of time curves are plotted for heaters #4, #5 and #8. This plot clearly indicates that between the period of 10,000 to 100,000 minutes, the heaters were turned off twice for servicing. Since the three curves are almost identical, only the curve for heater #5, which is located in the centre of the nine heaters, is used for the following discussion.

Figure 19 shows that the temperature at heater #5 increases linearly with logarithm time. The initial part of the curve is not linear because of the initial transient associated with the thermal inertia of the heater/8/. The linear portion of the curve indicates that the transient temperature increases in the heater and the surrounding domain without any change in the thermal conductivity of the domain. At t=8,000 minutes, a non-linearity is initiated at the temperature versus logarithm time curve for heater #5. The curve becomes linear once again, with a steeper slope, at t=20,000 minutes. The changes in steepness of the slope indicates a possible decrease in thermal conductivity of the buffer surrounding the heater.

In order to examine the possibility of thermal drying of the buffer, the temperature versus logarithm time relationship for thermocouple #150, which is located in the buffer at heater #5, is plotted in Figure 20. This curve has the same characteristic as the heater #5 curve. Deviation of the curve from linearity occurs at t=10,000 minutes and its linearity resumes at t=35,000 minutes. The curve clearly indicates the occurrence of thermal drying in the buffer zone.

The time for the occurrence of thermal drying at the buffer as is indicated by both curves, is very different. One cause of the problem for the time lag in response between heater #5 and thermocouple #150 is that at t=8,000 minutes, thermal drying occurs at the buffer and thus, the temperature versus logarithm time relationship of the heater starts to deviate from linear. At that time, the temperature difference between heater #5 and thermocouple #150 is about 12°C. With time, the thermal drying front moves further outward. At t=15,000 minutes , the temperature versus logarithm time curve for thermocouple #150 starts to deviate from its linearity. This response indicates that at that instant, the thermal drying front may be crossing the thermocouple location. With further migration of the thermal drying front away from thermocouple #150, the slope of the temperature versus logarithm time curve increases steadily. When the thermal drying front has moved a significant distance away from thermocouple #150, the effect of the movement of the drying front on the rate of temperature changes with logarithm time becomes negligible. At that time, the curve becomes linear again, but with a steeper slope caused by the reduction in thermal conductivity of the buffer due to thermal drying.

The temperature versus logarithm time plot for thermocouples #268, #269 and #270, which are located along the Y(+ve) axis in the backfill zone, are also presented in Figure 20. These curves indicate that neither thermal drying nor wetting have occurred in the backfill zone throughout the experiment.

The response of thermocouples #125, #138 and #143, located in the concrete mass, to the thermal loading condition is given in Figure 21. Because of the long distance from the heaters, about 7,000 minutes is required for the thermal front to reach the boundary of the model. The temperature profiles along the X-axis of the model at 5, 10, 30 and 60 days are plotted in Figure 22. These curves are symmetrical about the origin of the X-axis. This indicates that the buffer, backfill and concrete portions of the test model have uniformity in compaction and properties.

Extremely high temperature gradients occurred in the buffer zone. At 60 days, the temperature gradient across the buffer zone at heater #5 was about 2.3 °C/mm.

Figure 22 also indicates that the rate of temperature increase in the boundary decreases with time. This implies the occurrence of heat loss through the insulation boundary. In the numerical simulation of the experiment, the heat loss across these adiabatic boundaries was considered.

The temperature at the central heater (#5) is higher than the other heaters around it. With perfect adiabatic boundaries, heaters #4 and #5 should have the same temperature. The thermal regime of heater #5 is not affected by the imperfect boundaries of the model. Such results prove the design consideration that with the provision of multiple heaters, the effect of the imperfect adiabatic boundary on the temperature regime could be reduced.

6.2 Theoretical Analysis

A theoretical analysis was performed to study the heat and moisture flow in the experimental model. The computer program, TRUCHAM, developed in 1982 by the Civil Research Department/9,10/, was used for this study. The computer code is based on the mathematical model of Philip and DeVries, and utilizes the integrated finite difference technique for the analysis of transient, coupled heat and moisture flow in soils. The code can accommodate a variety of linear and non-linear boundary conditions and non-linear material properties.

In order to use TRUCHAM to predict the heat and moisture movement within the experimental model, the material properties that need to be known are the hydraulic conductivity, thermal moisture diffusivity, isothermal moisture diffusivity, isothermal vapour diffusivity, volumetric heat capacity and thermal capacity of the materials which comprise the model.

Currently, difficulties involved in the measurement of isothermal vapour diffusivity, isothermal moisture diffusivity and thermal moisture diffusivity are still unresolved. Thus, only the transient heat flow in the experimental model was studied. The thermal dryout conditions of the buffer was simulated by modifying the input thermal conductivity of the buffer zone based on the results of the laboratory experiments reported earlier/6/.

The effect of the thermal conductivity of the buffer on the thermal regime in the model was investigated through a parametric study.

Because of symmetry on the Y-Z and Y-X planes, a one-quarter segment of the laboratory scale model comprising one, one-quarter heater, two half heaters and one full heater was simulated.

The material properties of the compacted buffer and backfill materials were determined on test specimens prepared to the same moisture and density conditions as those in the experimental model.

In the analysis, the heaters were treated as having uniform material properties with a constant volumetric heat capacity and a constant thermal conductivity. Because of the complex configuration and multiple components of the heaters, both insulation and calorimetric laboratory methods were used to determine their volumetric heat capacity. These methods yielded values for the volumetric heat capacity of 1.677 and 1.616 $J/^{o}C\ cm^3$, with a difference of about 4 per cent. An average value was used for the analysis. The thermal conductivity of the heater was taken as equal to that of steel.

The function of the insulated boundaries was to control the loss of heat to the atmosphere. The insulated boundary consisted of a sandwich of two 19 mm plywood sheets with 150 mm polystyrene between. Initially in the analysis, a no heat flow boundary condition was applied to the insulated boundaries. However, after preliminary analysis, it was recognized that although the thermal conductivity of the insulated boundaries was several orders of magnitude less than that of the concrete, with time, the temperature gradients across the insulated boundary increased. Due to the large surface area of the insulated boundary, these temperature gradients caused significant heat losses through the insulated boundary.

In order to model each of these insulating materials separately, the number of elements required in the analysis would have been very large. Since the temperature distribution across the insulated boundaries was not of concern in this study, the insulation was treated as an equivalent material and the volumetric heat capacity and thermal conductivity which were calculated as follows:

$$\bar{k}_e = (l_1 + l_2)/(\frac{l_1}{k_1} + \frac{l_2}{k_2})$$

$$\bar{c} = (l_1c_1 + l_2c_2)/(l_1 + l_2)$$

where l_1, c_1, k_1 are the thickness the volumetric heat capacity and the thermal conductivity of material 1 (plywood). l_2, c_2, k_2 are the thickness, the volumetric heat capacity and the thermal conductivity of material 2 (polystyrene).

In addition, the thermal conductivity of the insulation boundary was also calculated with data from the thermocouples across the boundary. This measured thermal conductivity of the insulation boundary is a lumped parameter and depends on the insulation, plywood and also the workmanship in assembling. Four cases were analyzed. The material properties and boundary conditions used are listed in Tables I and II.

The predicted and measured temperature profile at 5, 10, 30 and 60 days along the X-axis of the model are presented in Figures 23 to 26 respectively.

The steep thermal gradient measured between the heaters during the transient phase was not properly predicted by the computer model. This is due to the size of the element mesh used in the analysis. With a coarse mesh, in the region of large thermal gradients, the temperature distribution in that region will be averaged out such that the steep thermal gradients cannot be predicted. This situation can be rectified by refining the element mesh. With refinement of the element mesh, the accuracy of the prediction can be improved, but at the same time the computing time will also be increased. Thus in the selection of an element mesh, there must be a balance between the accuracy required and the amount of computing time which is required to achieve this accuracy. In this study, 4500 elements were used to simulate the experimental model. Such a choice was based on the optimization of both computing time and accuracy of the results. In Figures 27 to 30, the predicted and measured near field temperature data at 5, 10, 30 and 60 days along the X-axis are plotted. The purpose of these plots was to confirm the existence of the steep thermal gradients which were measured between the heaters.

Both the measured and predicted temperature profiles along the Y-axis at 5, 10, 30 and 60 days are plotted in Figures 31 to 34 respectively. The correlation between the measured and predicted temperature profile along the Y-axis is better than those along the X-axis. This is because the thermal gradient along the Y-axis is not as steep as it is along the X-axis. This finding confirms that the accuracy of the predicted temperature profile along the X-axis can be improved with the refinement of the element mesh.

The results of the parametric study on the effect of the thermal conductivity of the buffer zone and the insulation boundary on the thermal regime are presented in Figures 35 to 38. The effect of the thermal conductivity of the buffer zone is rather local. At any given time, the temperature at the heaters increases with the decreases in thermal conductivity of the buffer. The difference in heater temperature at 60 days could be as high as 10°C with a reduction of the thermal conductivity of the buffer by one half.

The thermal conductivity of the insulation boundary in the model has a significant effect on the temperature regime. Laboratory measurements indicate that due to thermal leakage, the measured thermal insulation properties were considerably less than those given by the manufacturer of the insulation. As a result, the temperatures regime predicted with the insulation material properties as supplied by the manufacturer and those calculated from data obtained from the experiment, at 60 days, differ by approximately 10°C.

The temperature distribution along the Y-axis with different buffer and insulation thermal conductivity are shown in Figures 39 to 42. The effect of the buffer and insulation thermal conductivity on the temperature profile along the Y-axis is similar to those on the X-axis.

7.0 CONCLUSIONS AND RECOMMENDATIONS

The effect of thermal drying on the performance of buffer and backfill materials was studied by both an experimental model test and a numerical simulation. An evaluation was made of the near-field instrumentation. The performance of the water injection system was also studied in the model at the end of the thermal drying test. From this study the following conclusions can be drawn:

1. The measured temperature regime from the model tests can be simulated with the computer program TRUCHAM developed by the Civil Research Department.

2. In the transient state in the model, extremely high thermal gradients existed in the buffer zone between the heaters. Due to scaling effects between the model and prototype, the thermal gradients in the prototype will be less than those predicted by the experimental model. However, the steeper thermal gradients in the model subjected the buffer to more stringent and demanding thermal drying conditions. The computer model TRUCHAM will prove to be invaluable in the prediction of the true thermal gradients in the prototype.

3. As predicted by the computer model TRUCHAM, under steady state conditions, the thermal gradient between the heaters will be reduced to less extreme values.

4. The rate of migration of the thermal drying front was determined from the temperature records of the experiment.

5. The effect of the insulation boundaries on the thermal regime in the model is very significant. In the design of the experimental model to simulate the disposal vault, special attention should be paid to the design of the adiabatic boundary.

6. The effect of the thermal conductivity of the buffer on the thermal regime is very local. In the analytical study using TRUCHAM, the temperature at the heater at 60 days increased by $10^{o}C$ with a decrease in the thermal conductivity of the buffer by 50 per cent.

7. At the present time, information on material properties such as thermal moisture diffusivity, isothermal moisture diffusivity and isothermal vapour diffusivity is limited. Additional research on the methods for determining these parameters is required.

8. The thermocouples and Petur pressure cells functioned well throughout the thermal drying test stage. At the water injection stage, water passed through the plastic sleeves of the thermocouple cables and into the data logger, damaging a data acquisition card. It is proposed that in Phase 4 of the research program, a junction box should be provided to disconnect such a flow path. In addition, the tip of the thermocouple junctions should be sealed with a coating of impervious epoxy.

9. During the water injection test stage, three heaters were burnt out. This was caused by the influx of water through the ceramic epoxy of the heaters and thereby short circuiting the heating coils. Thus, in Phase 4 of the study, the heaters should be designed as impervious units.

10. The adiabatic boundaries simulated with 150 mm of polystyrene and 19 mm of plywood were not very effective. In order to reduce such effects a greater thickness (300 mm) of insulation should be provided.

11. The water injection system functioned well when it was subjected to a water pressure of about 35 kPa. With higher water pressures, leakage occurred. In the Phase 4 study, if the anticipated water injection pressure is higher than 35 kPa, redesign of the current system is required.

12. The Wescor psycrometer used in the current experiment is not suitable for the monitoring of moisture movement in areas which are subjected to high thermal gradients.

13. Modifications should be made to the computer code, TRUCHAM, to allow for the analysis of the rewetting of the buffer as is required in Phase 4 of the research program. Such changes to TRUCHAM will require the formulation of the program using pressure head, rather than moisture

content, as the dependent variable. Such a change in the variable is necessary to allow for the inclusion of prescribed head boundary conditions to the analytical model of the prototype repository.

14. TRUCHAM is a sophisticated numerical code, and the system to be analyzed in the near field of the waste canisters is very complicated. Time and effort should be committed to the building up of experience in the use of this model for analysis of the URL experiment.

Approved by:

TWK

T.W. Klym
Manager
Civil Research Department

Prepared by:

HSRadhakrishna

H.S. Radhakrishna
Senior Engineer
Soil Sciences Section

KCLau

K.C. Lau
Engineer
Soil Sciences Section

Reviewed by:

T.J. Carmichael

T.J. Carmichael
Supervising Engineer
Soil Sciences Section

HSR/KCL:LM

REFERENCES

1. R.S. Lopez, S.C.H. Cheung, and D.A. Dixon. "The Canadian Program for Sealing Underground Nuclear Fuel Waste Vaults". Canadian Geotechnical Journal, Vol 21, No 3, 1984.

2. Acres Consulting Services Ltd and Associates. "A Disposal Centre for Irradiated Nuclear Fuel: Conceptual Design Study". Atomic Energy of Canada Limited, Report No AECL-6415, 1980.

3. Acres Consulting Services Ltd and Associates. "A Disposal Centre for Immobilized Nuclear Waste: Conceptual Design Study". Atomic Energy of Canada Limited, Report No AECL-6416, 1980.

4. K. Nuttall, D.J. Cameron, and F.P. Sargent. "The Canadian Engineered Barriers Program". Proceedings, International Conference on Radioactive Waste Management, Winnipeg. Canadian Nuclear Society, Toronto, pp 46-53, 1982.

5. G.W. Bird and D.J. Cameron. "Vault Sealing for the Canadian Nuclear Fuel Waste Management Program". Atomic Energy of Canada Limited Technical Record, TR-145, 1982.

6. H.S. Radhakrishna. "Thermal Properties of Clay-Based Buffer Materials in a Nuclear Fuel Waste Disposal Vault". Atomic Energy of Canada Limited, Report No AECL-7805, 1984.

7. H.S. Radhakrishna, K.C. Lau and A.M. Crawford. "Near-Field Thermal Analysis of the Nuclear Waste Disposal Vault". Nineth Waste Management Conference, Stockholm, pp 559-566, Sept 1985.

8. J.K. Mitchell. "Backfill Materials for Underground Power Cables, Phase 4: Theory and Field Testing of Backfill Thermal Stability". Department of Civil Engineering, University of California, Berkeley, EPRI, EL-4856, Oct 1986.

9. H.S. Radhakrishna, K.C. Lau and A.M. Crawford. "Coupled Heat and Moisture Flow Through Soils". Journal of Geotechnical Engineering, ASCE, Vol 110, No 12, pp 1766-1784. Dec 1984.

10. A.M. Crawford, H.S. Radhakrishna and K.C. Lau. "Application of the Integrated Finite Difference Technique to Heat Transfer Through Unsaturated Particulate Media". Fifth Int Conf on Heat Transfer, Montreal, 1987.

TABLE I

Material Properties Used in the Analytical Study

Material	Thermal Conductivity W/°C m	Heat Capacity cal/cm^3°C
concrete	0.418	0.55
backfill	0.167	0.875
plywood	0.028	0.158
polystyrene	0.0069	0.016
fibreglass	0.01	0.0064

TABLE II

Material Properties Used in the Parametric Studies

Case	Buffer Thermal Conductivity W/°C m	Boundary
1	0.7238	equivalent properties
2	0.9999	equivalent properties
3	1.3221	equivalent properties
4	0.7238	calculated with data from thermocouples across the boundary

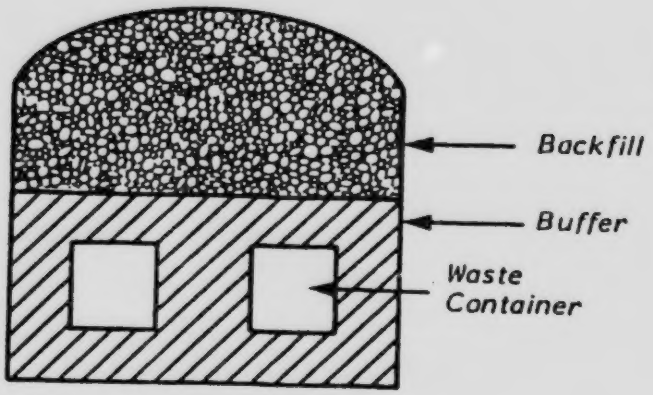
Backfill
Buffer
Waste Container

(a) In-Room Emplacement (TEC-1 Design)

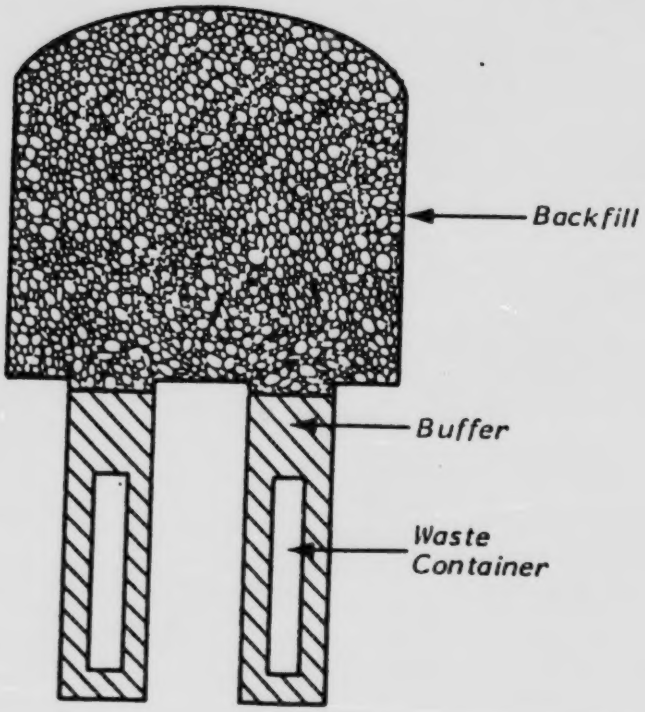
Backfill
Buffer
Waste Container

(b) Borehole Emplacement (TEC-2 Design)

FIGURE 1

SCHEMATIC ILLUSTRATION OF TWO METHODS OF NUCLEAR FUEL WASTE DISPOSAL

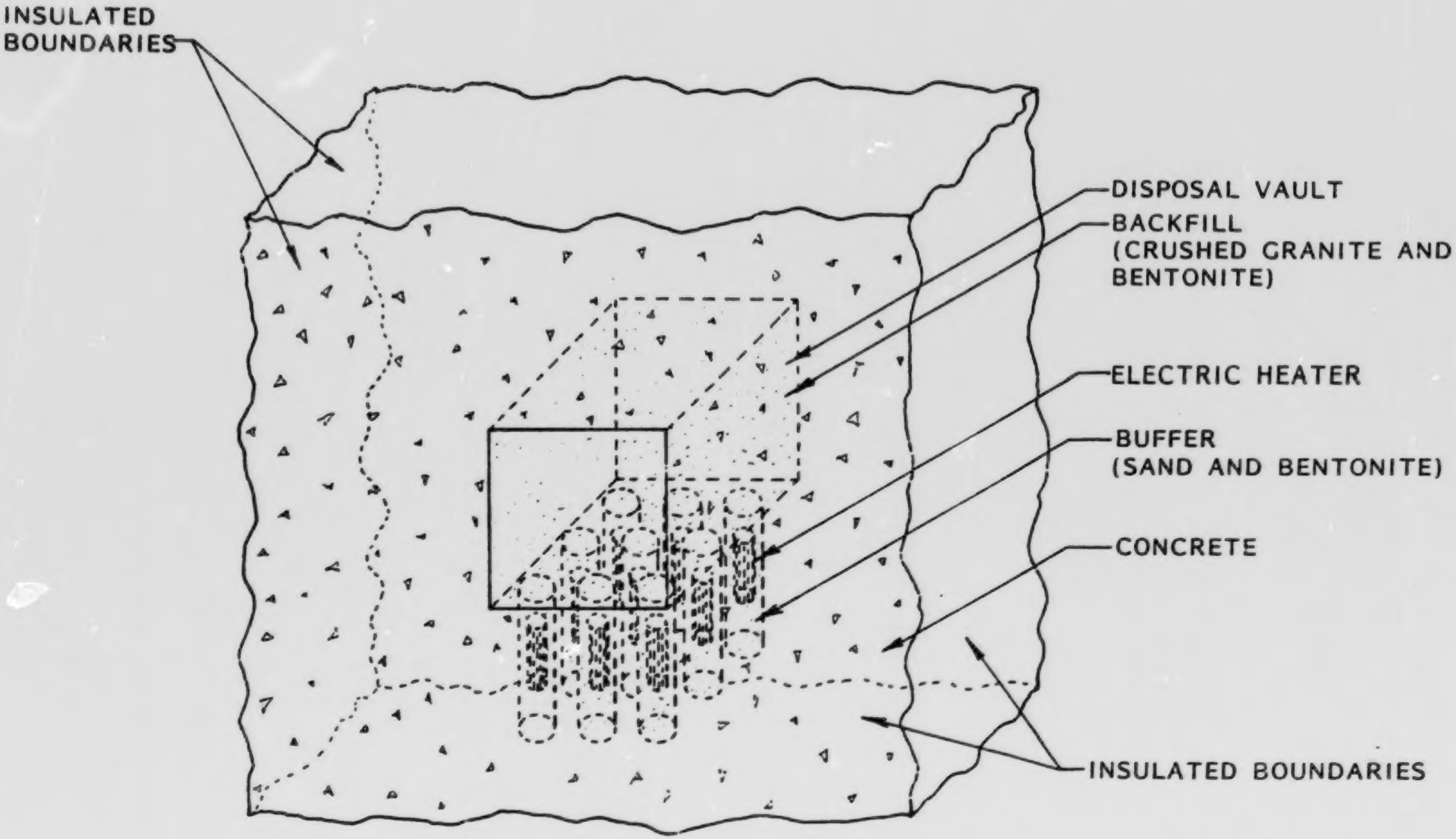
INSULATED BOUNDARIES
DISPOSAL VAULT
BACKFILL (CRUSHED GRANITE AND BENTONITE)
ELECTRIC HEATER
BUFFER (SAND AND BENTONITE)
CONCRETE
INSULATED BOUNDARIES

FIGURE 2

EXPERIMENTAL MODEL SIMULATING THE NEAR FIELD THERMAL ENVIRONMENT IN A BACKFILLED DISPOSAL VAULT

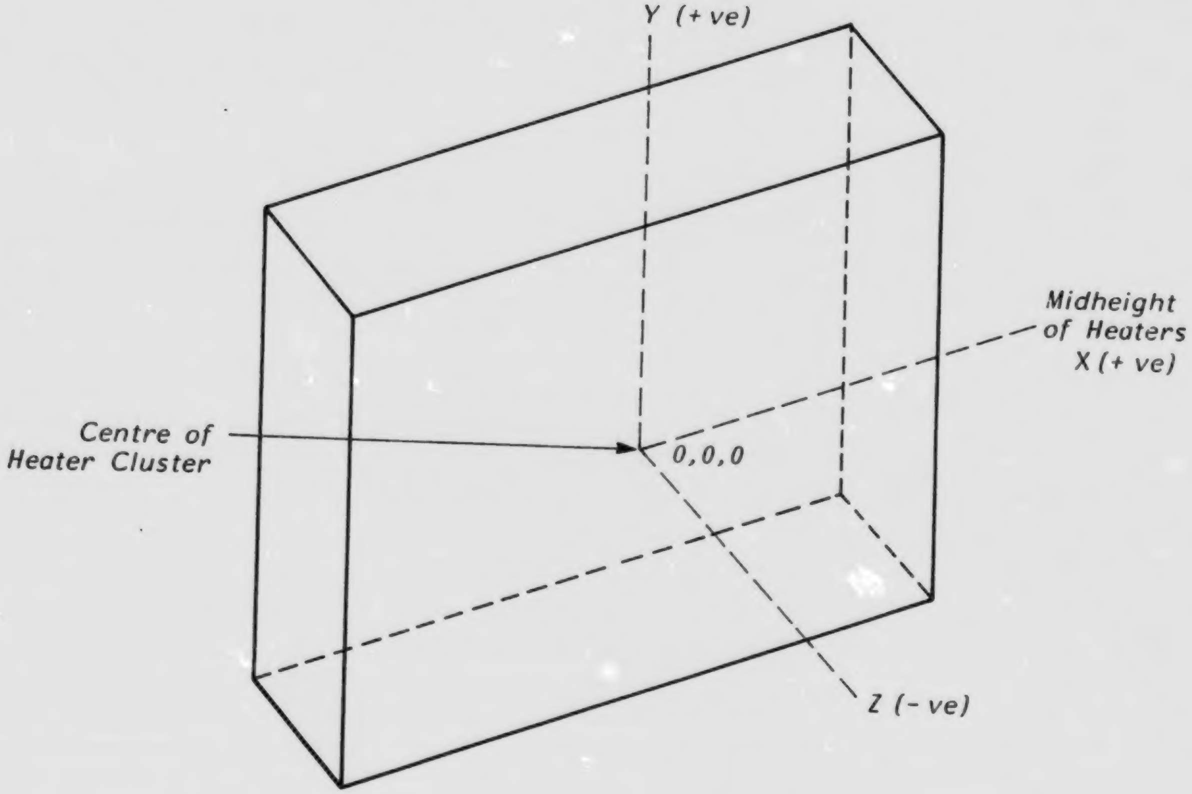
Y (+ ve)
Midheight of Heaters X (+ ve)
Centre of Heater Cluster
0,0,0
Z (- ve)

Note:

North	X (+ve)
South	X (-ve)
West	Z (+ve)
East	Z (-ve)

FIGURE 3

COORDINATE SYSTEM USED FOR MULTIPLE HEATER EXPERIMENTAL MODEL

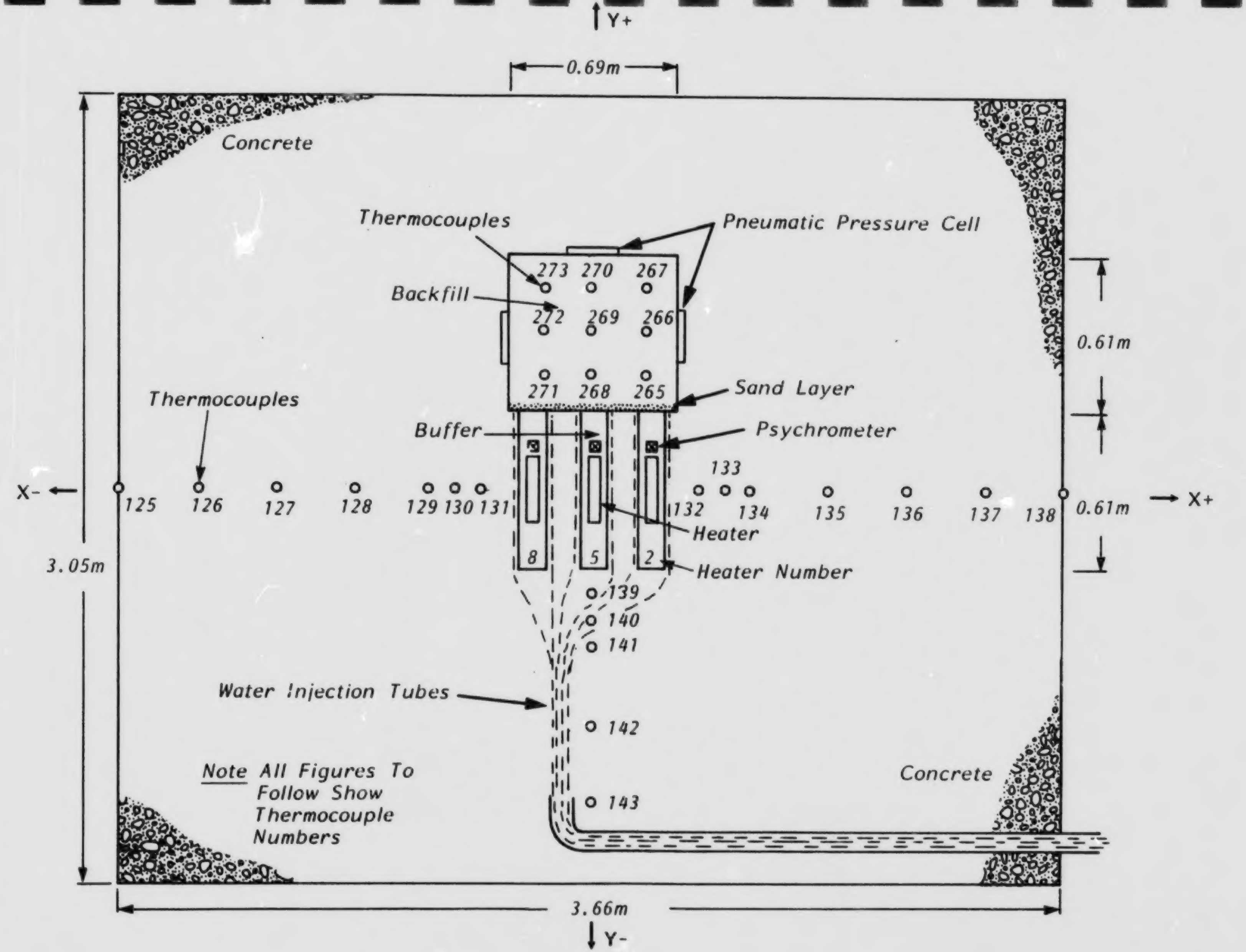
Y+
0.69m
Concrete
Thermocouples
Pneumatic Pressure Cell
273
270
267
Backfill
272
269
266
0.61m
271
268
265
Sand Layer
Thermocouples
Buffer
Psychrometer
133
X-
125
126
127
128
129
130
131
132
134
135
136
137
138
0.61m
X+
Heater
3.05m
8
5
2
Heater Number
139
140
141
Water Injection Tubes
142
Note All Figures To Follow Show Thermocouple Numbers
Concrete
143
3.66m
Y-

FIGURE 4

CROSS SECTION VIEW THROUGH X-Y PLANE, SHOWING HEATER, BUFFER AND BACKFILL ARRANGEMENT

173500-RD

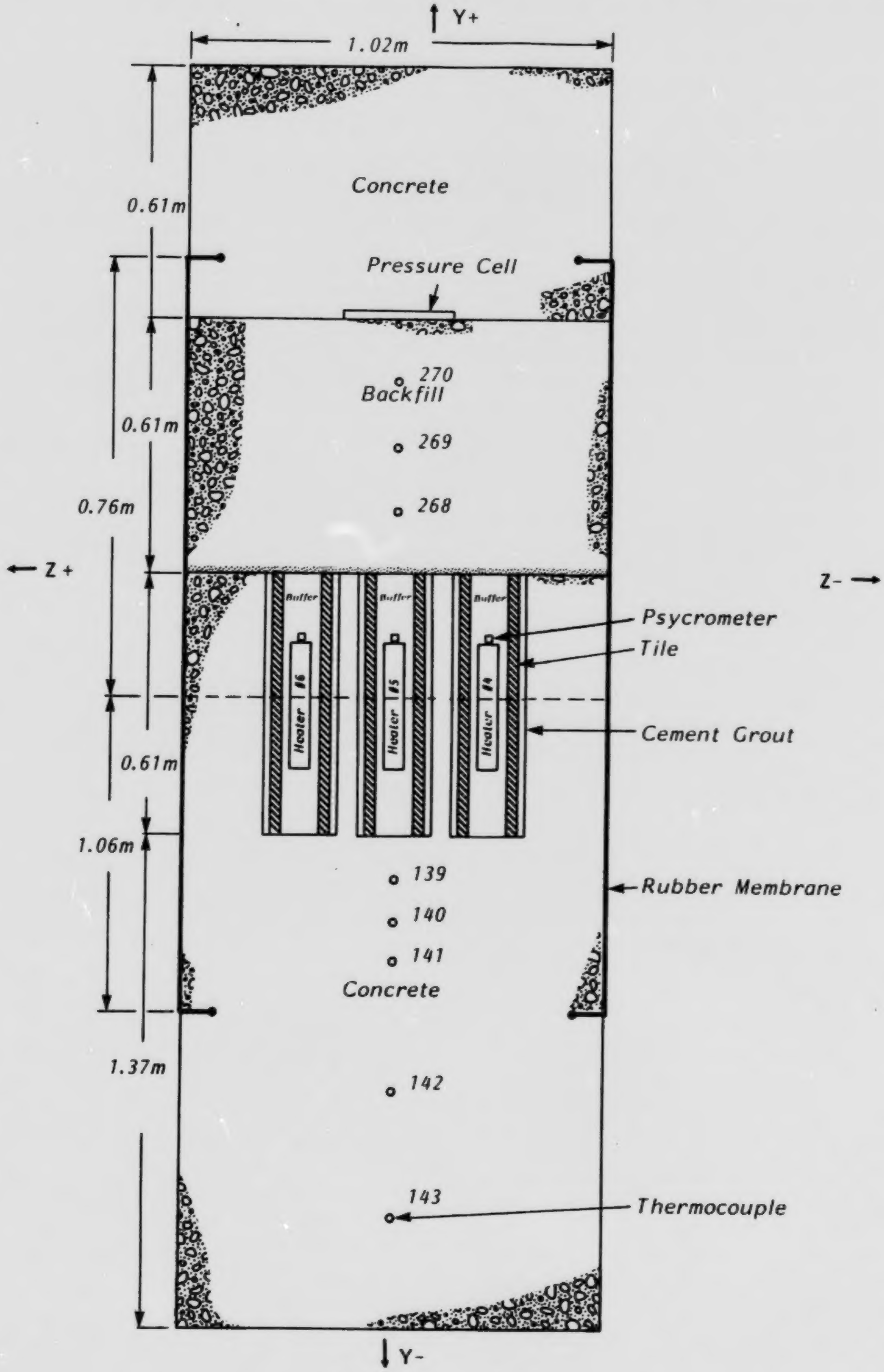
Y+
1.02m
Concrete
0.61m
Pressure Cell
270
Backfill
269
0.61m
0.76m
268
Z+
Z-
Buffer
Buffer
Buffer
Psycrometer
Tile
Heater #6
Heater #5
Heater #4
Cement Grout
0.61m
1.06m
139
Rubber Membrane
140
141
Concrete
1.37m
142
143
Thermocouple
Y-

FIGURE 5
CROSS SECTION OF MODEL IN Y-Z PLANE

173541 RD

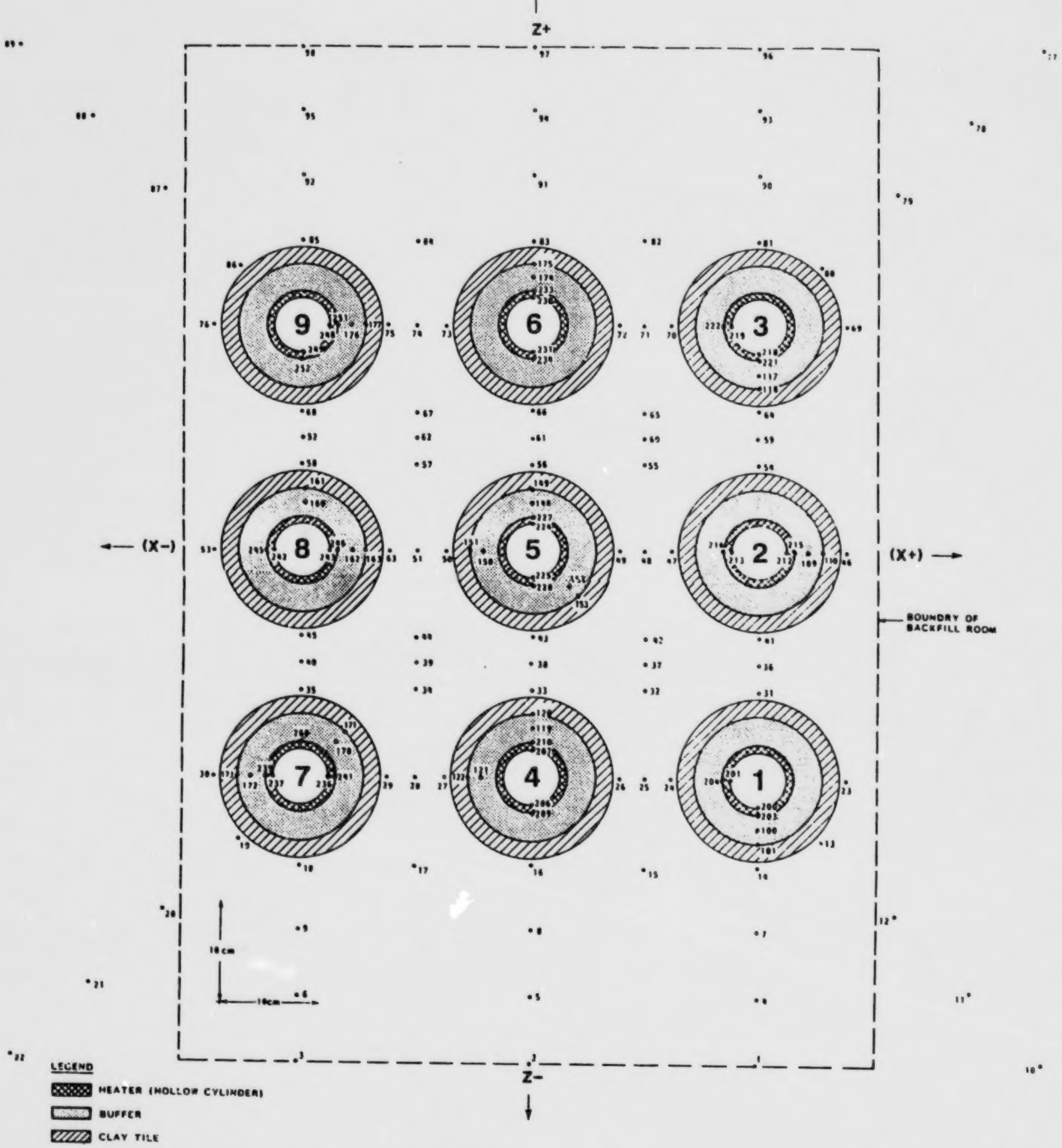
Z+
Z-
(X-)
(X+)
9
6
3
8
5
2
7
4
1
BOUNDRY OF BACKFILL ROOM
10cm
10cm
LEGEND
HEATER (HOLLOW CYLINDER)
BUFFER
CLAY TILE

NOTE: FOR ADDITIONAL THERMOCOUPLES ON XX AXIS, SEE FIGURE 8

FIGURE 6

PLAN VIEW THROUGH MID HEIGHT OF THE HEATERS IN X-Z PLANE SHOWING THERMOCOUPLE LOCATIONS

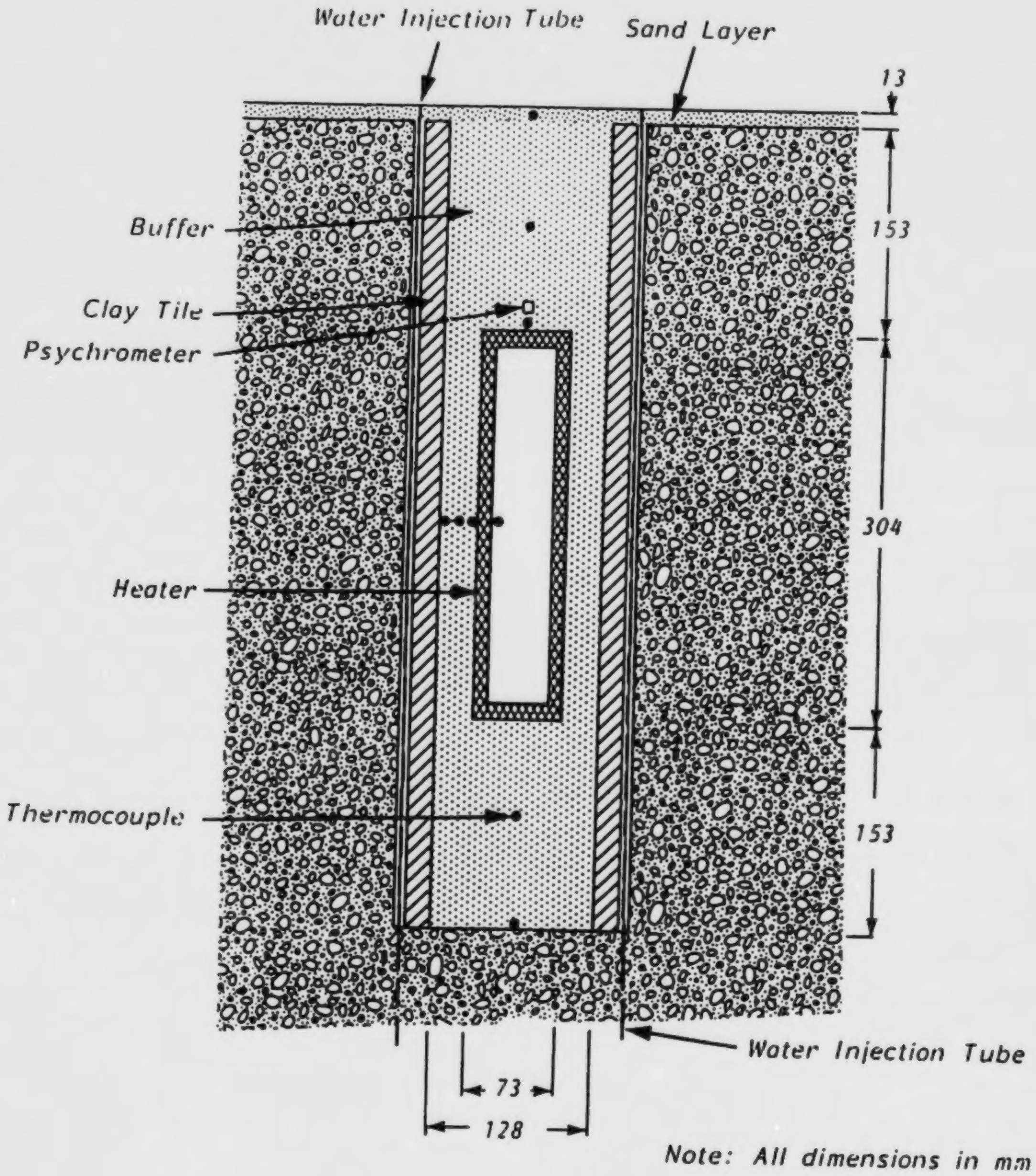
Water Injection Tube
Sand Layer
13
Buffer
153
Clay Tile
Psychrometer
304
Heater
Thermocouple
153
Water Injection Tube
73
128
Note: All dimensions in mm

FIGURE 7
DETAILS OF HEATER-BUFFER ARRANGEMENT IN BOREHOLE

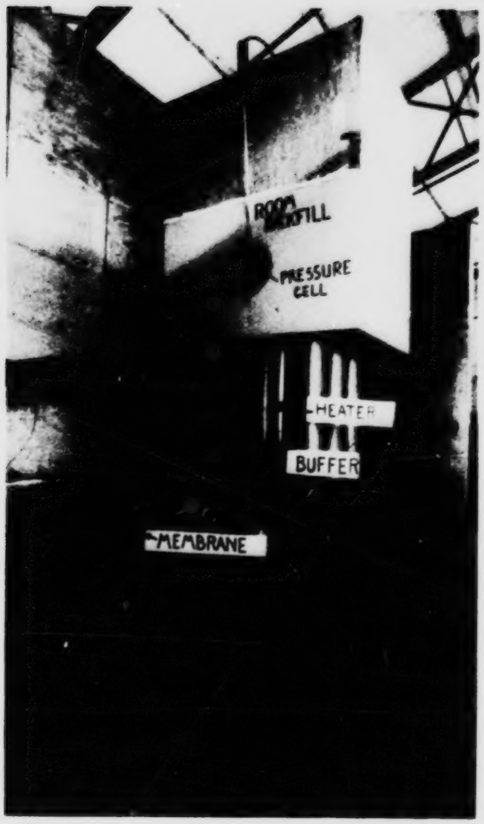
ROOM BACKFILL
PRESSURE CELL
HEATER
BUFFER
MEMBRANE

Note: Nine Fibreglass cans were cast into concrete to form boreholes for emplacing heaters and buffer

FIGURE 8

FORMWORK USED FOR CASTING THE CONCRETE MODEL FOR MULTIPLE HEATER EXPERIMENT

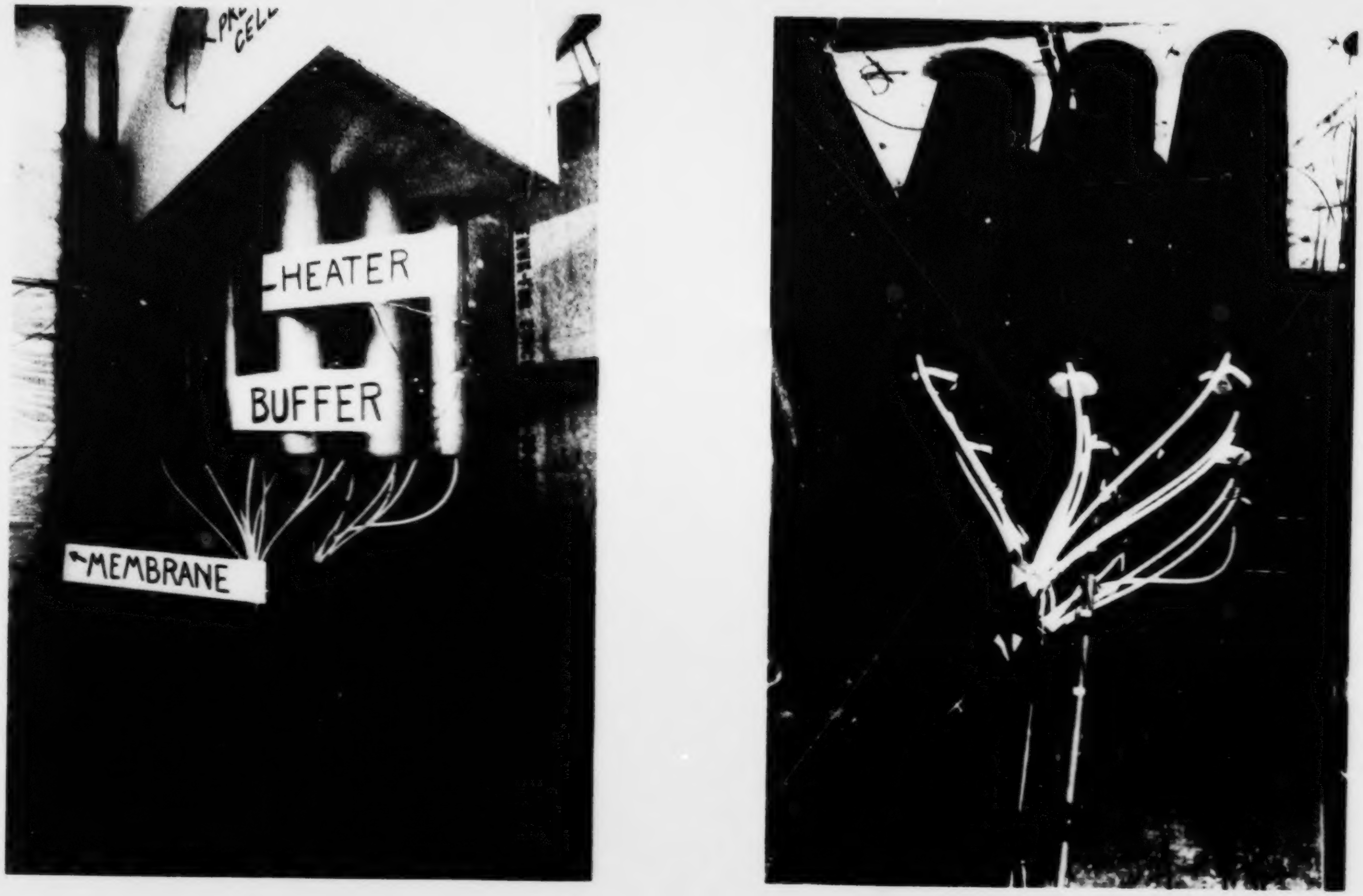
PR CELL
HEATER
BUFFER
MEMBRANE

FIGURE 9

DETAILS OF WATER INJECTION TUBES AND THERMOCOUPLES CAST INTO CONCRETE MODEL
(Note: Fibreglass cans were embedded in concrete to form boreholes for installing heaters and buffer)

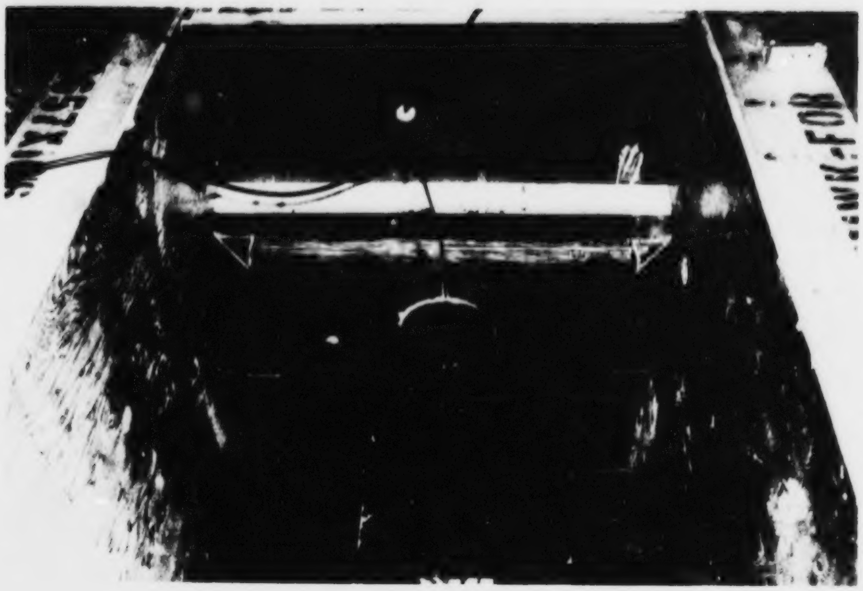

Inside view of the form work ready for concreting

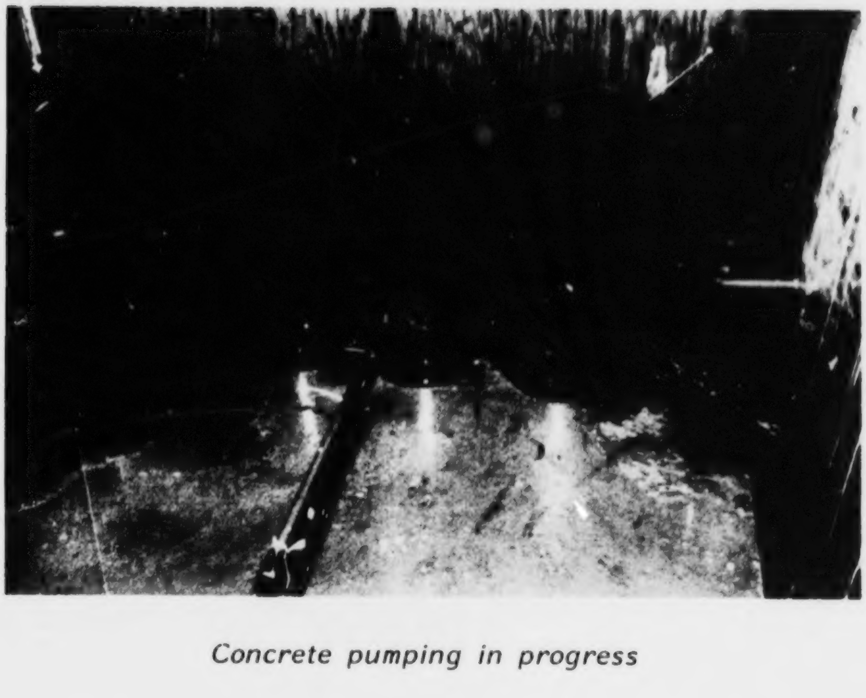

Concrete pumping in progress

FIGURE 10
CONSTRUCTION OF MODEL IN PROGRESS

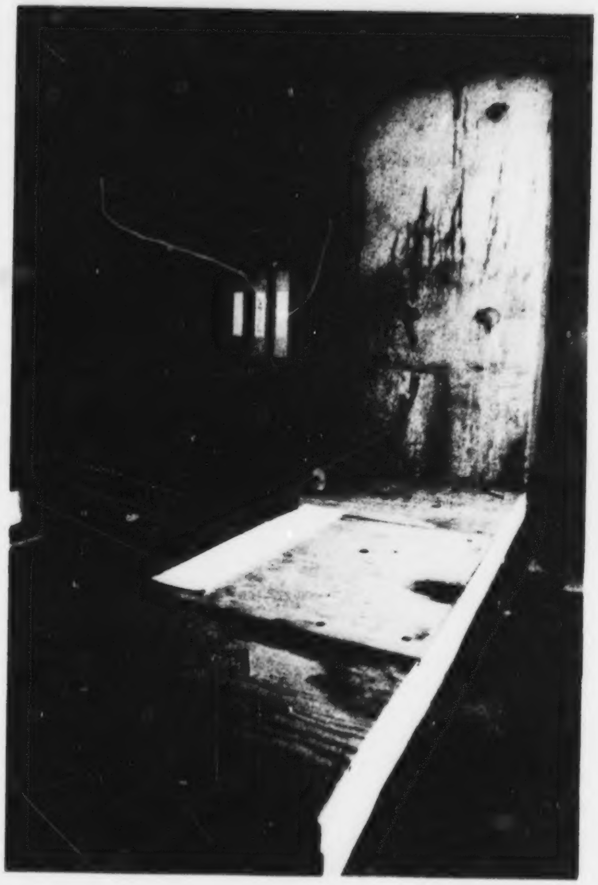

Note: Outline of Buffer and Backfill areas marked on the membrane for illustration only.

FIGURE 11

CONCRETE MODEL AFTER THE REMOVAL OF FORMWORK

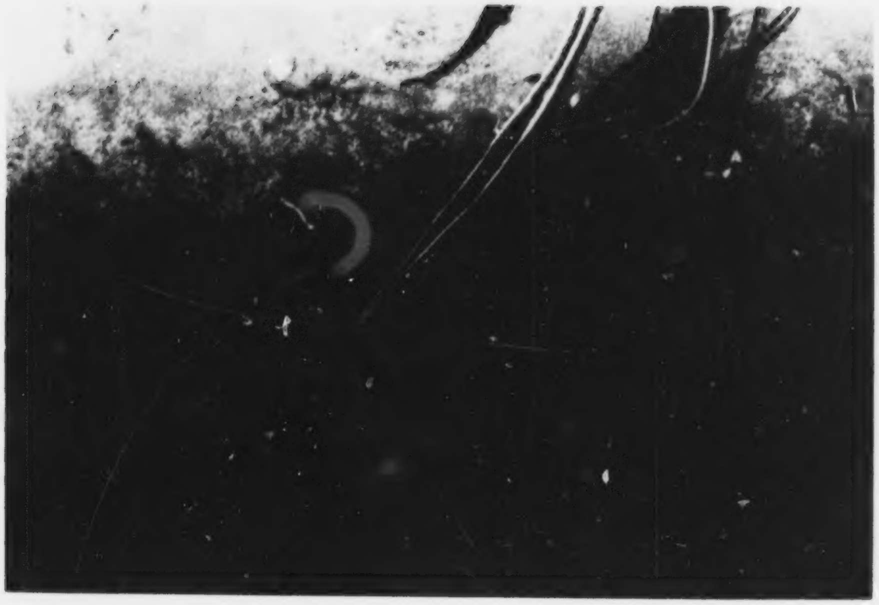

FIGURE 12

CLOSE UP VIEW OF BOREHOLE AFTER
EMPLACING HEATER AND BUFFER
*(Note the clay tile, and water injection
tube embeded in grout)*

Heaters installed, buffer filled and sand layer being poured on the floor of the backfill room.

Pneumatic pressure cell embeded in the side wall of backfill room.

FIGURE 13

LOOKING DOWN INTO THE BACKFILL ROOM

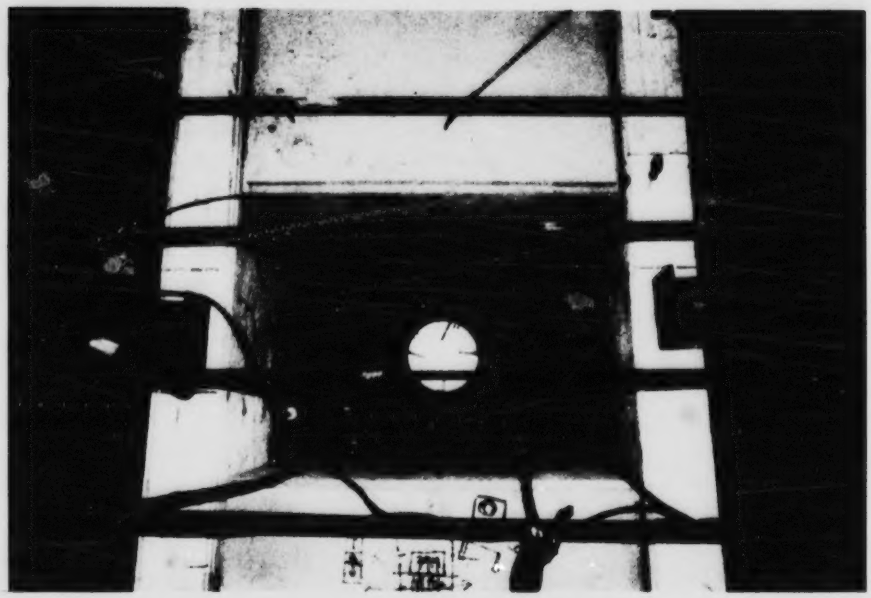

Side panels and bracing in place

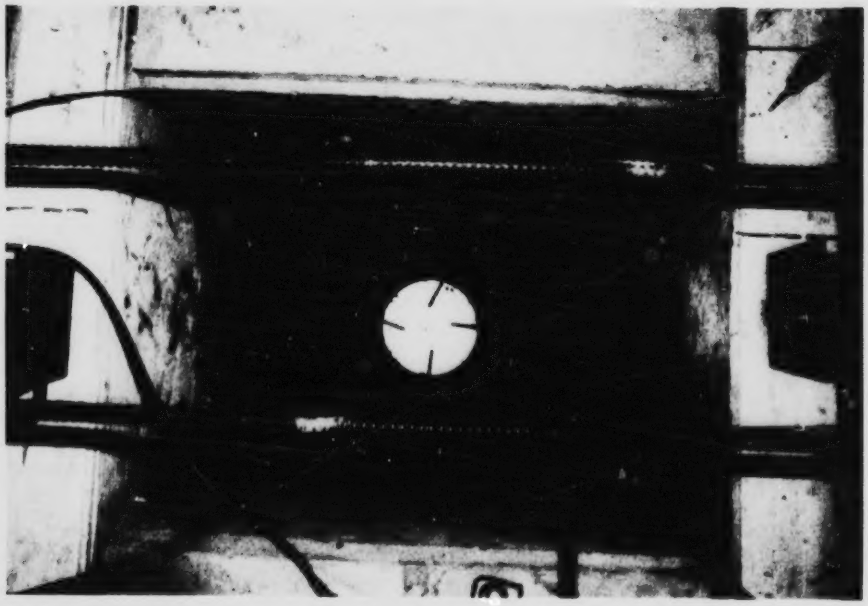

Pneumatic pressure cell located on the backfill.
Ready for concrete keyway pour.

FIGURE 14
VIEW OF TOP OF BACKFILL

Thermocouple (Copper-Constantan Junction) for monitoring temperature

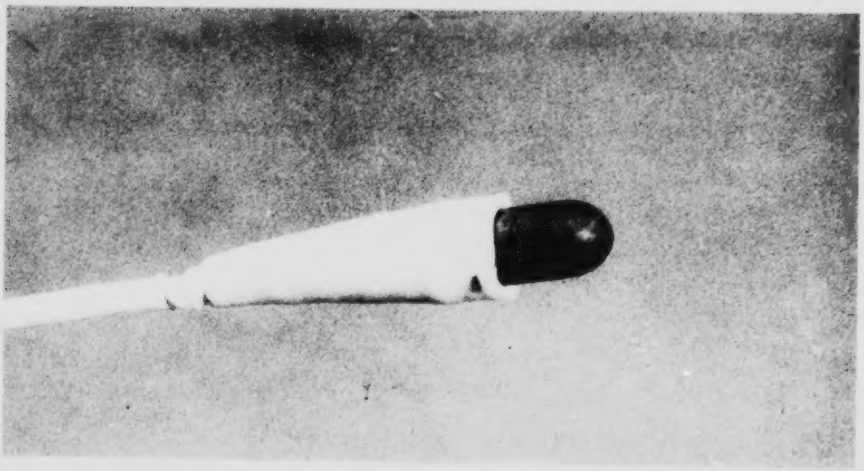

Psychrometer for monitoring the soil moisture content

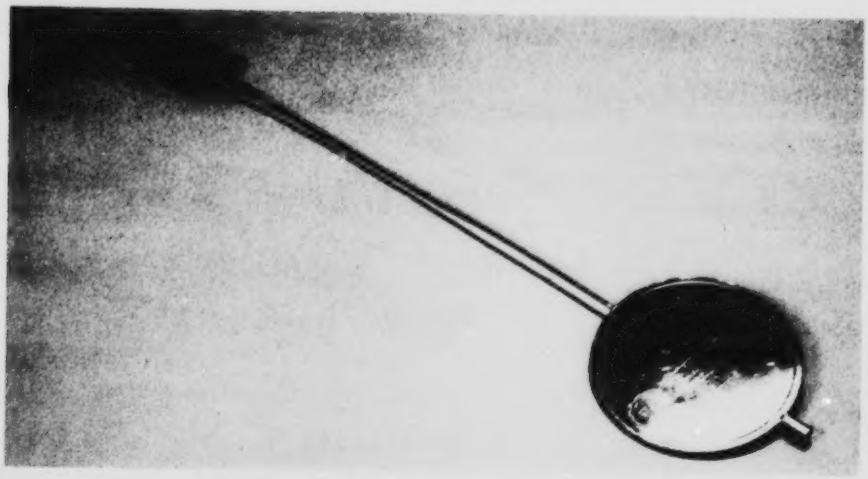

Pneumatic pressure cell for monitoring swelling pressures at concrete-backfill interface

FIGURE 15

INSTRUMENTS USED IN THE MODEL

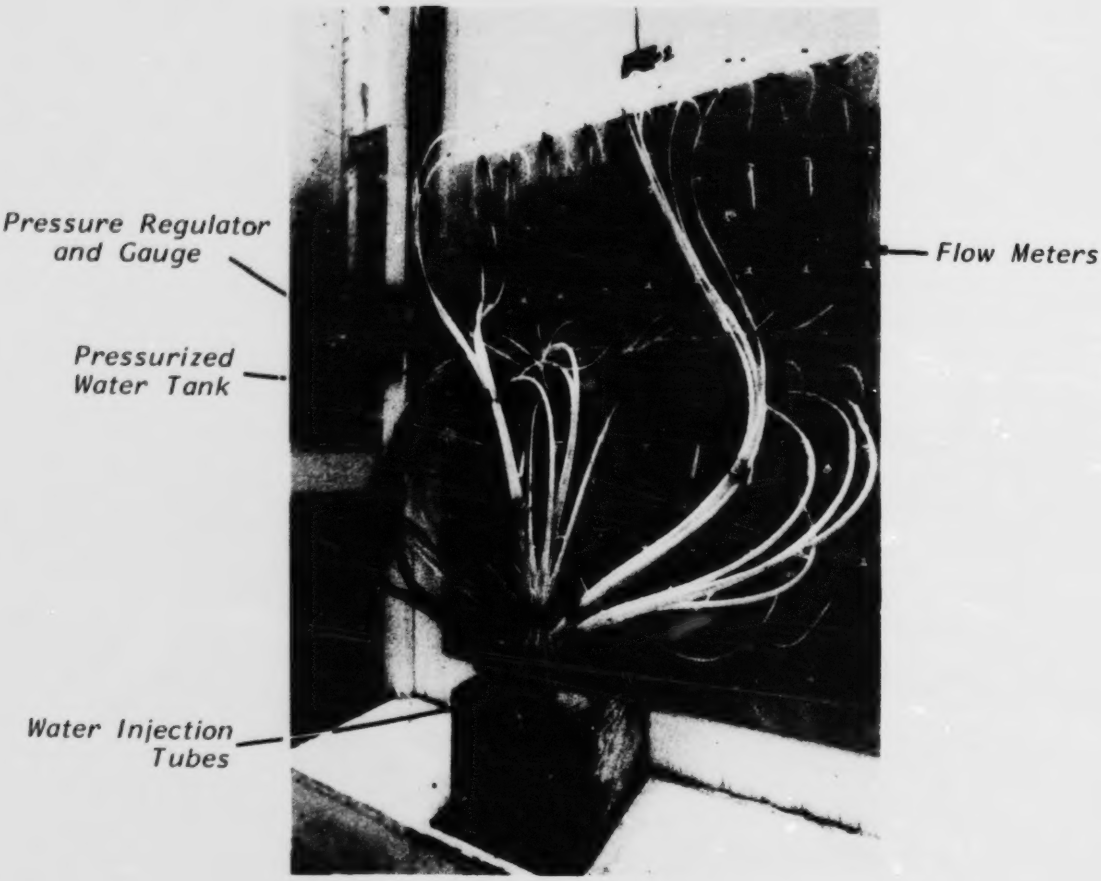
Pressure Regulator and Gauge
Pressurized Water Tank
Water Injection Tubes
Flow Meters

FIGURE 16
WATER INJECTION SYSTEM

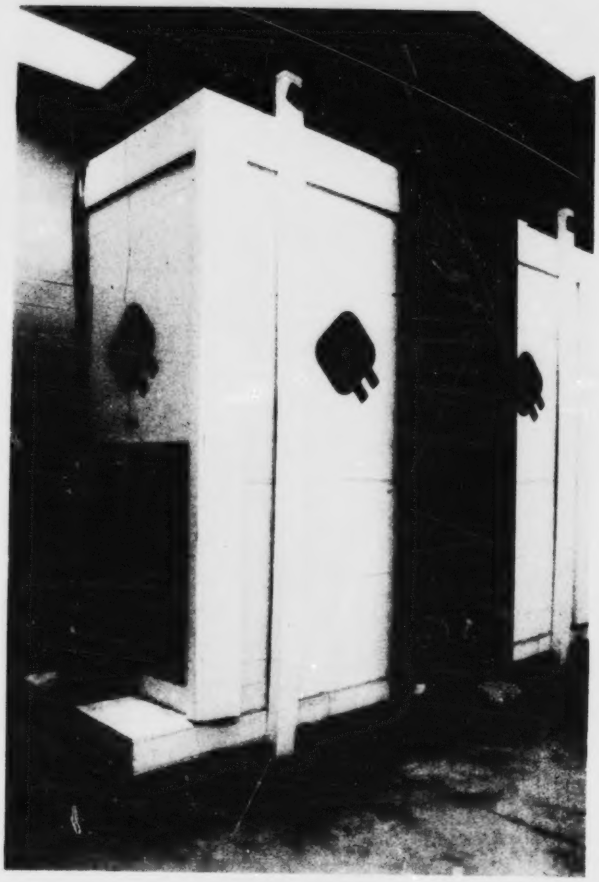

Completed model with insulated sides, cross bracing and water injection system

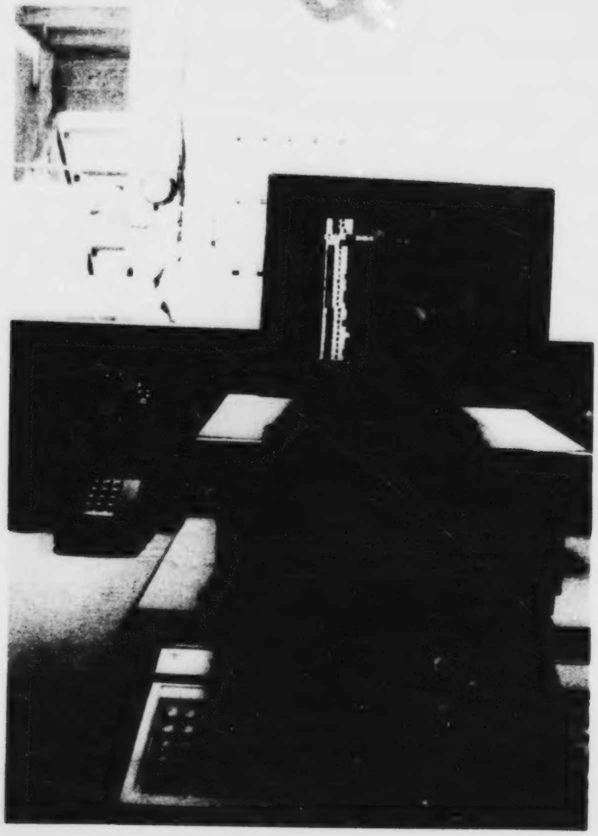

Computer controlled data aquisition system

FIGURE 17

COMPLETED MODEL TEST IN PROGRESS

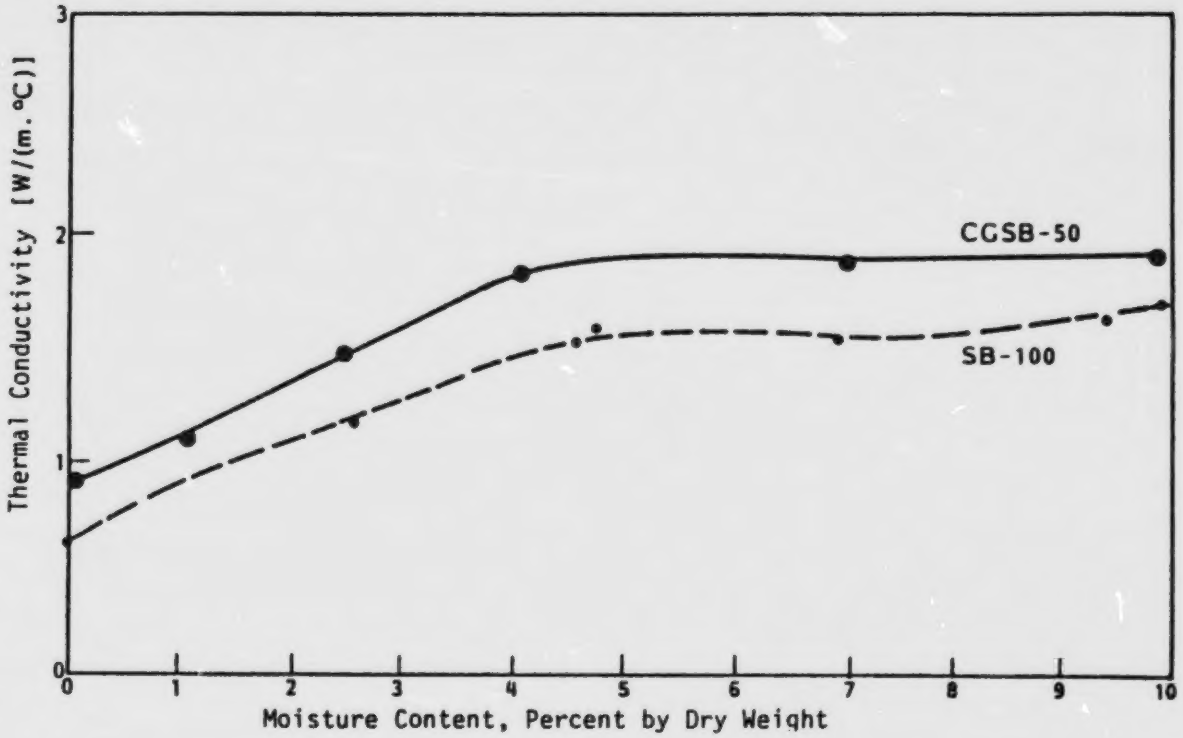

FIGURE 18

THERMAL CONDUCTIVITY VS. MOISTURE CONTENT RELATIONSHIP AT CONSTANT DENSITY FOR CRUSHED GRANITE AND SEALBOND BUFFER

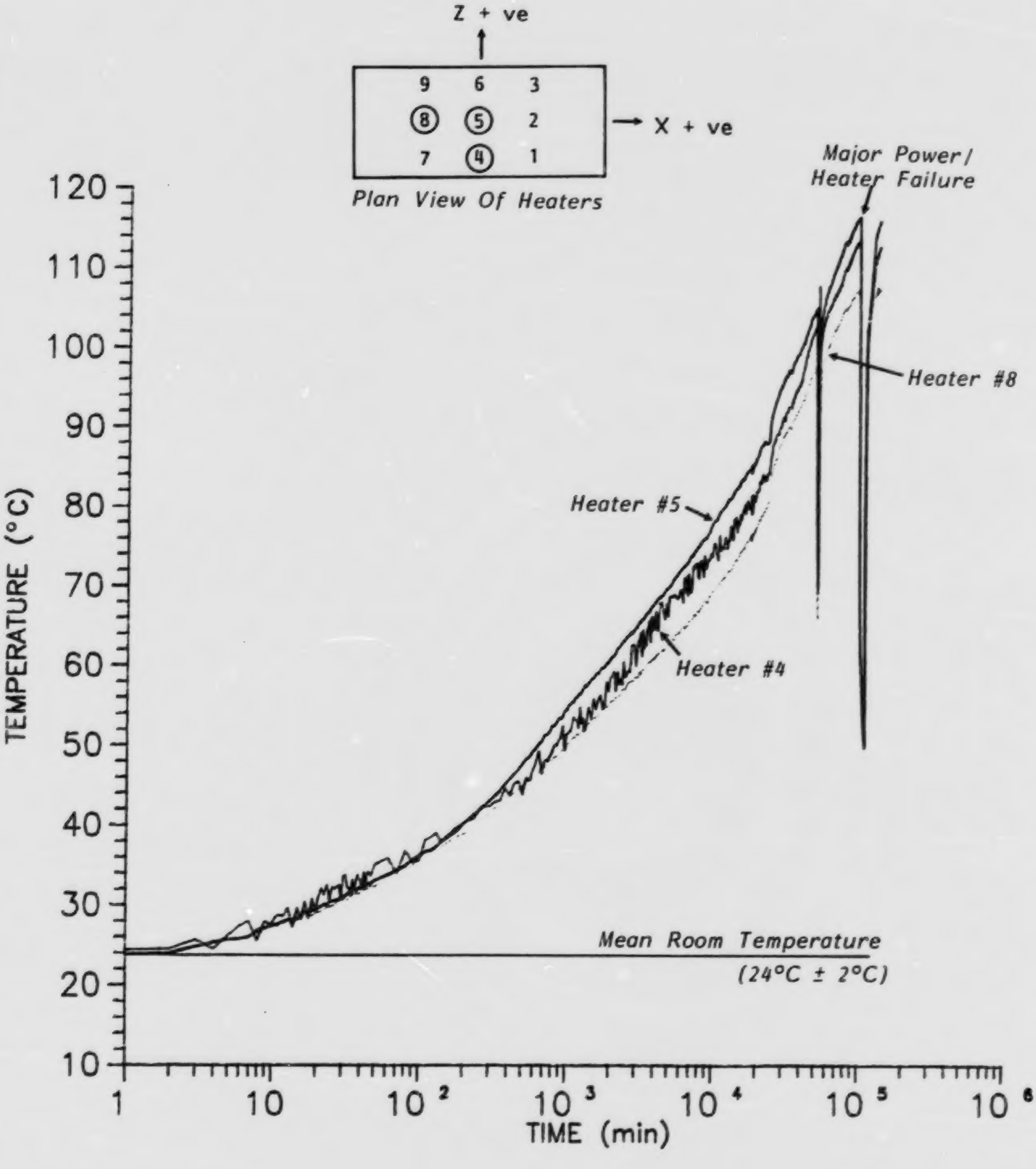

FIGURE 19

HEATER TEMPERATURE VS LOG TIME

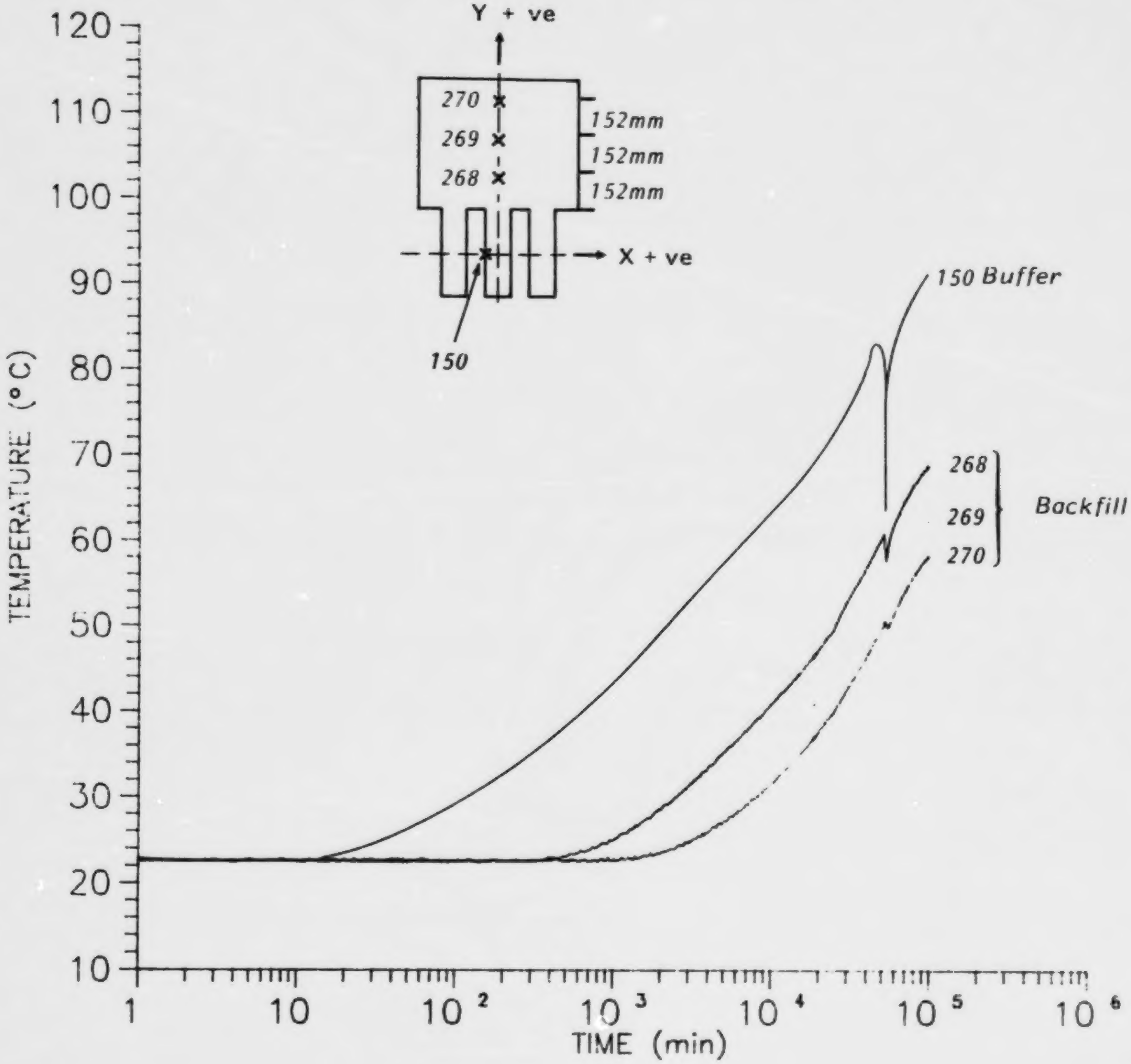

FIGURE 20
BACKFILL TEMPERATURE VS LOG TIME

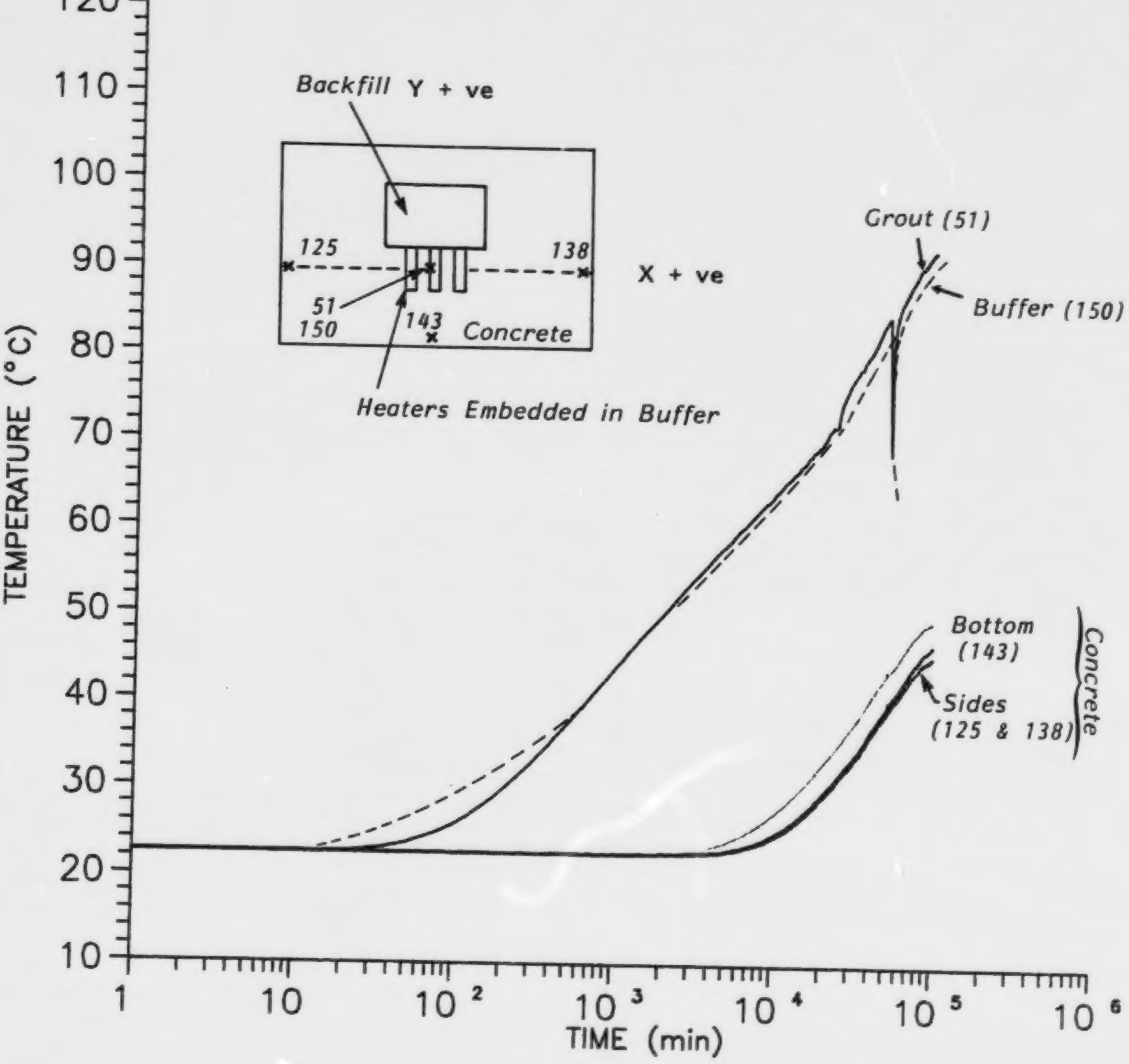

FIGURE 21
BUFFER, BACKFILL AND CONCRETE TEMPERATURE VS LOG TIME

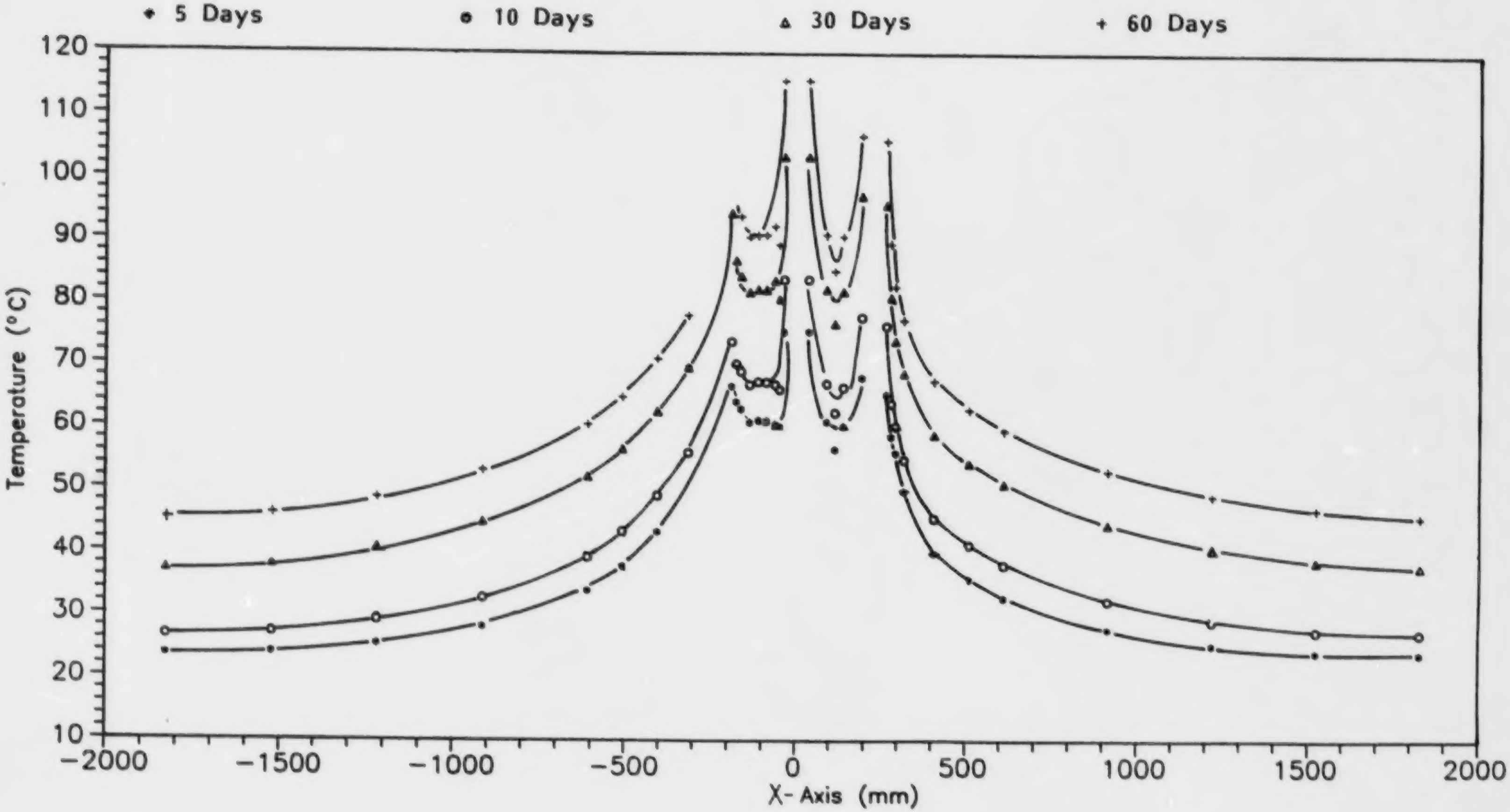

FIGURE 22

TEMPERATURE PROFILE ALONG X-AXIS OF THE BLOCK

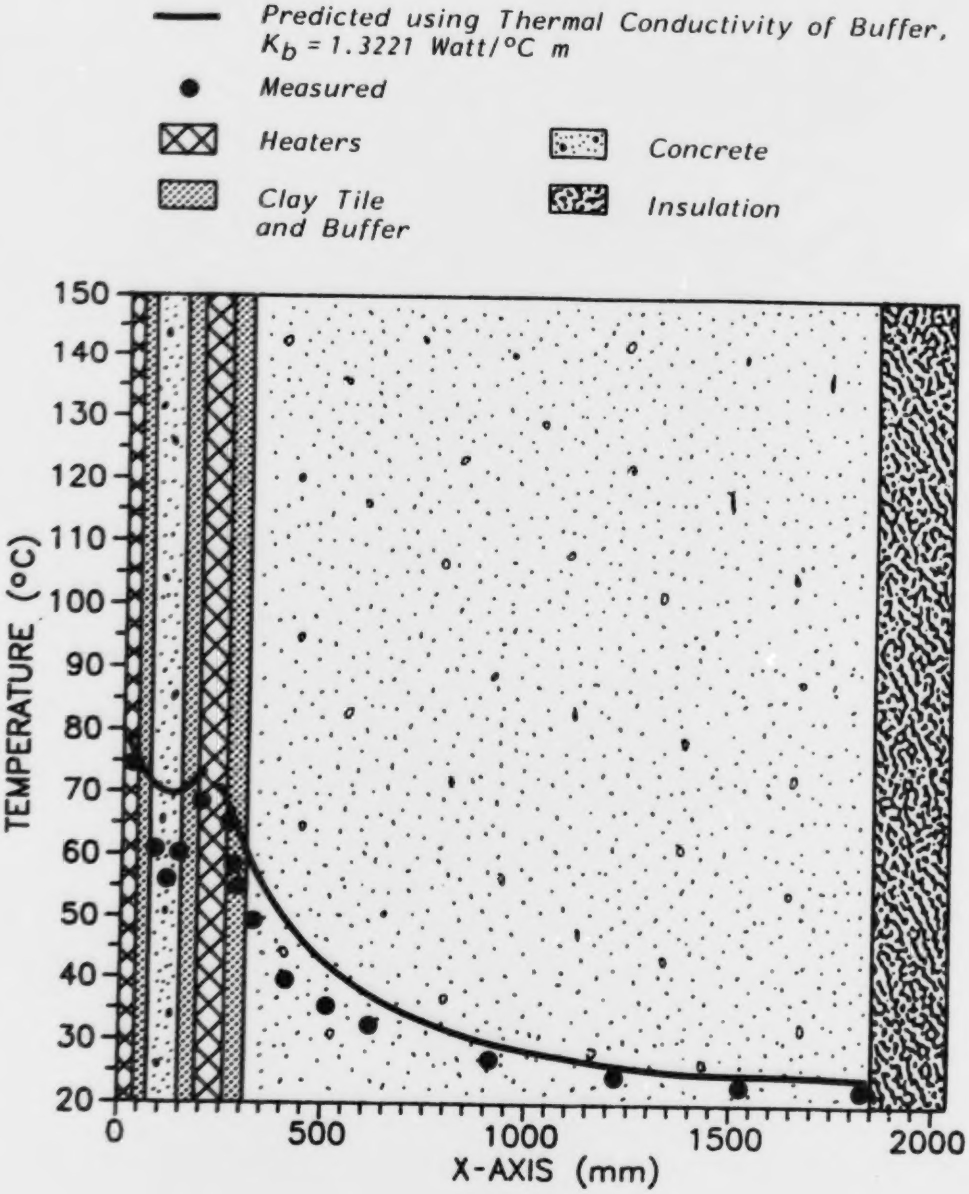

FIGURE 23

TEMPERATURE DISTRIBUTION ALONG THE X-AXIS OF MODEL AT 5 DAYS

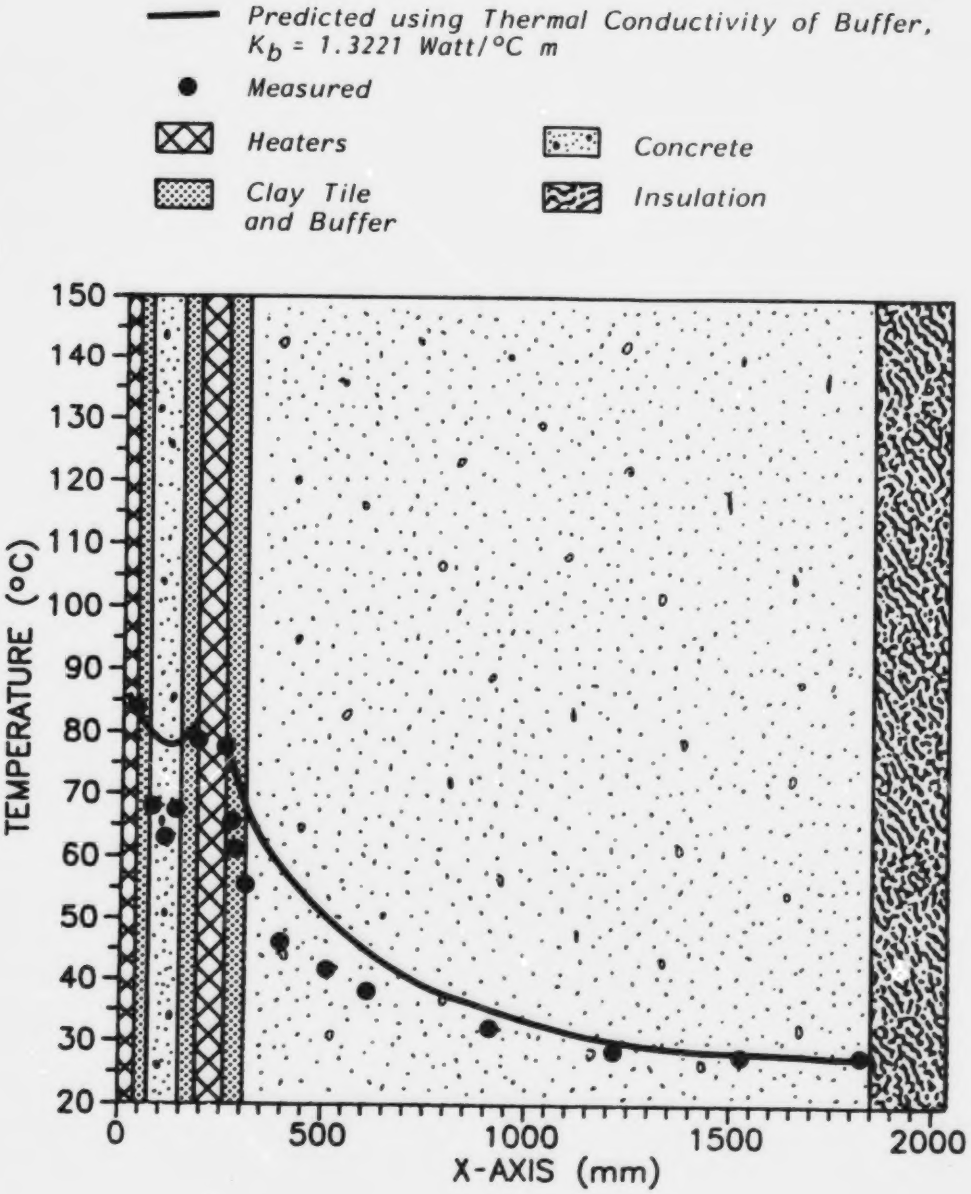

FIGURE 24

TEMPERATURE DISTRIBUTION ALONG THE X-AXIS OF MODEL AT 10 DAYS

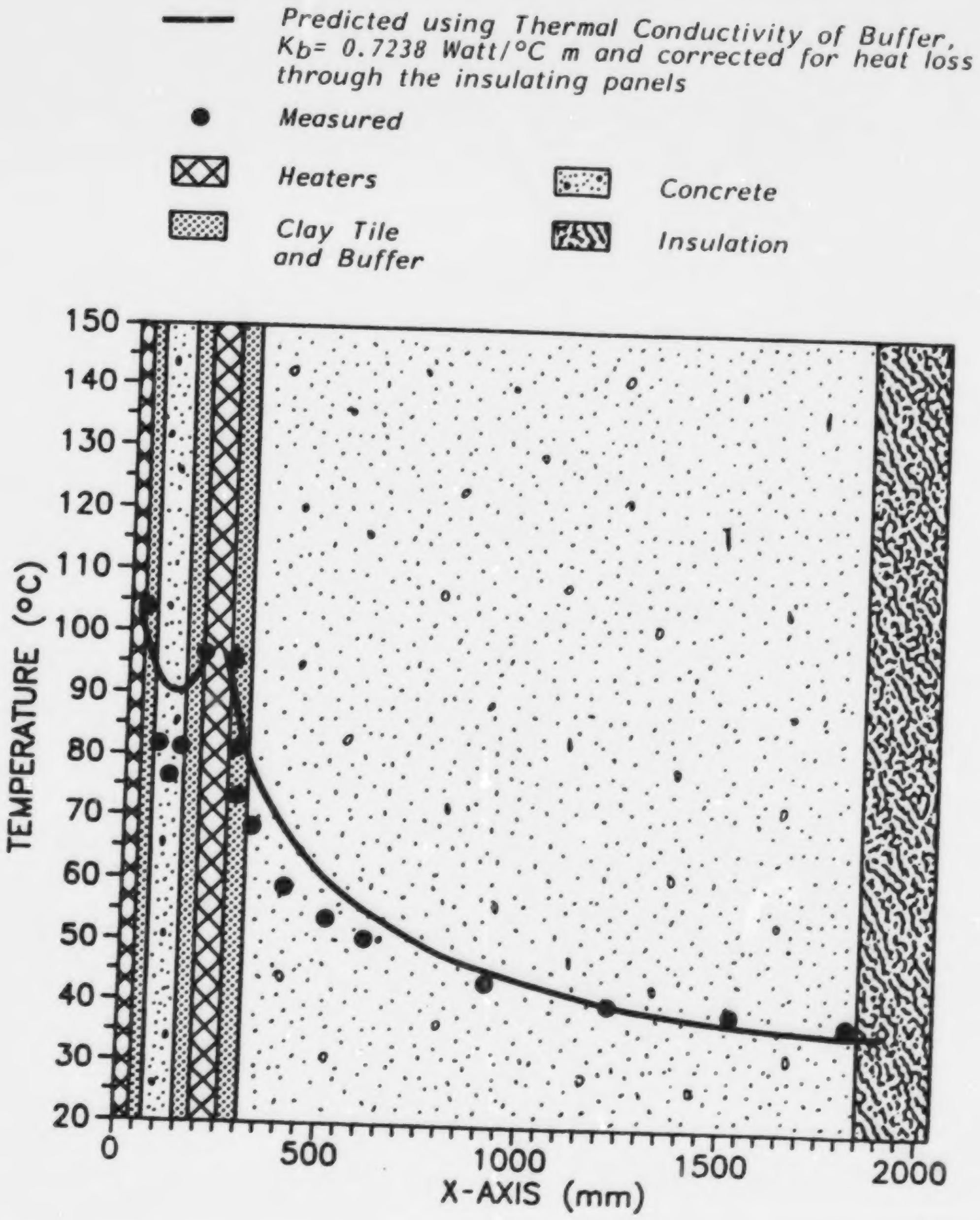

FIGURE 25

TEMPERATURE DISTRIBUTION ALONG THE X-AXIS OF MODEL AT 30 DAYS

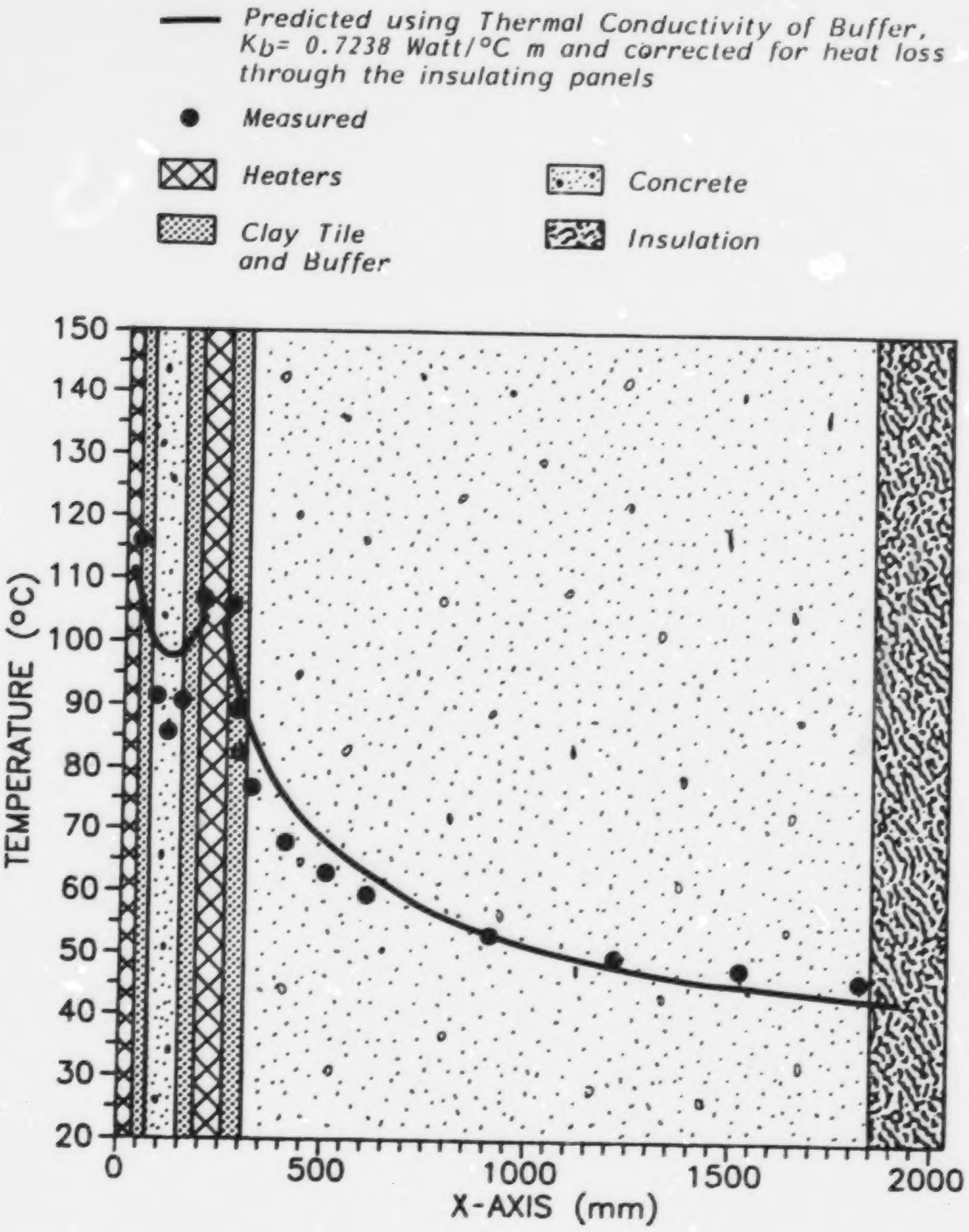

FIGURE 26

TEMPERATURE DISTRIBUTION ALONG THE X-AXIS OF MODEL AT 60 DAYS

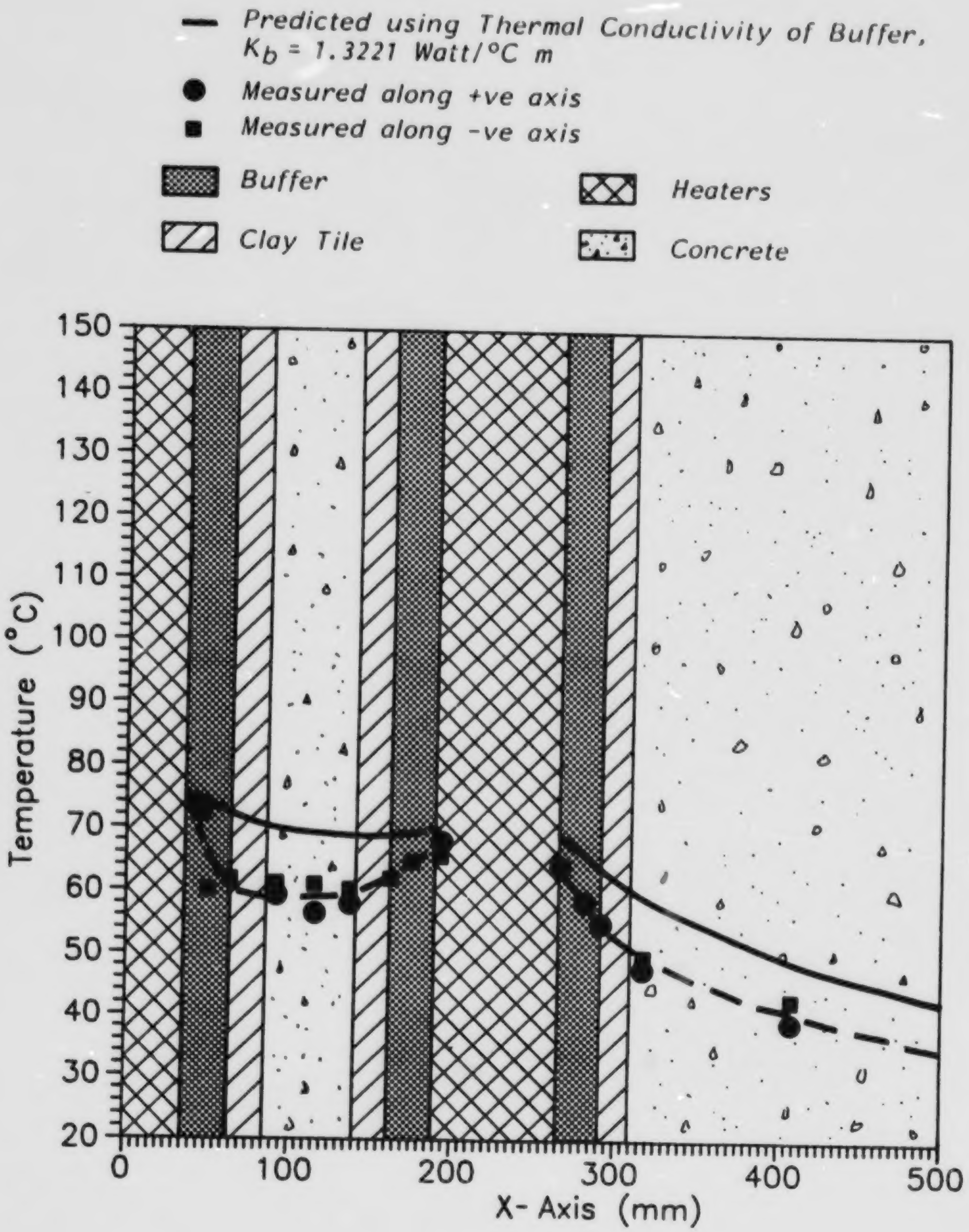

FIGURE 27

NEAR FIELD TEMPERATURE DISTRIBUTION IN BUFFER AND CONCRETE ALONG THE X-AXIS AT 5 DAYS

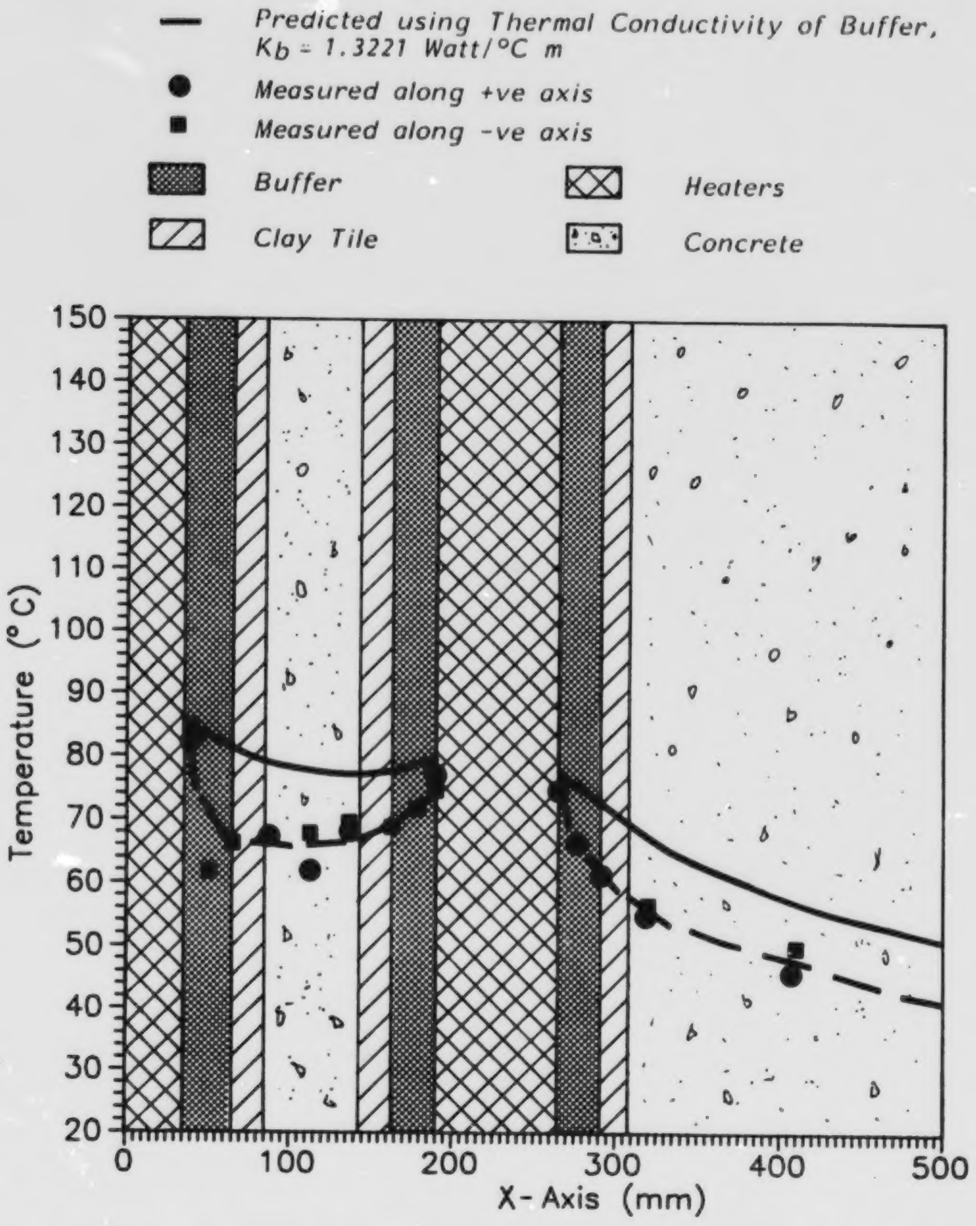

FIGURE 28

NEAR FIELD TEMPERATURE DISTRIBUTION IN BUFFER AND CONCRETE ALONG THE X-AXIS AT 10 DAYS

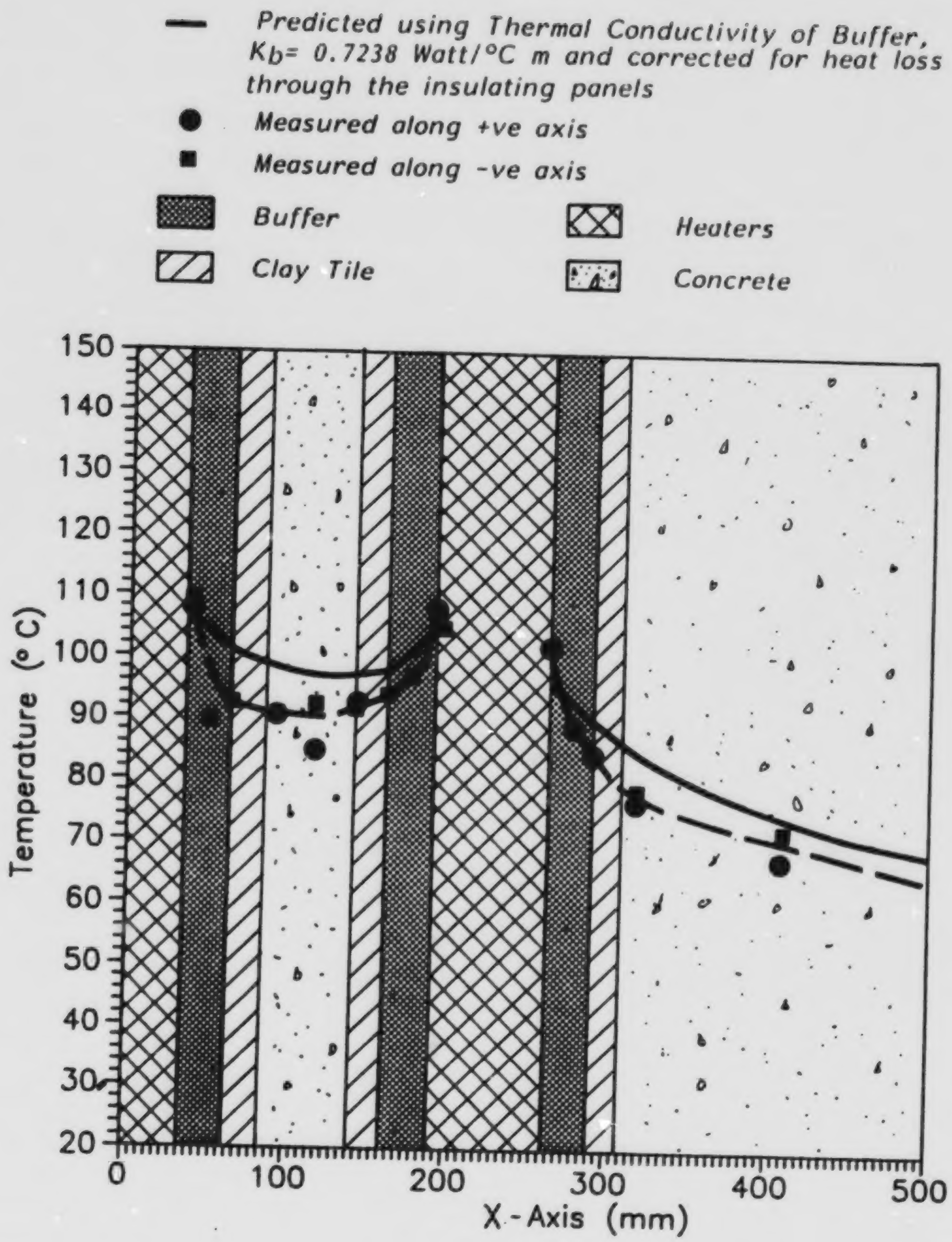

FIGURE 29

NEAR FIELD TEMPERATURE DISTRIBUTION IN BUFFER AND CONCRETE ALONG THE X-AXIS AT 30 DAYS

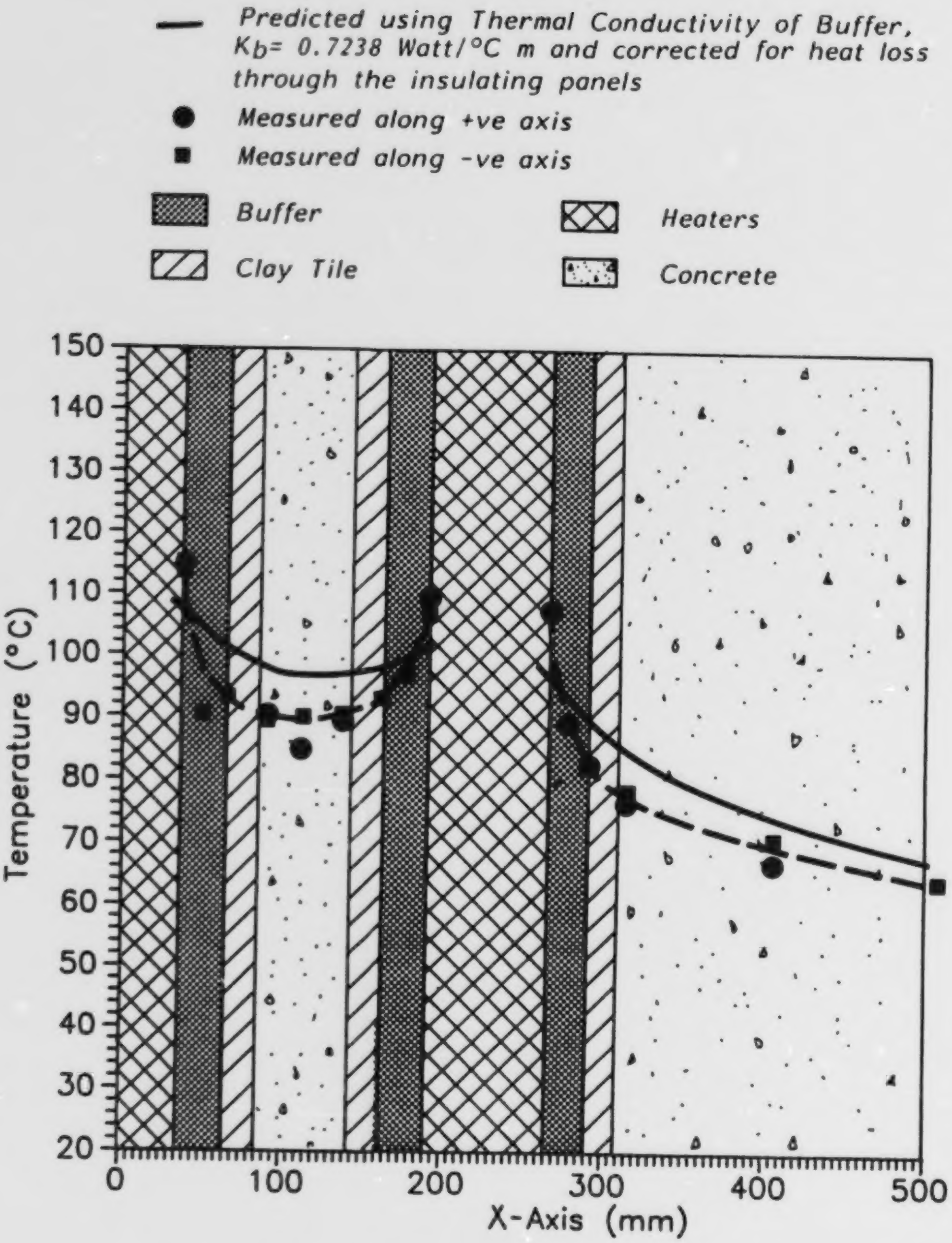

FIGURE 30

NEAR FIELD TEMPERATURE DISTRIBUTION IN BUFFER AND CONCRETE ALONG THE X-AXIS AT 60 DAYS

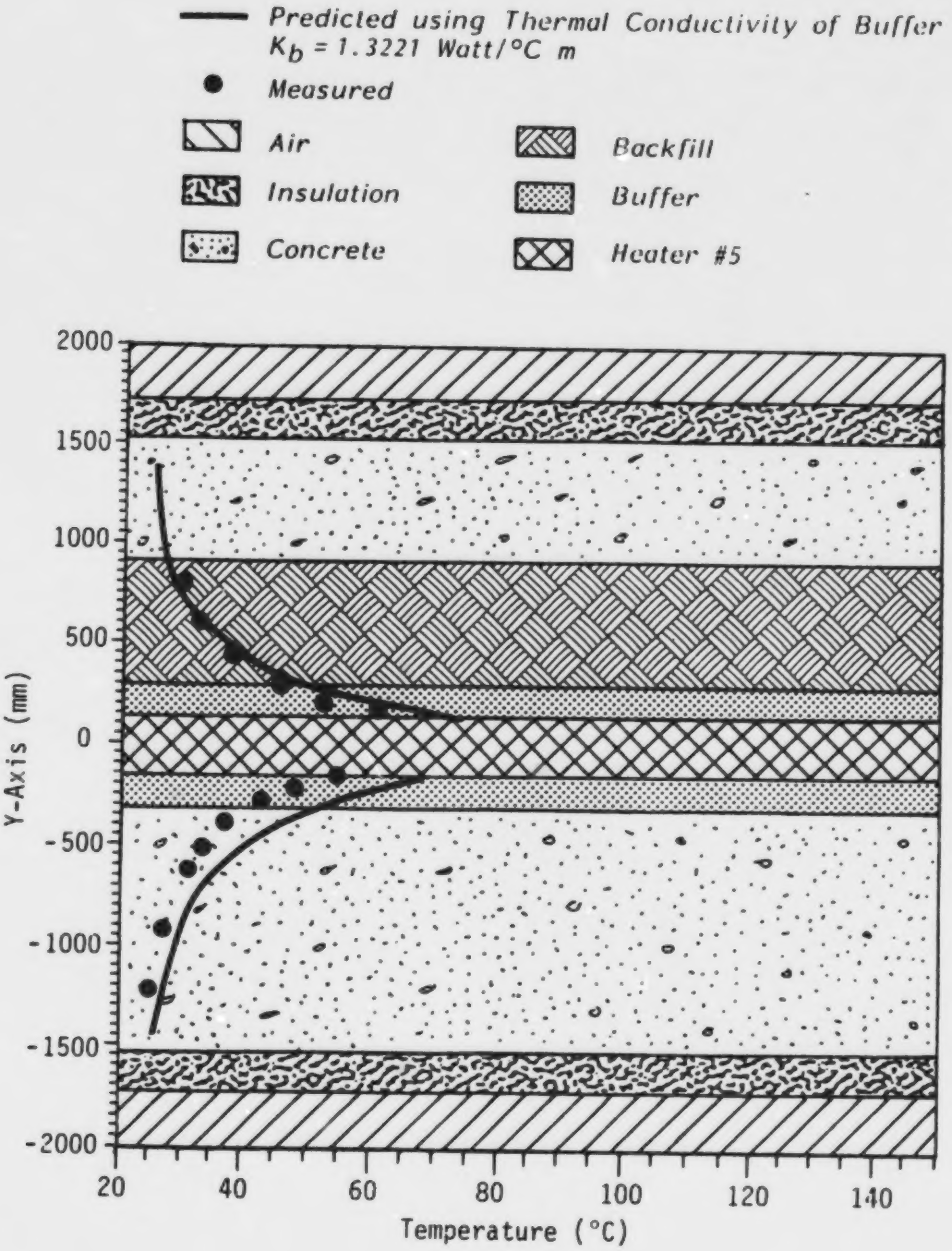

FIGURE 31

TEMPERATURE DISTRIBUTION ALONG THE Y-AXIS OF MODEL AT 5 DAYS

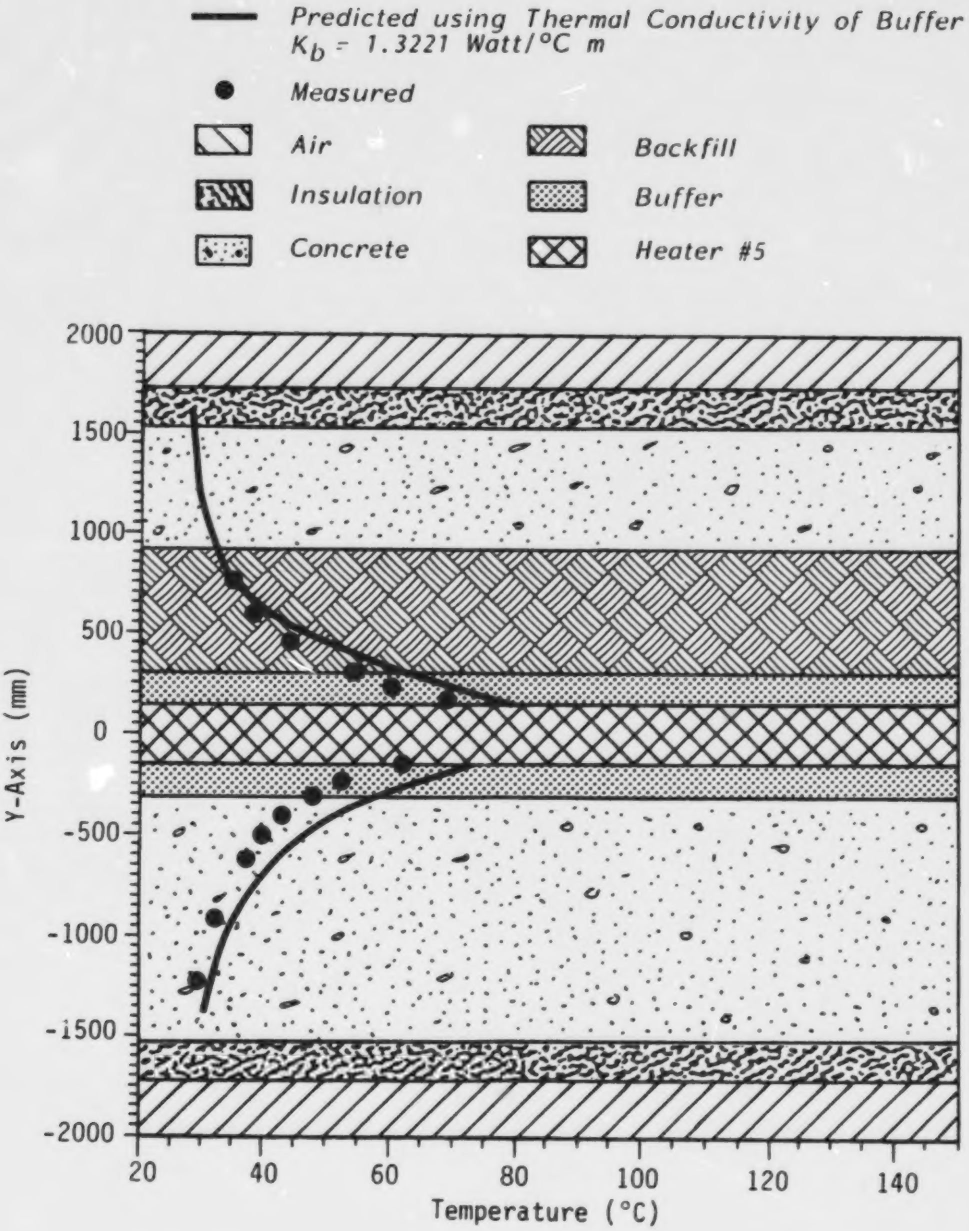

FIGURE 32

TEMPERATURE DISTRIBUTION ALONG THE Y-AXIS OF MODEL AT 10 DAYS

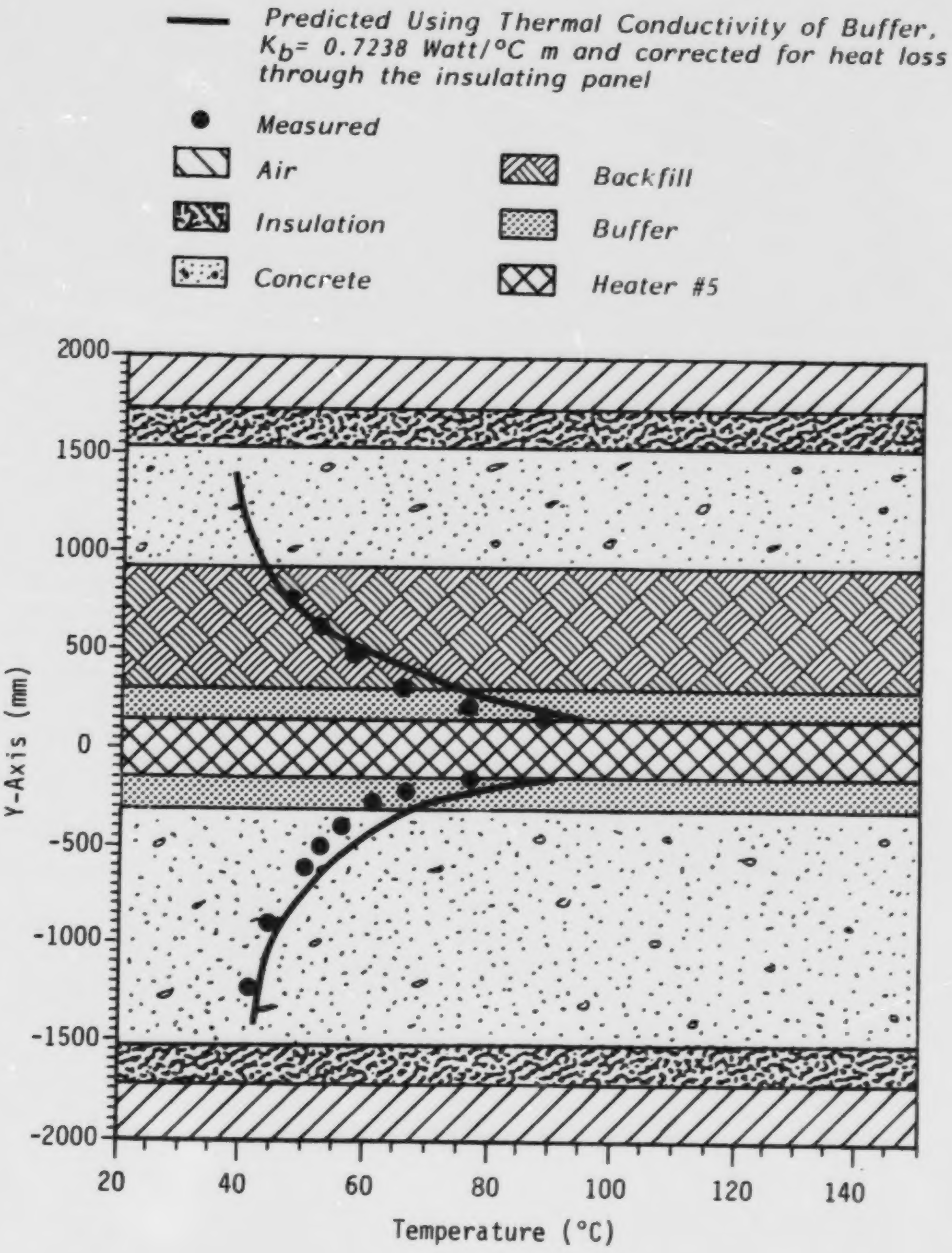

FIGURE 33

TEMPERATURE DISTRIBUTION ALONG THE Y-AXIS OF MODEL AT 30 DAYS

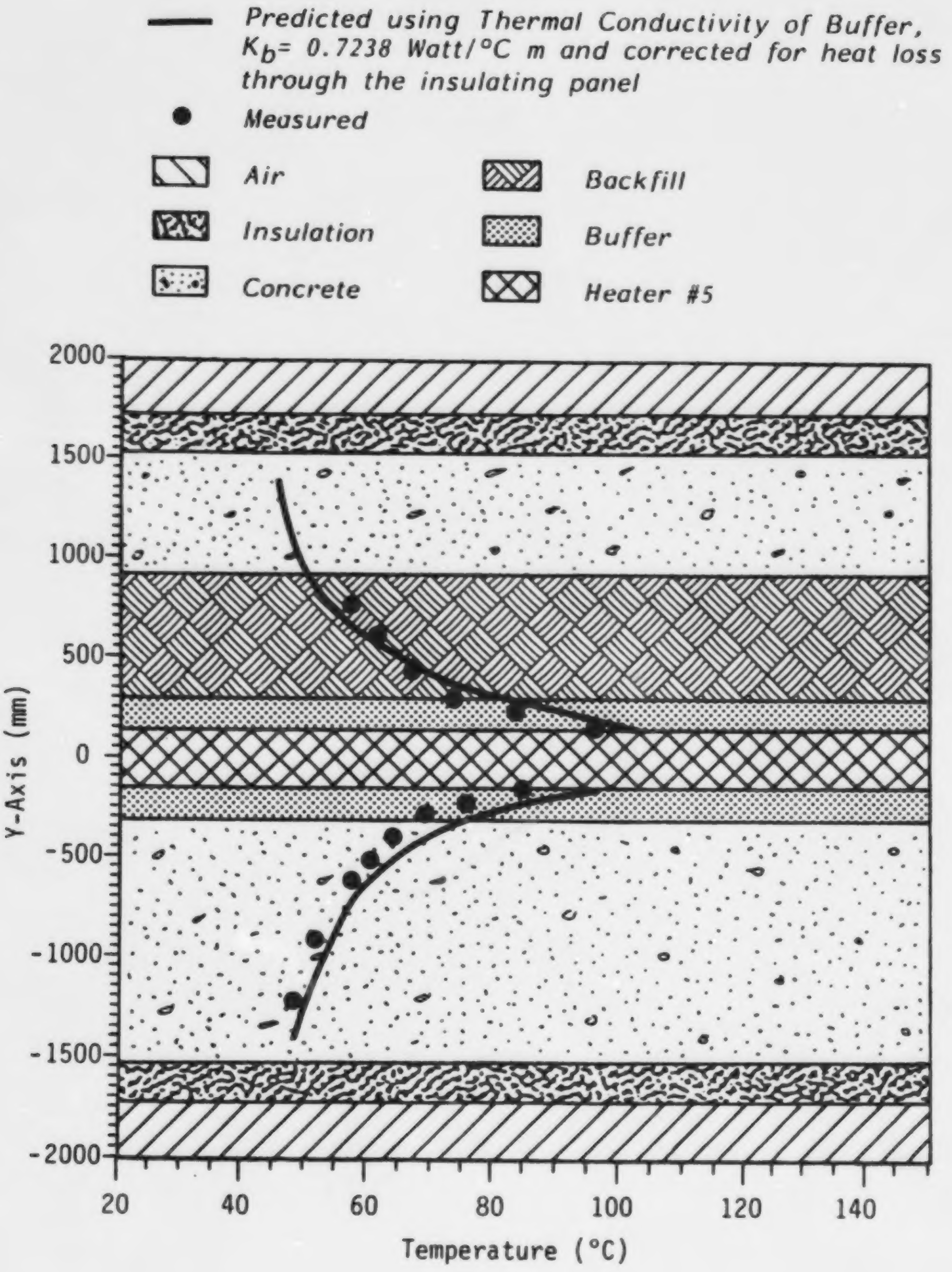

FIGURE 34

TEMPERATURE DISTRIBUTION ALONG THE Y-AXIS OF MODEL AT 60 DAYS

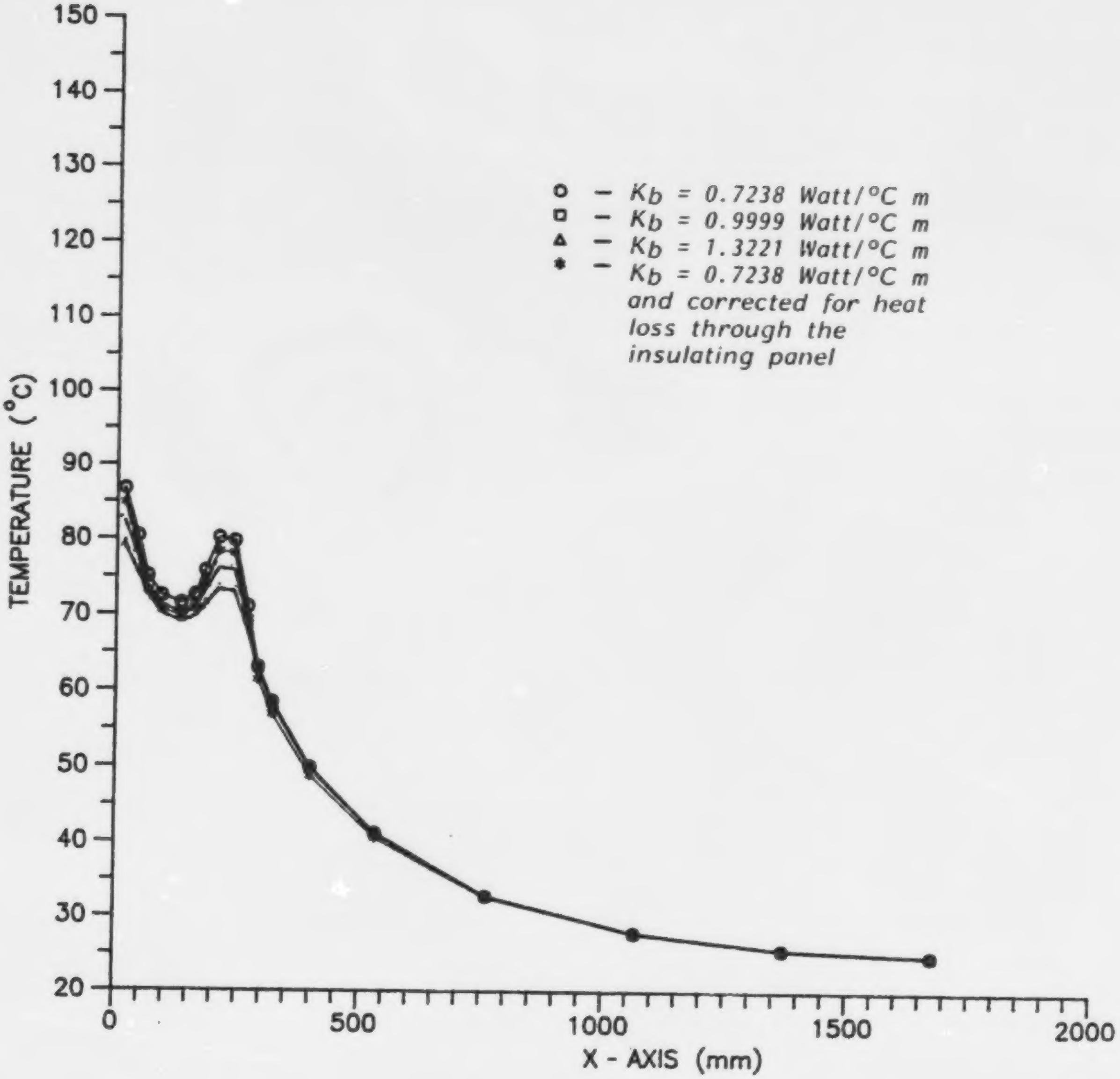

FIGURE 35

PREDICTED TEMPERATURE PROFILES ALONG X-AXIS FOR DIFFERENT THERMAL CONDUCTIVITY VALUES OF BUFFER AND HEAT LOSS ACROSS THE BOUNDARIES AT DAY 5

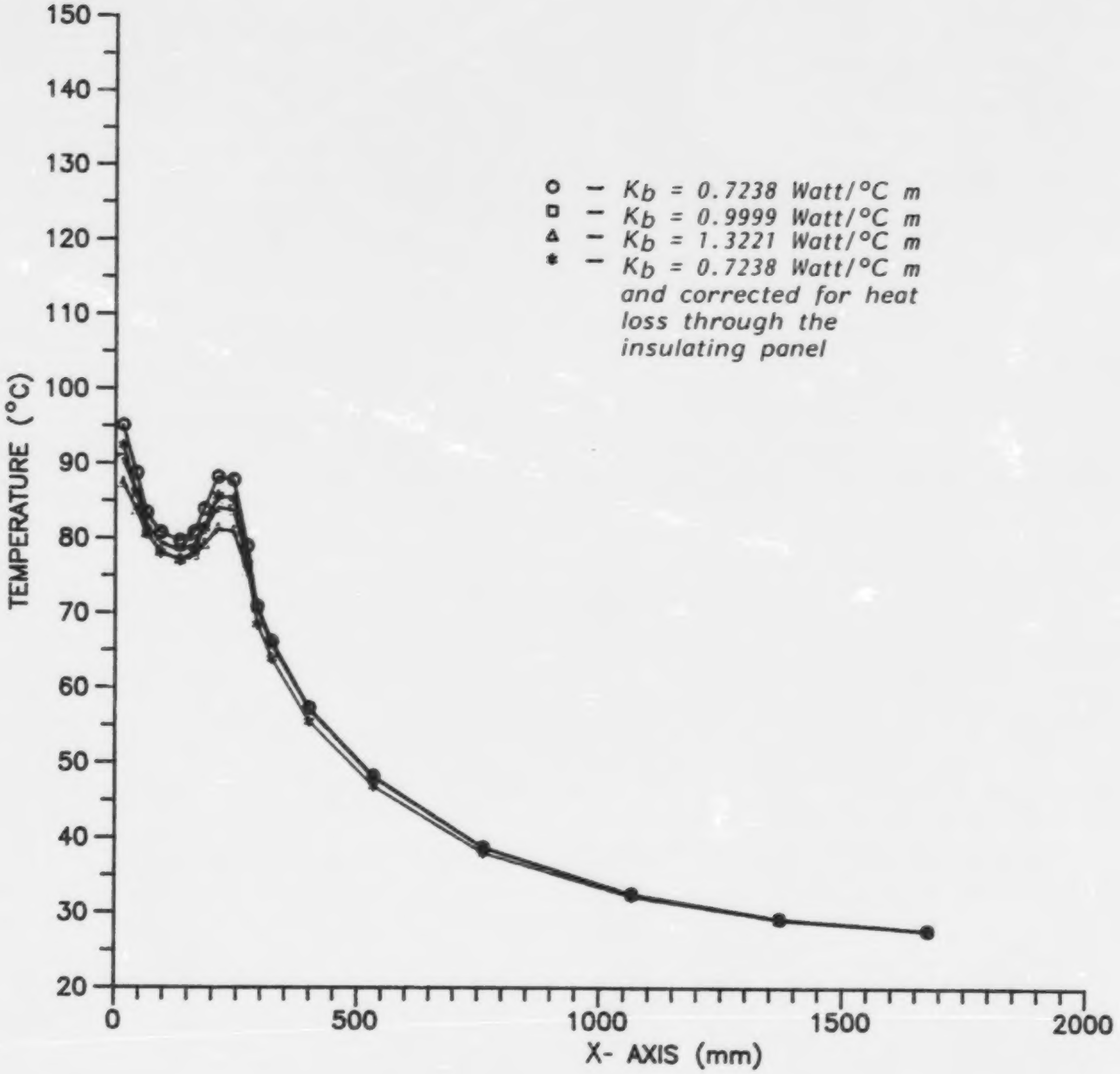

FIGURE 36

PREDICTED TEMPERATURE PROFILES ALONG X-AXIS FOR DIFFERENT THERMAL CONDUCTIVITY VALUES OF BUFFER AND HEAT LOSS ACROSS THE BOUNDARIES AT DAY 10

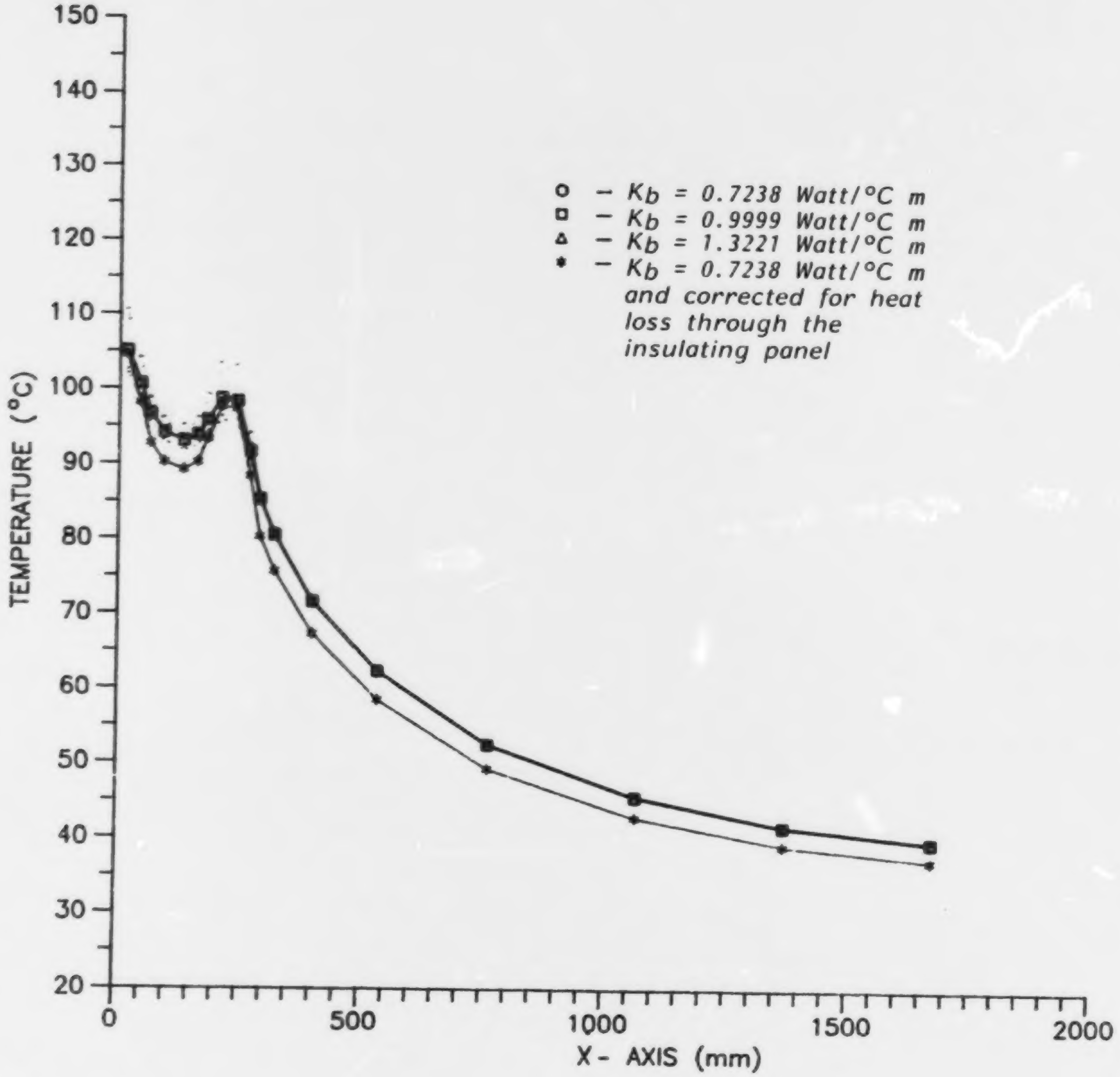

FIGURE 37

PREDICTED TEMPERATURE PROFILES ALONG X-AXIS FOR DIFFERENT THERMAL CONDUCTIVITY VALUES OF BUFFER AND HEAT LOSS ACROSS THE BOUNDARIES AT DAY 30

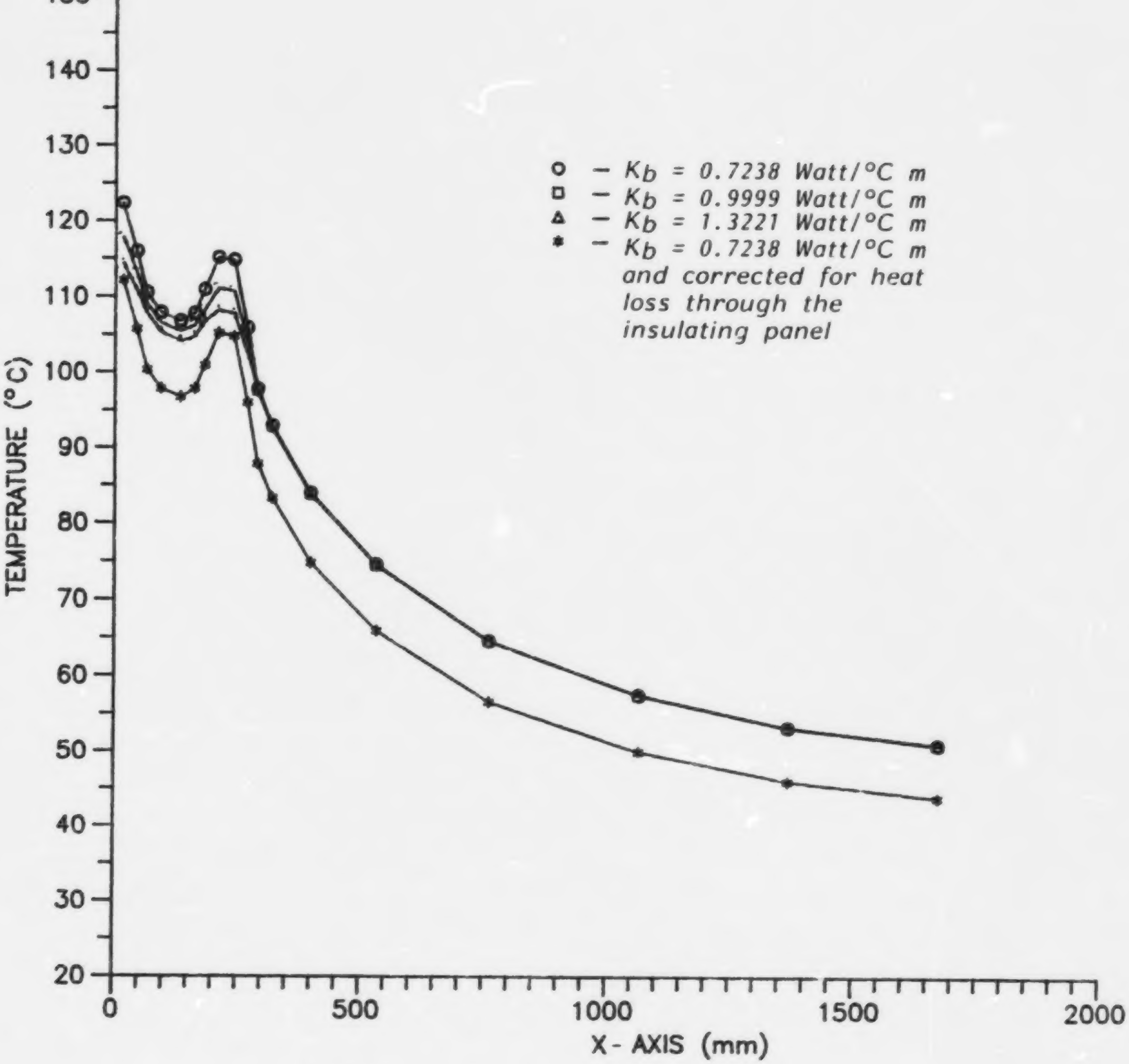

FIGURE 38

PREDICTED TEMPERATURE PROFILES ALONG X-AXIS FOR DIFFERENT THERMAL CONDUCTIVITY VALUES OF BUFFER AND HEAT LOSS ACROSS THE BOUNDARIES AT DAY 60

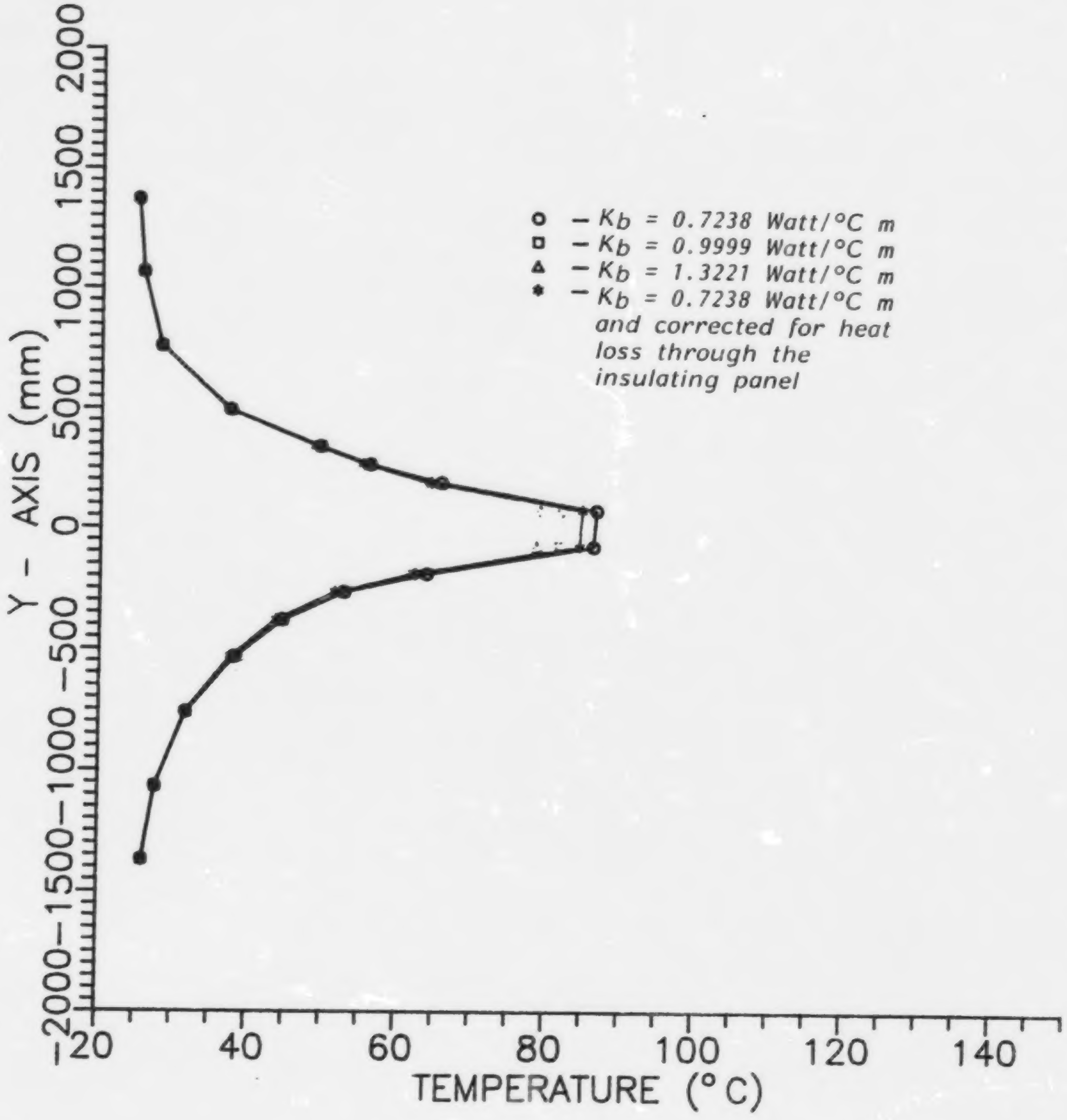

FIGURE 39

PREDICTED TEMPERATURE PROFILES ALONG Y-AXIS FOR DIFFERENT THERMAL CONDUCTIVITY VALUES OF BUFFER AND HEAT LOSS ACROSS THE BOUNDARIES AT DAY 5

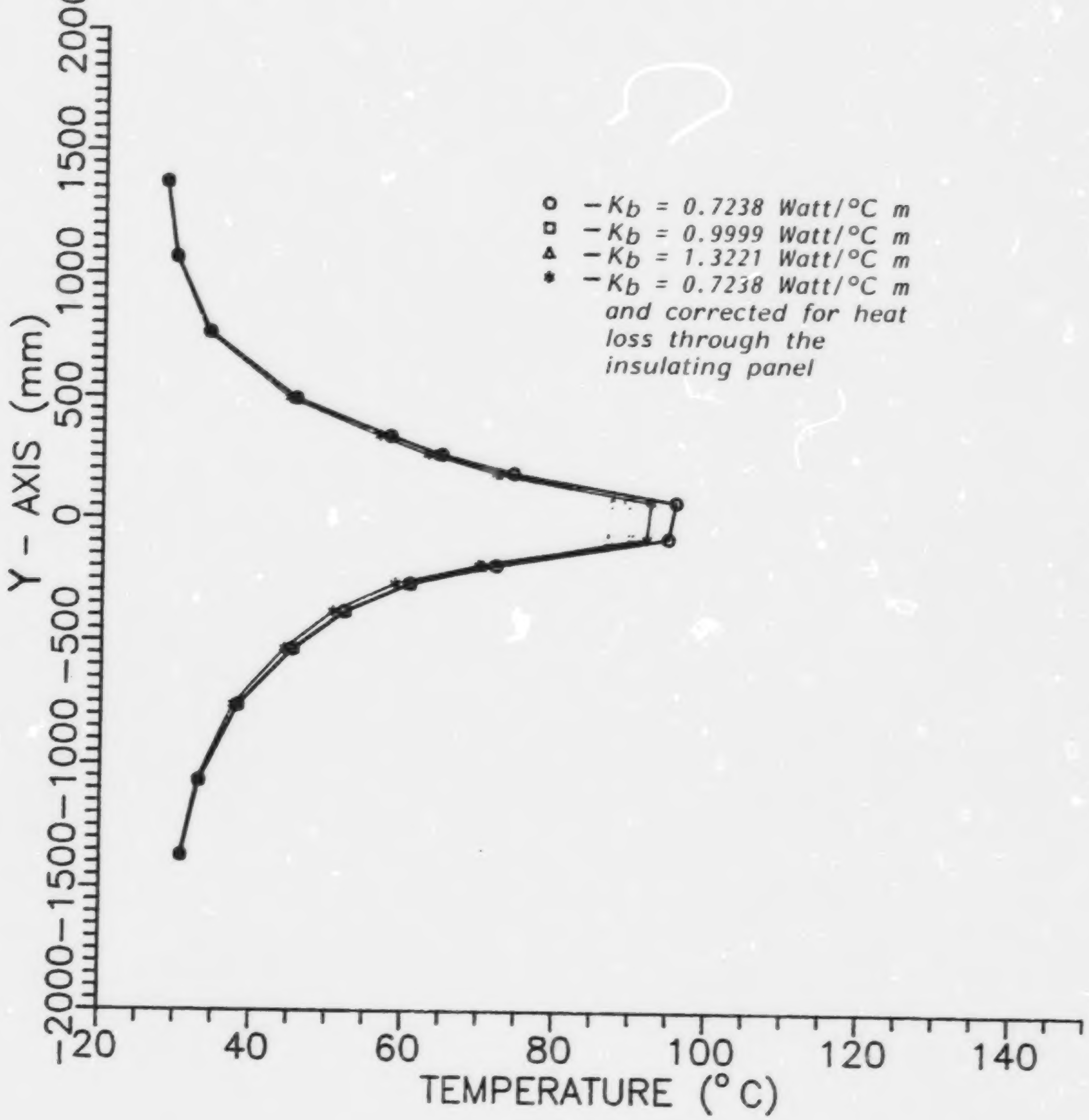

FIGURE 40

PREDICTED TEMPERATURE PROFILES ALONG Y-AXIS FOR DIFFERENT THERMAL CONDUCTIVITY VALUES OF BUFFER AND HEAT LOSS ACROSS THE BOUNDARIES AT DAY 10

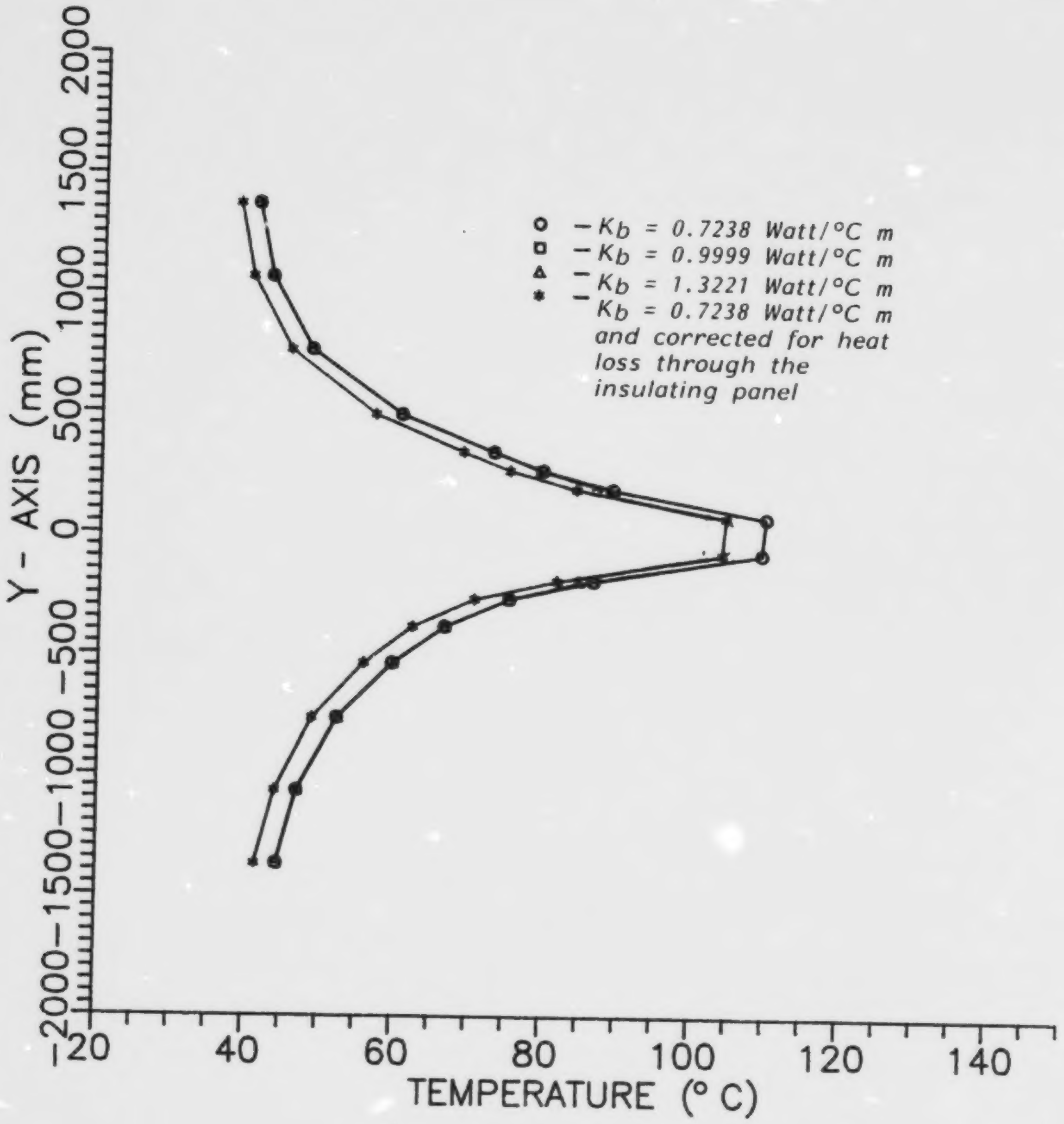

FIGURE 41

PREDICTED TEMPERATURE PROFILES ALONG Y-AXIS FOR DIFFERENT THERMAL CONDUCTIVITY VALUES OF BUFFER AND HEAT LOSS ACROSS THE BOUNDARIES AT DAY 30

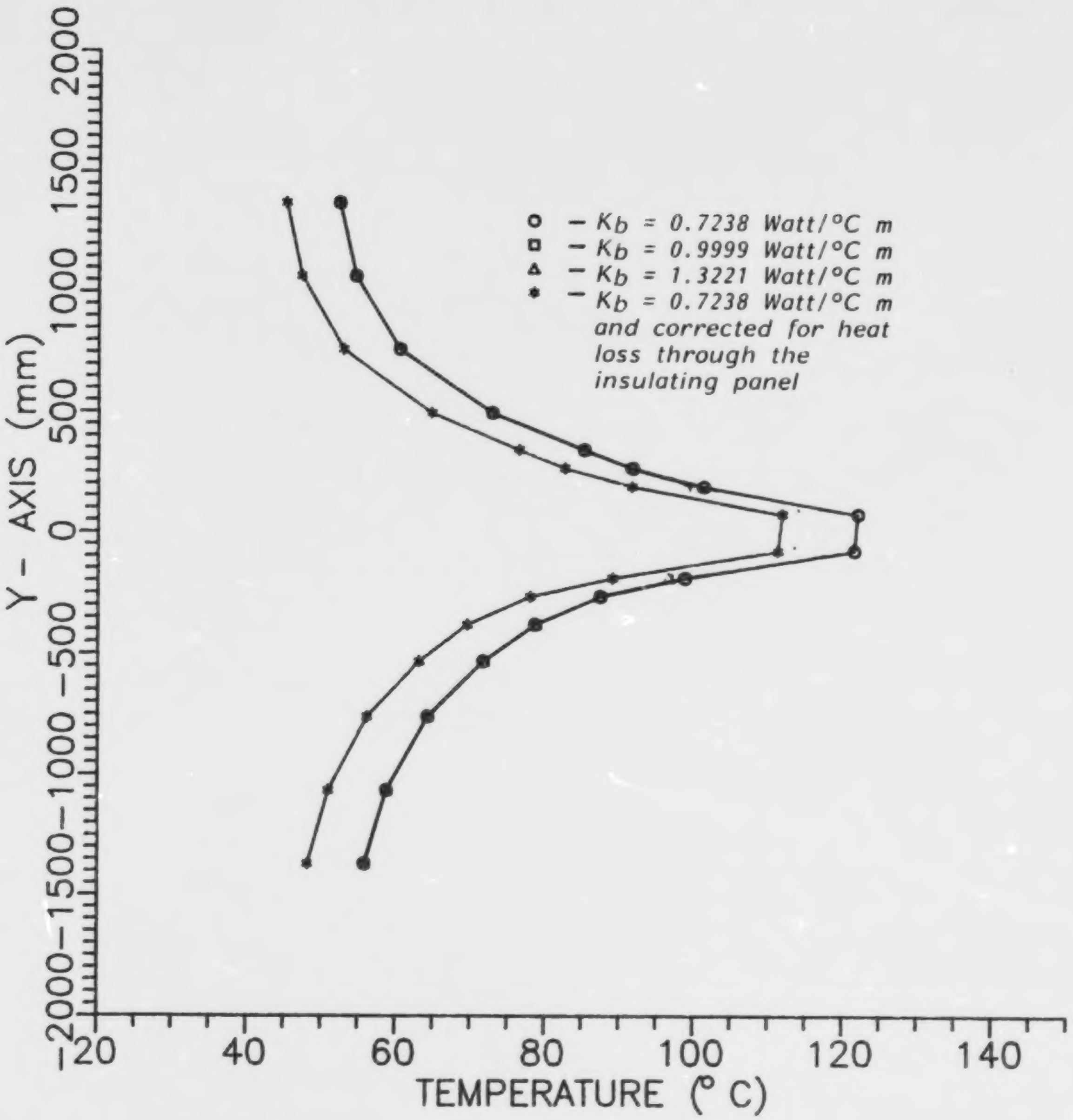

FIGURE 42

PREDICTED TEMPERATURE PROFILES ALONG Y-AXIS FOR DIFFERENT THERMAL CONDUCTIVITY VALUES OF BUFFER AND HEAT LOSS ACROSS THE BOUNDARIES AT DAY 60

APPENDIX A

Factors Influence the Thermal Conductivity of Clay-Based Buffers - Results from Phase I Study

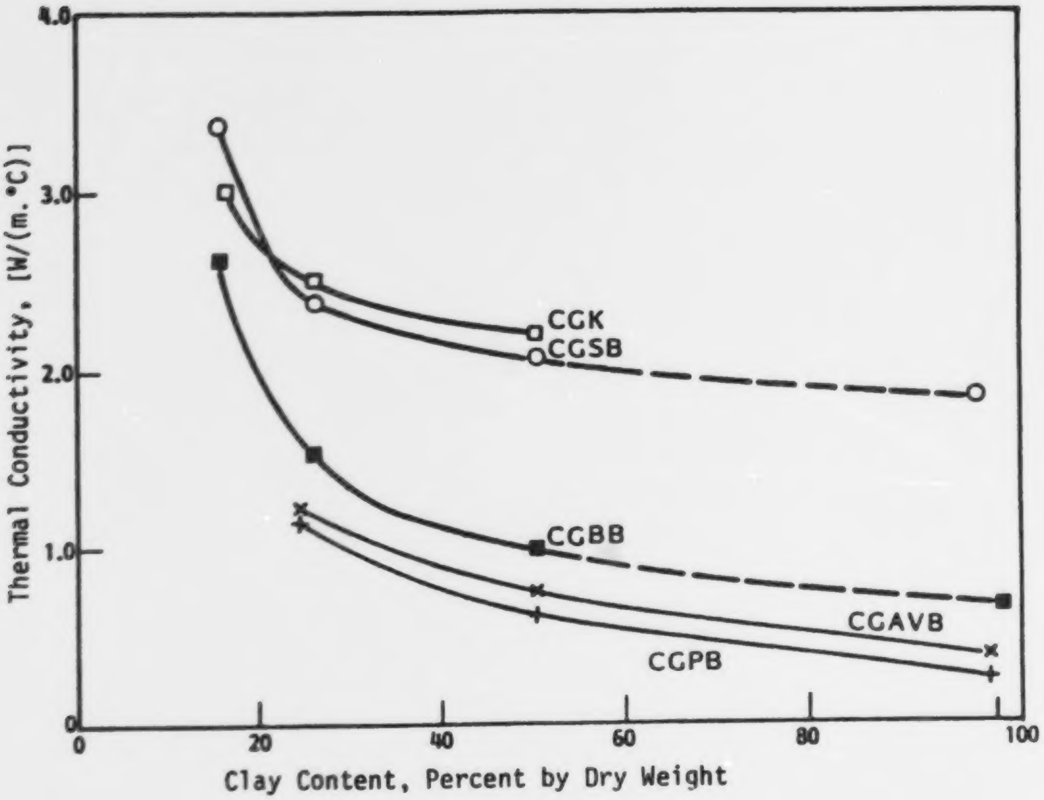

FIGURE 1A

THERMAL CONDUCTIVITY AS A FUNCTION OF CLAY CONTENT IN CRUSHED GRANITE AND CLAY MIXES

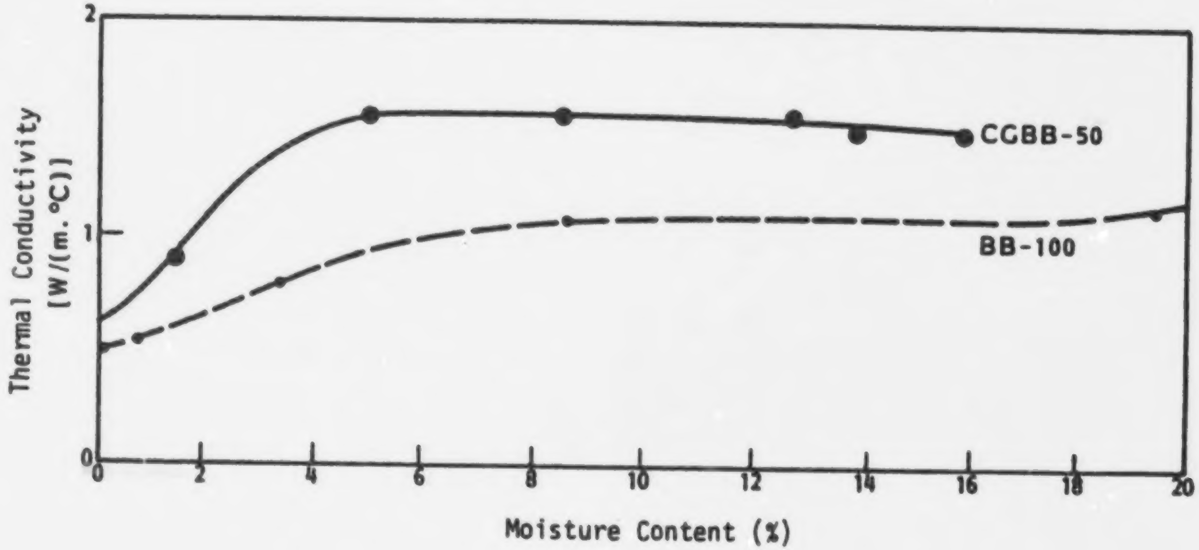

FIGURE 2A

THERMAL CONDUCTIVITY VS MOISTURE CONTENT RELATIONSHIP AT CONSTANT DENSITY FOR CRUSHED GRANITE AND BENTONITE BUFFER

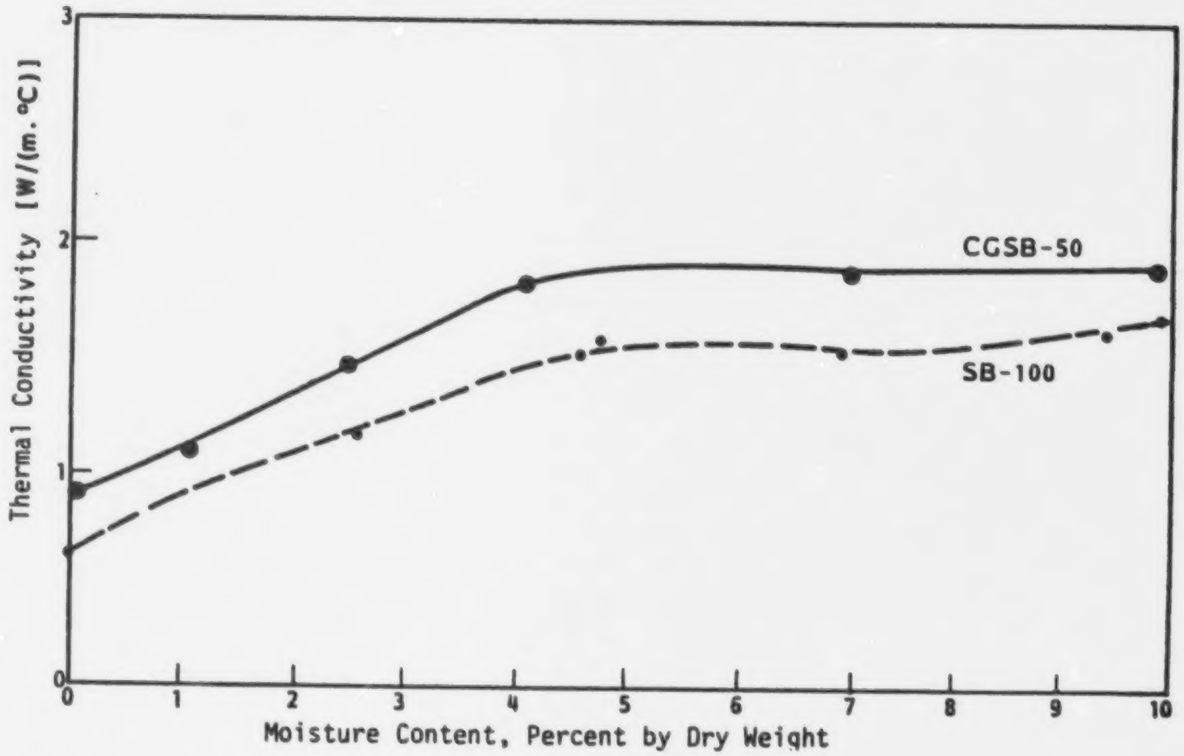

FIGURE 3A

THERMAL CONDUCTIVITY VS MOISTURE CONTENT RELATIONSHIP AT CONSTANT DENSITY FOR CRUSHED GRANITE AND SEALBOND BUFFER

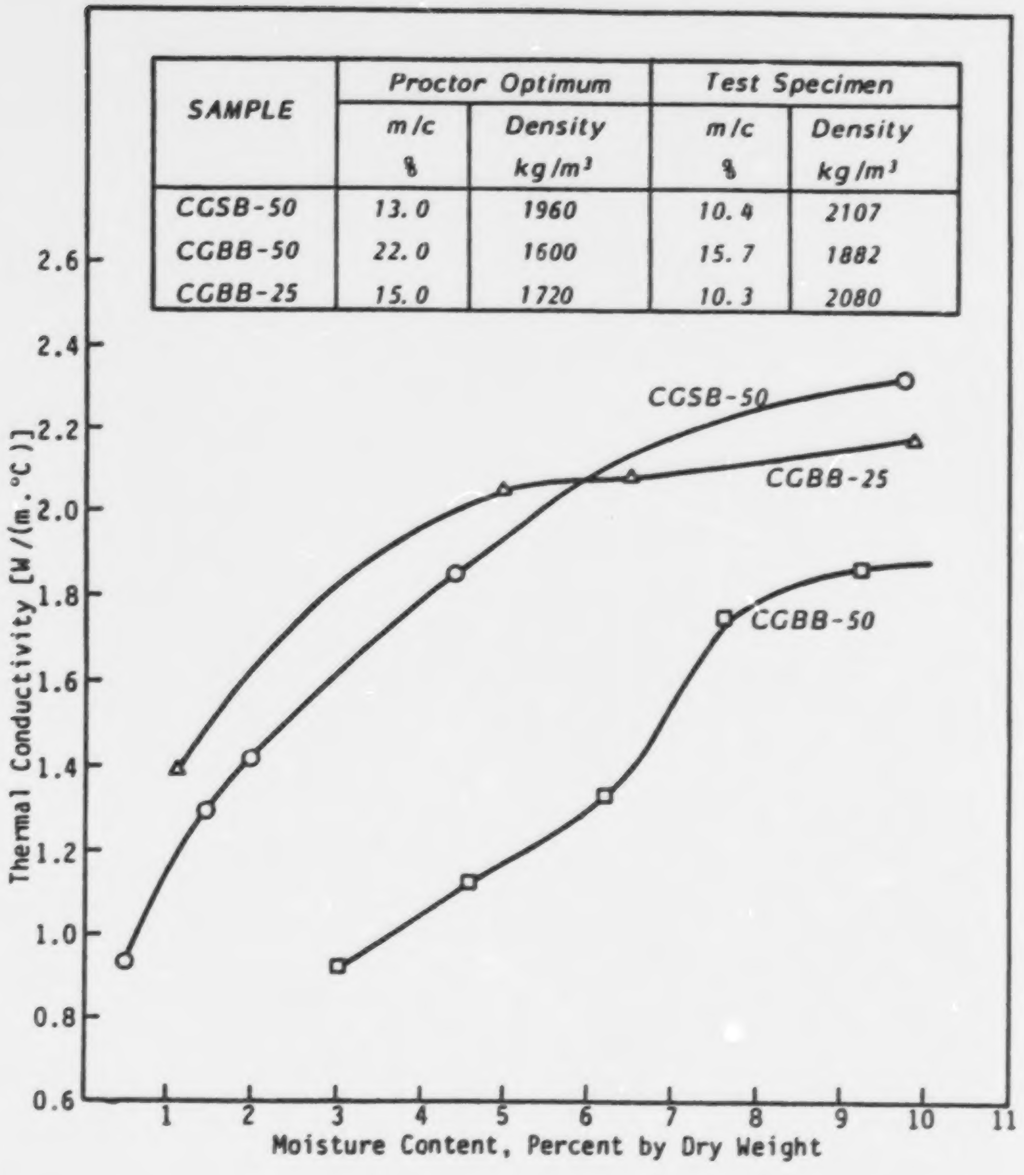

SAMPLE	Proctor Optimum		Test Specimen	
	m/c %	Density kg/m³	m/c %	Density kg/m³
CGSB-50	13.0	1960	10.4	2107
CGBB-50	22.0	1600	15.7	1882
CGBB-25	15.0	1720	10.3	2080

FIGURE 4A

THERMAL CONDUCTIVITY VS MOISTURE CONTENT OF STATICALLY COMPACTED CRUSHED GRANITE AND CLAY MIXTURES

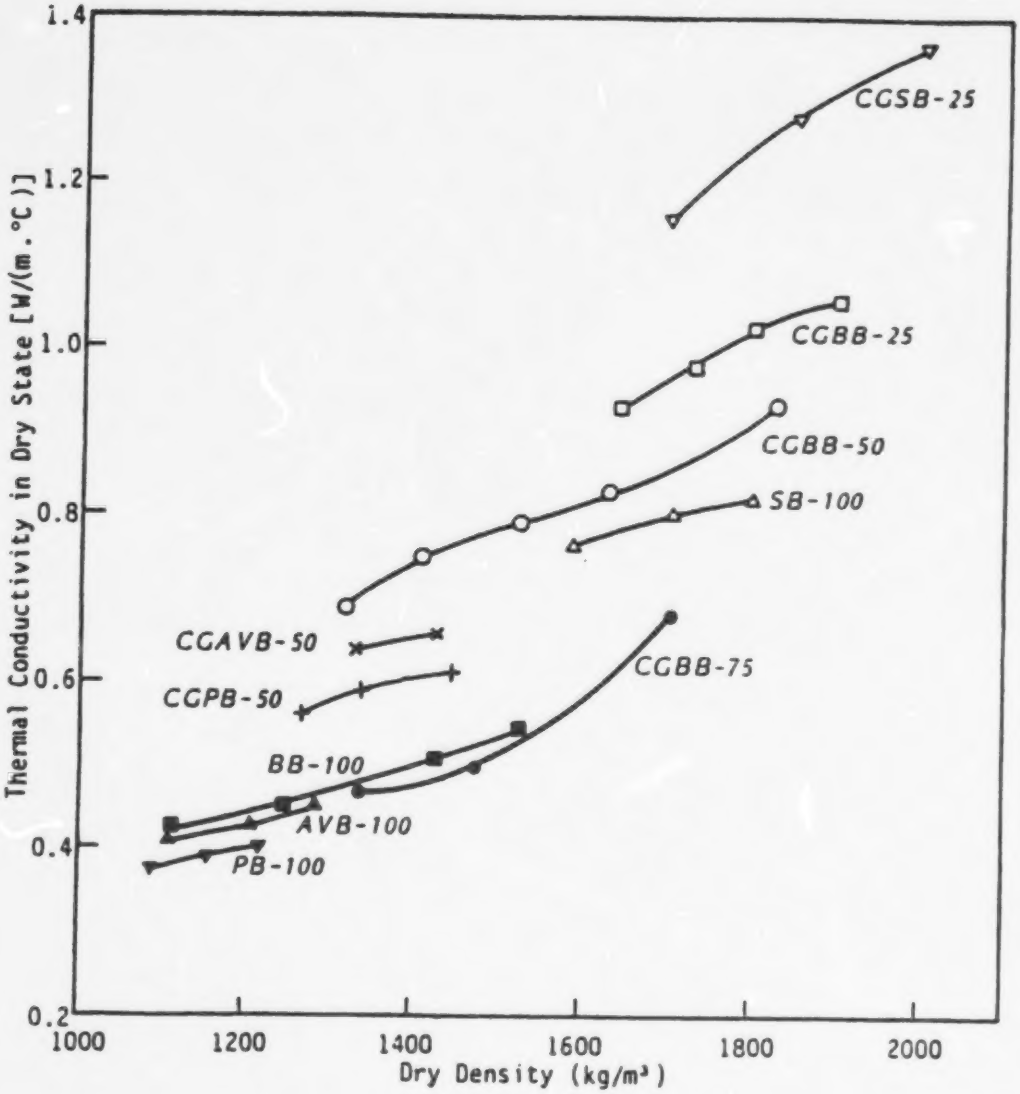

FIGURE 5A

DRY THERMAL CONDUCTIVITY VS DRY DENSITY RELATIONSHIP FOR CRUSHED GRANITE AND CLAY MIXES

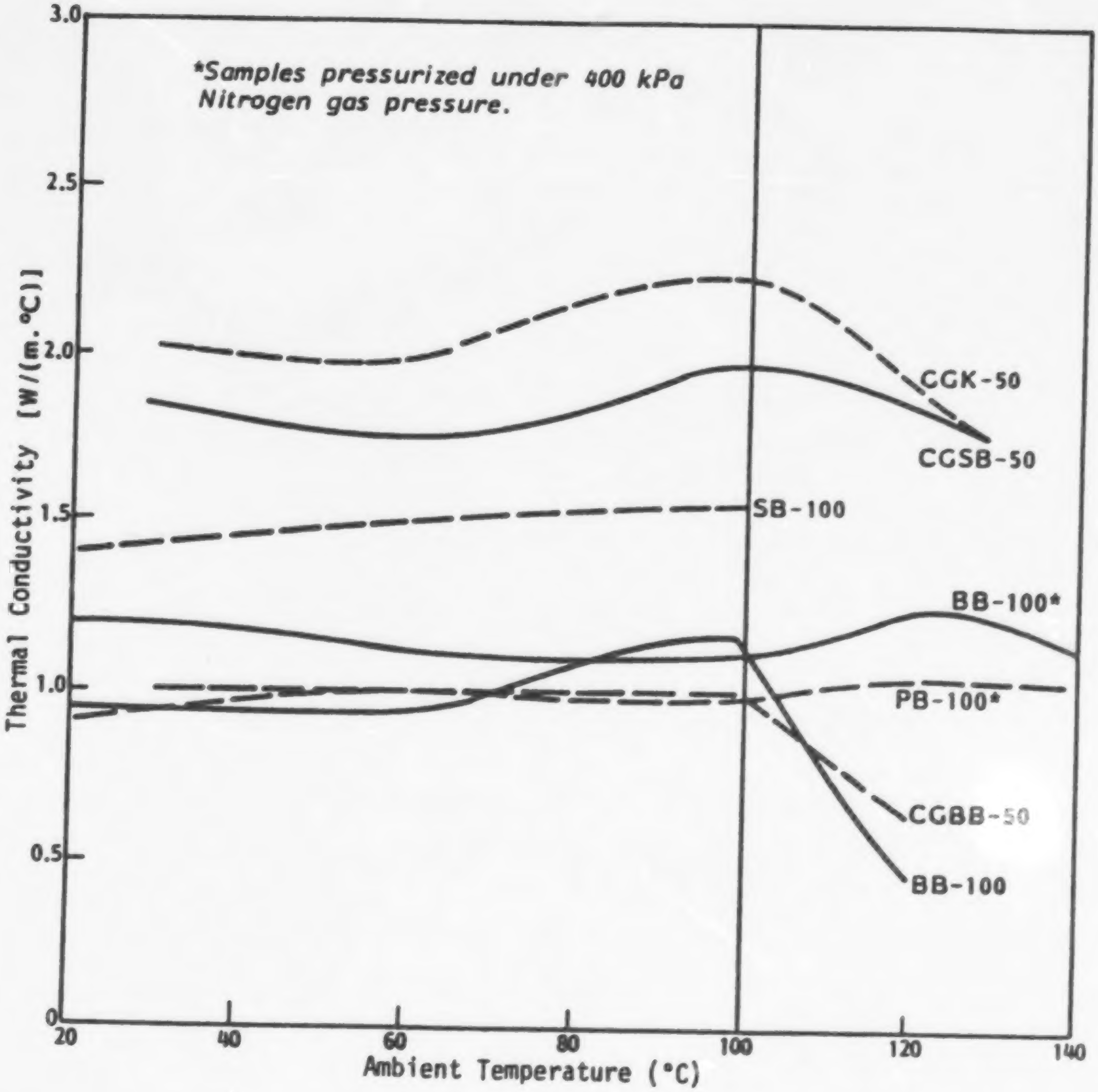

FIGURE 6A
THERMAL CONDUCTIVITY AS A FUNCTION OF AMBIENT TEMPERATURE

APPENDIX B

The Heater

GEOTHERM INC.
CONSULTANTS & INSTRUMENTATION SPECIALISTS IN GEOTECHNICAL
AND GEOTHERMAL ENGINEERING & TESTING

ONTARIO HYDRO RESEARCH DIVISION

CIVIL RESEARCH DEPARTMENT

HEATER CALIBRATIONS
FOR
BUFFER MASS STUDY

188 DEERFIELD RD., NEWMARKET, ONT. CANADA L3Y 2L9 – TELEPHONE (416) 898-7555

GEOTHERM INC.

CONSULTANTS & INSTRUMENTATION SPECIALISTS IN GEOTECHNICAL
AND GEOTHERMAL ENGINEERING & TESTING

January 31, 1986

Ontario Hydro
Civil Research Department
800 Kipling Avenue
Toronto, Ontario
M8Z 5S4

ATTENTION: Dr. H.S. Radhakrishna P. Eng;

Dear Sir;

RE: Calibration of heaters for buffer mass study;

Please find enclosed herewith a brief report on the calibration of heaters supplied to you for the aforementioned research study.

A total number of 10 (ten) heaters were designed and manufactured by us in accordance with the specification given by you. The report contains the physical dimensions of various components, fabrication techniques, thermal parameters of components and details on locations of temperature sensors. Test results for the thermal parameters of the filler epoxy are also appended.

We hope you find this report to be satisfactory. Should you require any further details or clarification, please contact us. Thanking you for the opportunity of being of service to you.

Yours truly,

GEOTHERM INC:

Deepak Parmar,
President

Encl;

DP:kb

188 DEERFIELD RD., NEWMARKET, ONT. CANADA L3Y 2L9 – TELEPHONE (416) 898-7555

GEOTHERM INC.
CONSULTANTS & INSTRUMENTATION SPECIALISTS IN GEOTECHNICAL
AND GEOTHERMAL ENGINEERING & TESTING

HEATERS FOR BUFFER STUDY

This report contains the full specifications and calibrations for the heaters to be used by the Civil Research Departmant of Ontario Hydro for the radio active waste disposed studies. Full fabrication details are given with the understanding that this may be of importance for theoratical analysis of the heat transfer mechanism.

Components;

The heaters consist of seven basic components namely;

1) Outer shell
2) Temperature sensors
3) Ceramic thermal epoxy
4) Electrical insulating media
5) Heater winding
6) Inner core
7) Sealed volume of air

Outer Shell:

Appendix "A" contains all the details on the dimensions and weights of various components. The material for the shell is stainless steel #304 pipe of wall thickness of 2.8mm and outer diameter 73.2mm. The average overall length of each heater shell is 303.5mm. Appropriate length of the pipe was cut and faced both ends. On one end, a stainless steel plate of similar material was silver soldered and machined to the exact outside diameter. For the top end (end cap) a similar plate was machined to close tollerance to the inner diameter. For all practical purposes, the very small amount of silver solder used is regarded as stainless steel. A small hole was drilled through the end cap to allow vapour to escape during heat curing of thermal epoxy. Four holes of 1.5mm diameter were drilled through the wall of the outer shell to faciliate thermo-couple junctions to measure temperatures at the soil-heater interface. The locations of these holes are detailed in Appendix "C".

Inner Core;

Appendix "B" contains all the details on dimensions and weight. The inner core is fabricated from a stainless steel pipe of 48.4 mm outer diameter and 2.54 mm wall thickness. Two end caps 2.54 mm thickness were silver soldered on the pipe and machined to exact outside diameter. The purpose of the inner core was to form the base for two parallel heater windings and also to reduce the overall heat capacity of the heaters by creating a large volume of sealed air. It also allows the heater windings to be close to the our shell and reduces the volume of the annular space to be filled by thermal epoxy.

Temperature Sensors;

These were type "T" copper constantan thermocouples double insulated fused capton of 250°C rating. For the mechanical durability, 24 gauge wires were chosen. Each heater contains six thermocouples. Two of these are mounted on the heater windings and the remaining four are brought out through the wall of the outer shell. The purpose of this configuration was to determine the thermal gradient between the heater winding and the soil / heater interface. The temperature lag is clearly depicted in Appendix "D" during calibration for heat capacity in insulation.

Ceramic Thermal Epoxy;

A commercially available electrical insulating cement was modified to enhance thermal conductivity. The two part (powder/liquid) epoxy was blended with a high percentage of silica sand to yield an end product of high dielectric constant, low thermal resistivity (40°C - cm/watt), thermally stable to 1200°C and impervious to water. A sample of this epoxy was cast and tested with a thermal needle installed prior to curing. The test results are enclosed herewith and the test speciman is also supplied for you for in-house testing. The specifications for the termal needle are written on the base of the test specimen. The dry density of the epoxy is 2.319 g/cc.

Electrical insulation;

Prior to the winding of the heater, the inner core was wound with one layer of glass fibre cloth tape (one-half over lap) and two layers of mylar tape. The breakdown voltage of this insulating media is in excess of 2000 volts under hi-pot test. A further two layers of mylar tape were wound on the heater windings. These procedures were performed using a special winding machine. Mylar tape and glass fibre sleeve insulation were used on all connections of heater lead wires. The total weight of all the insulating materials was neglibible in comparison to the total weight of the heaters.

Heater Windings;

Two parallel heaters were wound on each inner core. Manganin heater wire of 19 gauge was used to fabricate the heaters. Manganin has the lowest coefficient of resistance change with temperature (about 18 ppm/°C/cm/ohm). This particular wire gauge was chosen for three reasons;

1) heater windings to be as close as possible (1.5mm separation between turns) for uniform heat field.

2) optimise various combinations of total resistances (each heater could be of 8.8 ohms or 17.6 ohms or 4.4 ohms)

3) to be compatible for use with existing Ontario Hydro's D.C. power supply (100 volts and 5 amps maximum).

Heater length is the full length of the core - 275mm. The two heater windings were joined together at one end to form a common return lead and the top end were individually connected to extension leads for individual or parallel or series connections. The extension lead wires were 21 gauge stranded copper teflon coated. The rating was 3.5 amps and 200°C continuous operation. All lead wires for heaters and thermocouples are 3m long.

Heater configuration and T/C designations;

Please refer to Appendix "C" for the heater arrangements and the thermocouple identification. Heater #10 is the spare heater used for calibration and for future referance.

HEAT CAPACITY CALIBRATIONS:

Volumetric heat capacity calibrations were performed by two methods;

Insulation method;

Temperature rise of a well insulated heater (no heat loss to the surrounding) is proportional to time for a constant power input. Therefore, mass or volumetric heat capacity is also proportional to time - temperature relationship. i.e. $\text{Heat capacity} = \text{power} \times \frac{\Delta \text{ time}}{\Delta \text{ temp}}$.

This theory is valid for short time - temperature measurements and small temperature rise. The heater under test was wrapped with 15cm. of pink glass fibre insulation all around and then contained in a totally enclosed wooden box. Our thermal property analyser was used to conduct the test. A constant power of 0.95 watt/cm was applied and time - temperature data monitored. The graphs are shown in Appendix "D" for the middle thermocouple on the heater and the one through the wall diagonally opposite. The volumetric heat capacity was found to be $\underline{1.677\ \text{J}/^\circ\text{C cm}^3}$. A temperature lag of approximately 5°C was found between the heater winding on the core and the surface temperature on the outer shell. During this calibration, no boundary effects were evident for the test duration.

Calorimeter method;

A well insulated plexiglass container was used as the calorimeter containing 2500ml. of water. A constant power was applied to the heater for 2000 seconds and the average of the six thermocouples was taken as mean initial heater temperature. The heater was immediately transferred into the calorimeter and temperatures for the heater and the water were monitored by the thermal property analyser until a steady state was reached (i.e. until a relatively constant average temperature was attained). For the calculation of the volumetric specific heat, the specific heat of the plexiglass container (0.35 cal/°C/gm) and it's weight were accounted for. The findings are reported on Appencix "E". Assuming minimal loss of heat to the external environment, the volumetric heat capacity by this method was found to be 1.616J/°C cm^3.

Comments;

Although the two methods of calibration for volumetric heat capacity are different in concept and theory, the findings are very close. The results differ by only 3.6% and this could be attributed to the experimental errors in averaging mean temperatures, some heat losses into the ambient and some deviations from the theory etc.

GEOTHERM INC:

Deepak Parmar,
President

DP:kb

APPENDIX "A"

GEOTHERM INC.
P.O. Box 699
Bradford, Ontario
Canada L0G 1C0
Tel. (416) 775-7141

JOB ONTARIO HYDRO - CIVIL RESEARCH
SHEET NO ______ OF ______
CALCULATED BY D.P. DATE January/86
CHECKED BY ______ DATE ______
SCALE NOT TO SCALE

HEATERS FOR BUFFER TESTS OUTER SHELL

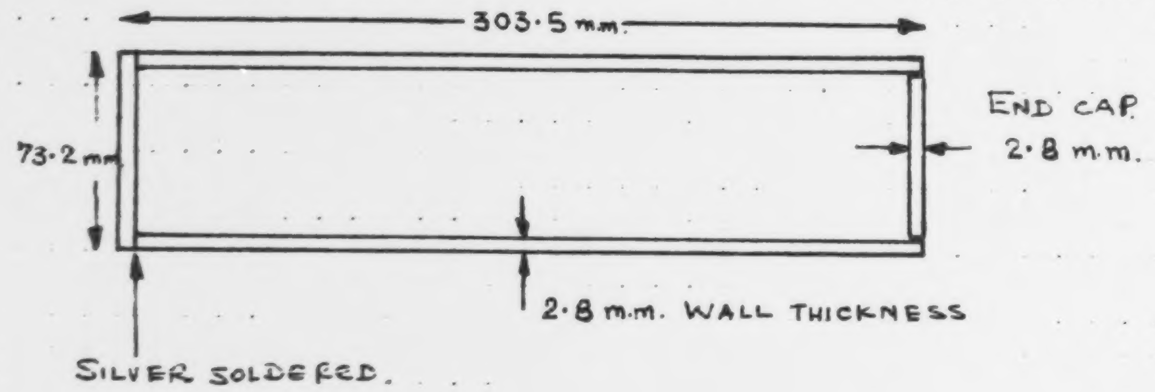

MATERIAL: Stainless Steel # 304
Thermal Conductivity: 16.26 W/deg.C- m.
Specific Heat: 0.00805 J/c.c.-deg.C

Weight of shell with both end caps: 1650 gms.

ALL THERMOCOUPLES (EXCEPT THE ONES ON THE HEATER WINDINGS) ARE BROUGHT OUT THROUGH THE WALL OF THE OUTER SHELL.

THERMOCOUPLES: Six (6) per heater.
Type "T" copper-constantan 24 gauge with fused Capton insulation rated at 250 deg.C.

TOTAL WEIGHT OF COMPLETE HEATER = 3960 gms.

Weight of all lead wires (six thermocouples and three for the heater windings) = 162 gms.

Weight of ceramic thermal epoxy = 1198 gms.

HEATER WEIGHT EXCLUDING LEAD WIRES = 3798 gms.

APPENDIX "B"

GEOTHERM INC.

P.O. Box 899
Bradford, Ontario
Canada L0G 1C0
Tel. (416) 775-7141

JOB ONTARIO HYDRO - CIVIL RESEARCH
SHEET NO ________ OF ________
CALCULATED BY D.P. DATE January/86
CHECKED BY ________ DATE ________
SCALE NOT TO SCALE

HEATERS FOR BUFFER TESTS

HEATER CORE

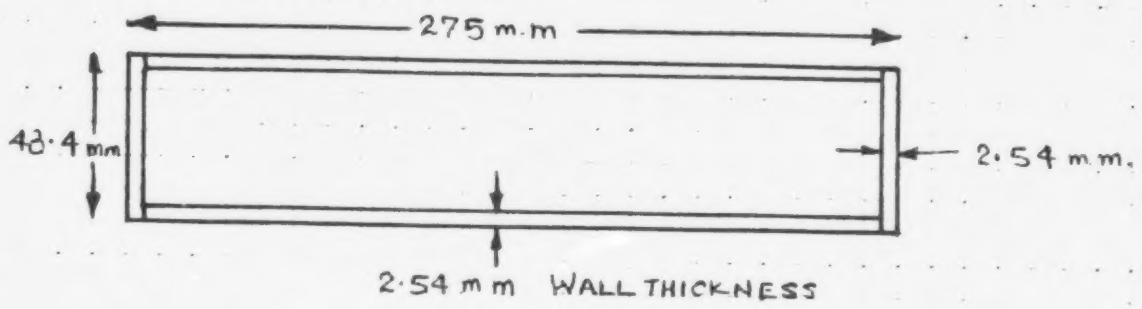

BOTH END CAPS SILVER SOLDERED.

MATERIAL: Stainless Steel # 304
Thermal Conductivity: 16.26 W/deg.C-m.
Specific Heat: 0.00805 J/c.c.-deg.C

Weight of Stainless Steel Core only: 863gm.
Weight of insulation and heater windings: 87gm.

INSULATION: 2 layers of glass fibre cloth tape.
2 layers of mylar tape
2 layers of mylar tape on heater windings

HEATER WINDINGS: 2 parallel windings
seperation between windings= 1.5mm.
Length of heater windings= 275m.m.
Each heater resistance= [illegible] ohms.
19 gauge heater wire made of Manganin uninsulated.

Heater lead wires: One separate lead for each heater plus one common return lead.
21 gauge stranded copper wire Teflon coated
Rating: 3.5 amps and 200 deg. C.

ALL LEAD WIRES ARE 3m LONG.

APPENDIX "C"

GEOTHERM INC.
P O Box 699
Bradford, Ontario
Canada L0G 1C0
Tel. (416) 775-7141

JOB ONTARIO HYDRO - CIVIL RESEARCH
SHEET NO ______ OF ______
CALCULATED BY D.P. DATE January/86
CHECKED BY ______ DATE ______
SCALE NOT TO SCALE

HEATERS FOR BUFFER TESTS

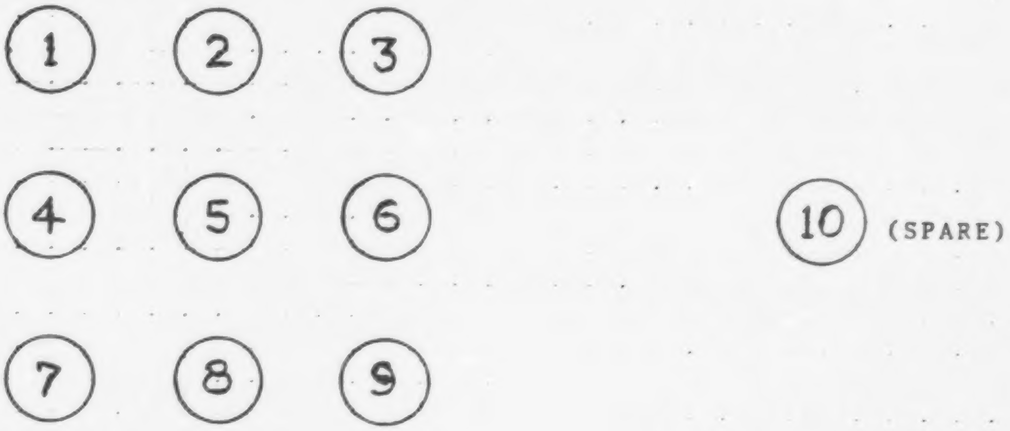

LOCATION OF THERMOCOUPLES:

Heaters 2,4,5,6,8 and 10: Six (6) thermocouples in each(total).

Two (2) on the heater windings at mid point of the length and are diogonally opposite.

Two (2) through the wall of shell at mid point of the length and are diogonally opposite.

Two (2) through the wall of shell at 1/4 way up from each end and in the same axis as the above two.

Heaters 1,3,7 and 9: Six (6) thermocouples in each (total)

Two (2) on the heater windings at mid point of the length and at 90 deg.

Two (2) through the wall of shell at mid point of the length and at 90 deg.

Two (2) through the wall of shell at 1/4 way up from each end and in the same axis as the above two (90 deg.).

DESIGNATIONS: U=upper, M=middle, L=lower, H=on heater and W=through wall.

APPENDIX "D"

GEOTHERM INC.
P O Box 699
Bradford, Ontario
Canada L0G 1C0
Tel. (416) 775-7141

JOB ONTARIO HYDRO - CIVIL RESEARCH
SHEET NO. ______ OF ______
CALCULATED BY D.P. DATE January/86
CHECKED BY ______ DATE ______
SCALE HEATERS FOR BUFFER TESTS

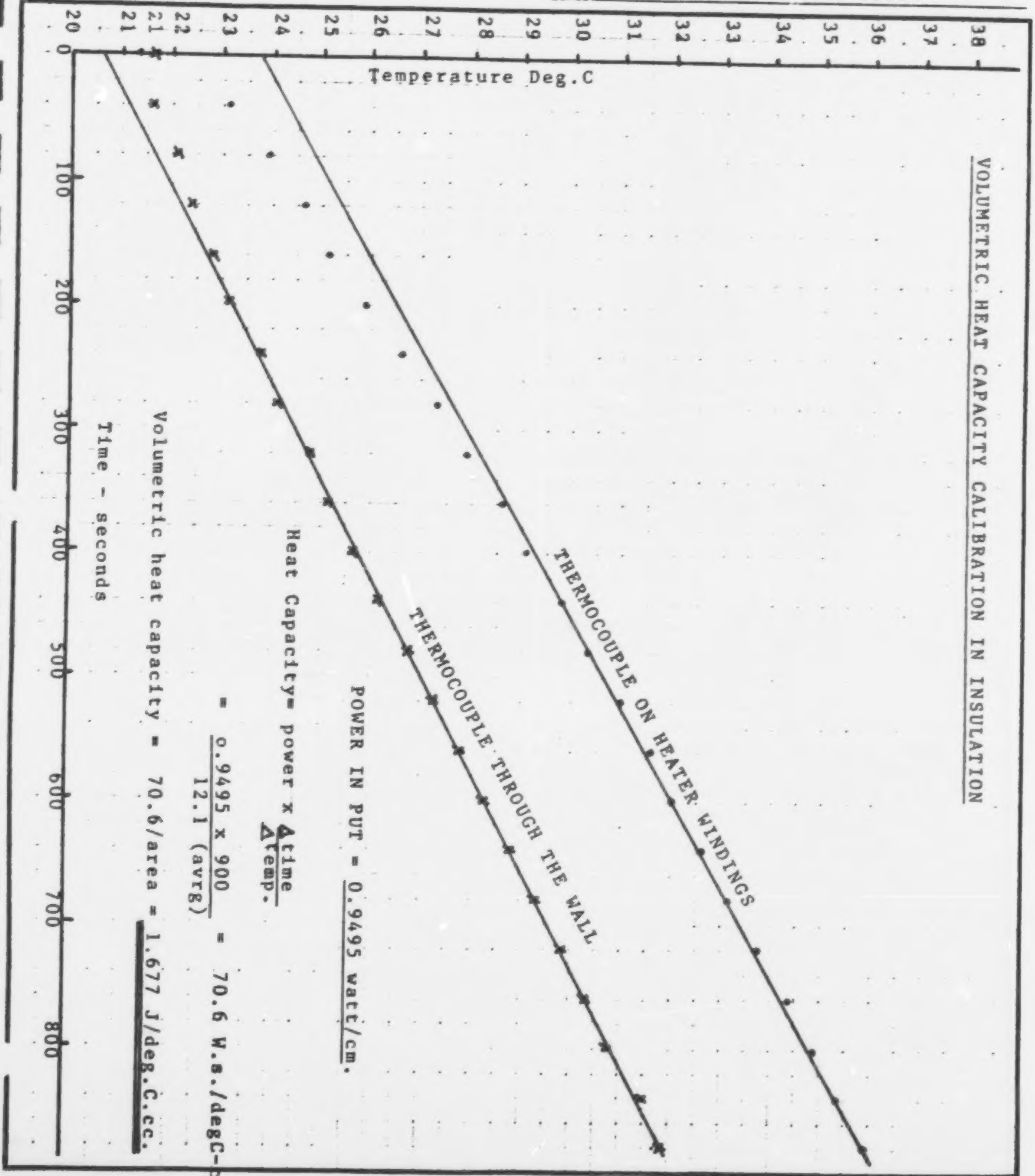

VOLUMETRIC HEAT CAPACITY CALIBRATION IN INSULATION

POWER IN PUT = 0.9495 watt/cm.

Heat Capacity = power x $\frac{\Delta \text{time}}{\Delta \text{temp.}}$

$= \frac{0.9495 \times 900}{12.1 \text{ (avrg)}} = 70.6$ W.s./degC-cm

Volumetric heat capacity = 70.6/area = 1.677 J/deg.C.cc.

APPENDIX "E"

JOB ONTARIO HYDRO - CIVIL RESEARCH
SHEET NO ______ OF ______
CALCULATED BY D.P. DATE January/86
CHECKED BY ______ DATE ______
SCALE HEATERS FOR BUFFER TESTS

VOLUMETRIC HEAT CAPACITY BY CALORIMETER METHOD:

Weight of Heater = 3798 gms.
Weight of Water = 2500 gms.
Weight of plexiglass container = 800 gms.

Specific heat of water = 1.0 Cal/gm. deg.C
Specific heat of plexiglass = 0.35 Cal/gm. deg.C

Initial average temperature of water = 19.0 deg.C
Initial average temperature of container = 19.0 deg.C
Initial average temperature of Heater = 68.8 deg.C

FINAL AVERAGE TEMPERATURE = 26.5 deg.C

Specific heat of Heater =

$$\frac{\text{Sp. ht. of water X mass X } \Delta t \text{ + sp.ht. of plexiglass Xmass X } \Delta t}{\text{mass of heater X } \Delta t}$$

$$= \frac{1.0 \text{ X } 2500 \text{ X } 7.5 + 0.35 \text{ X } 800 \text{ X } 7.5}{3798 \text{ X } 42.3} = \underline{0.1298}$$

$$\text{Volumetric heat capacity} = \frac{\text{sp.ht. X ht. cap. of water X wt. of heater}}{\text{volume of heater}}$$

$$= 0.1298 \text{ X } 1 \frac{\text{cal}}{\text{g. C}} \text{ X } 4.187 \frac{\text{J}}{\text{cal}} \text{ X } \frac{3798 \text{ g.}}{1277 \text{ c.c.}}$$

$$= \underline{\underline{1.616 \text{ J/deg.C cc.}}}$$

APPENDIX C

The Pneumatic Pressure Cell

PETUR™

INSTRUMENTS LTD.

PORTABLE PNEUMATIC READOUT INSTRUMENTS

FUNCTIONS

- Monitor all PETUR pneumatic piezometers, i.e., P-100, P-102, P-102-1, P-102-2, P-102-3, P-103, P-104, P-104-1, P-106, P-106-1
- Monitor TP-101 pressure cells
- Monitor SP-105 settlement systems when used in conjunction with SC-100 auxiliary settlement readout instrument.
- Bubbler readout for monitoring standpipe piezometers.
- C-102 WS controls PETUR water sampler/piezometer

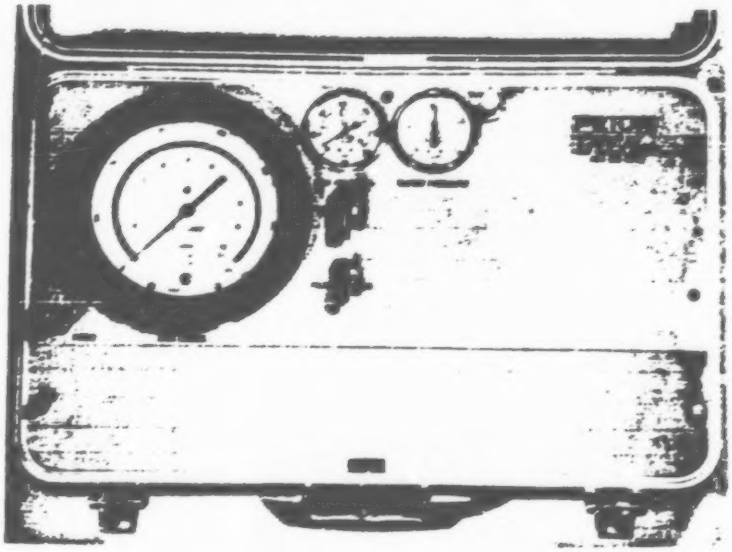

C-102

ADVANTAGES

- Patented PETUR FC-100 automatic flow controller eliminates operator and flow rate induced errors. The flow rate is unaffected by variable back pressure or tubing length.
- Low operating rate of 35 cc/min. insures most economical use of gas.
- Internal pressure cylinder is refilled without needing to be removed.
- No additional regulator is required to fill the internal cylinder. The necessary filler hose is supplied as standard.
- Specifically designed for cold weather operation and reliability.
- 6" (150 mm) diameter test gauges in 0.25% or 0.10% full scale accuracy.
- Dual scale (psi/kPa) standard on C-102 and C-102-1
- Pressure ranges to 2000 psi (13,790 kPa) available
- Design allows constant monitoring capability. If a charted record is required, Model PDM-101 utilizes a 12" circular chart for monitoring up to 4 transducers.
- PDM-101 may be provided in wall or pipe mount case for monitoring multiple transducers.
- Relief valves protect sensitive parts from over-pressurization.
- Made in Canada and competitively priced

OPERATING PROCEDURE

- Open the supply tank and turn the instrument on.
- Connect the transducer with quick-connect fittings provided.
- Open the by-pass valve and observe the data gauge. When the pointer stops rising, close the valve.
- Allow the data gauge to stabilize, tap the gauge and record the indicated pressure.
- Disconnect transducer, turn instrument off, and close the supply tank valve.

SPECIFICATIONS

MODEL	C-102	C-102-1	C-102-2	C-102-3
Scale length	14" (36 cm)	14" (36 cm)	32" (81 cm)	32" (81 cm)
Accuracy (% of full scale)	± 0.25%		± 0.10%	
Sensitivity (% of full scale)	± 0.13%		± 0.05%	
Temperature compensation	not available		-32° to + 52° C	
Zero Adjustment	MANUAL			
Parallax compensation	Mirrored dial with knife edged pointer			
Dimensions	21 x 13 x 6.5" (53 x 33 x 17 cm)			
Weight	24 lbs. (11 kg)		26 lbs. (12 kg)	
Cylinder capacity	0.033 cu. ft. (0.93 litres)			
Pressure Ranges	ranges up to 300 psi (2068 kPa)	ranges up to 2000 psi (13,790 kPa)	ranges up to 300 psi (2068 kPa)	ranges up to 2000 psi (13,790 kPa)

Dual scale (psi/kPa) standard for C-102 and C-102-1 models.

Models C-102-2 and C-102-3 calibrated in psi as standard. Other ranges upon request (cm of H_20, kPa, etc.)

All models available with water sampler (C-102 WS) capability.

PETUR™
INSTRUMENTS LTD.

No. 18 - 1780 McLEAN AVENUE, PORT COQUITLAM, B.C. V3C 4K9
TELEPHONE (604) 941-4848

APPENDIX D

The Psycrometer

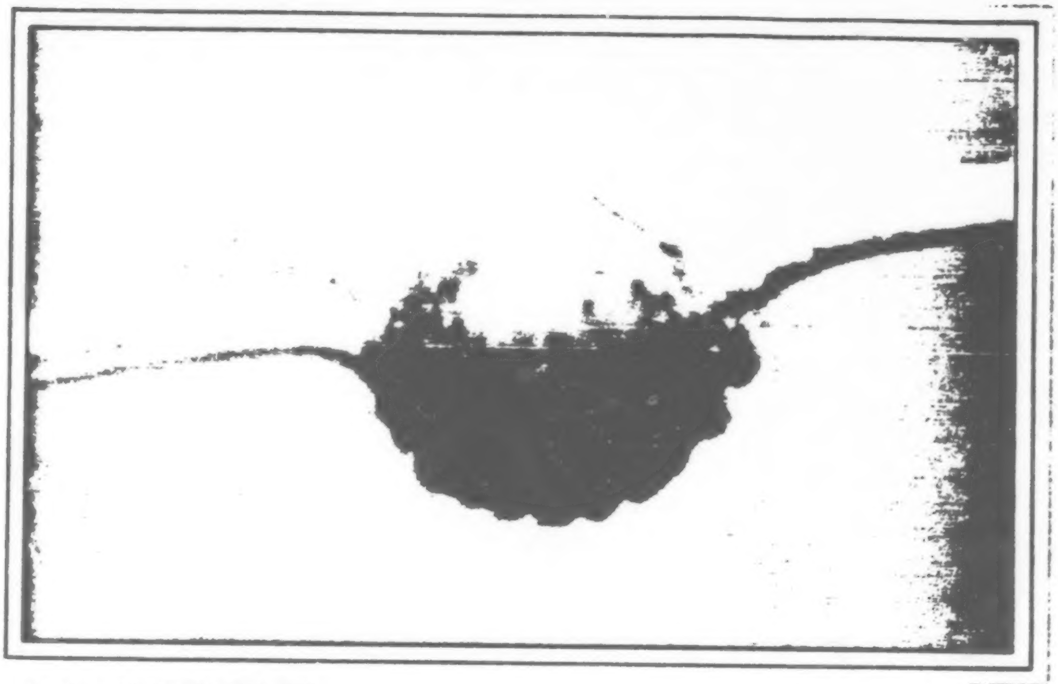

WATER
POTENTIAL SYSTEMS

WESCOR

WATER POTENTIAL AND THERMOCOUPLE PSYCHROMETRY

Water potential is defined in terms of the energy status of the water. Water potential is the energy required to remove water reversibly and isothermally from a standard reference state to the soil, plant or atmospheric system under consideration. The reference state chosen is usually pure free water at the same temperature as water in the system and at a pressure of one standard atmosphere.

Water moves from regions of high water potential to regions of lower water potential. The greater the difference in the potentials of the two regions, the greater will be the energy exchange in the transfer of the water. Growing plants respond to water according to the energy required from the plant to assimilate water into the plant and move the water through the plant.

Thermocouple psychrometers/hygrometers provide a means of measurement of the total water potential. The measurement is based on the energy and is an actual measurement of the water potential. Other methods measure water content, electrical conductivity or other conditions which are related to water potential. These other methods require a knowledge of the composition of the soil or other factors which affect the relationship between the measured parameter and the water potential, in order to obtain accurate results.

Water potential is related to relative humidity by the Kelvin equation.

$$\Psi = \frac{RT}{V_w} \ln e/e_o$$

Where:

Ψ is the water potential (Pa)
R is the universal gas constant (8.3143 J mol^{1} $^{\circ}$K^{1})
e/e_o is the relative humidity expressed as a fraction
T is the absolute Temperature (°K)
V_w is the molar volume of water ($1.8 \times 10^{5} m^{3} mol^{1}$)

In practice the soil psychrometers/hygrometers measure the relative humidity of a small sample of air which has been allowed to equilibrate with the soil or other material for which the water potential measurement is desired.

The use of Peltier cooled psychrometers was first proposed by D.C. Spanner in 1951. Since that time over 1000 papers have been published which report the use of this method of water potential measurement.

A comprehensive review of thermocouple psychrometery / hygrometry is available from Wescor. Request the publication "Thermocouple Psychrometry For Water Potential Measurement". Several additional publications of general interest are listed below:

1. Brown, R.W. and Van Haveren, B.P. (eds.) *Psychrometry in Water Relations Research*. Utah Agric. Res. Stat. and Utah State Univ., p. 328.
2. Spanner, D.C. The Peltier effect and its use in the measurement of suction pressure. *J. Exp. Bot.* 2:145-168. 1951.
3. Neuman, H.H. and Thurtell, G.W. A Peltier cooled thermocouple dewpoint hygrometer for *in situ* measurement of water potential. In: *Psychrometry in Water Relations Research* (R.W. Brown and B.P. van Haveren, eds.) Utah Agric. Exp. Stat. and Utah State Univ., pp. 103-112.
4. Campbell, E.C., Campbell, G.S. and Barlow, W.K. A dewpoint hygrometer for water potential measurement. *Agric. Meteorol.* 12:113-121. 1973.
5. Brown, R.W. and Collins, J.M. A screen-caged thermocouple psychrometer and calibration chamber for measurements of plant and soil water potential. *Agron. J.* 72:851-854. 1980.
6. Savage, M.J., Wiebe, H.H. and Cass, A. *In situ* field measurement of water potential using thermocouple psychrometers. *Plant Physiol.* 73:609-613. 1983.
7. Savage, M.J., Wiebe, H.H. and Cass, A. Effect of cuticular abrasion on thermocouple psychrometric *in situ* measurement of leaf water potential. *J. Exp. Bot.* 35:36-42. 1984.
8. Campbell, G.S. and Campbell, M.D. Evaluation of a thermocouple hygrometer for measuring leaf water potential *in situ*. *Agron. J.* 60:24-27. 1974.
9. Savage, M.J., and Cass, A. Measurement of water potential using *in situ* thermocouple hygrometers. *Advances in Agronomy* 37:73-126.
10. Wiebe, H.H., et al. Measurement of plant and soil water status. Bulletin 484, Utah Agric. Exp. Stat. May 1971.

Definition of Terms Used in this Catalog

Psychrometric (Wet Bulb) Method — The technique of measuring water potential by determining the wet bulb depression temperature. A thermocouple is cooled below the dew point by means of the Peltier Effect, thereby collecting micro-droplets of condensed water upon the junction surface. The water is then allowed to evaporate, causing the temperature of the junction to be depressed below the ambient temperature due to evaporative cooling. The wet bulb temperature depression persists until all the water has evaporated, then the thermocouple returns to the ambient temperature.

Hygrometric (Dew Point) Method — The technique of measuring water potential by determining the dew point depression temperature. The method is made possible through the use of a special electronic technique pioneered by Wescor. A thermocouple is cooled below the dew point as in the psychrometric method, but the temperature of the thermocouple is then controlled by the heat of condensation from the water condensing on its surface. This causes the thermocouple temperature to converge to the dew point, where it remains with a static amount of water. The dew point measurement is therefore continuous in nature, rather than transitory, as is the wet bulb depression measurement. Greater precision of measurement is possible, along with other advantages. For technical information regarding the dew point method, contact Wescor, Inc.

Thermocouple Cooling Coefficient, π_v — The Cooling Coefficient, π_v, of a given thermocouple transducer is defined as the emf in microvolts produced by the temperature differential that results from the passage of a specified nominally optimum cooling current through the junction.

π_v is related to the Peltier Coefficient π_{ab} which expresses the theoretical cooling capability of any junction composed of two dissimilar metals, a and b. The actual cooling capability of a thermocouple transducer is affected by a number of factors in addition to its theoretical cooling ability. These factors include geometric and metallurgical anomalies in the junction and lead wires, length of the lead wires, mounting structure and materials, mounting geometry, etc.

If the π_v of a thermocouple hygrometer is known, then its maximum range is also known. In specifying π_v, both the cooling current and the ambient temperature must also be specified. For example:

$$\pi_v\ (8\ \text{mA},\ 25^\circ\text{C}) = 66\ \text{microvolts}$$

We invite your inquiries for further information or technical assistance in special applications.

PCT-55 and PST-55
Soil Hygrometer/Psychrometer

For Water Potential Measurements (In Situ)

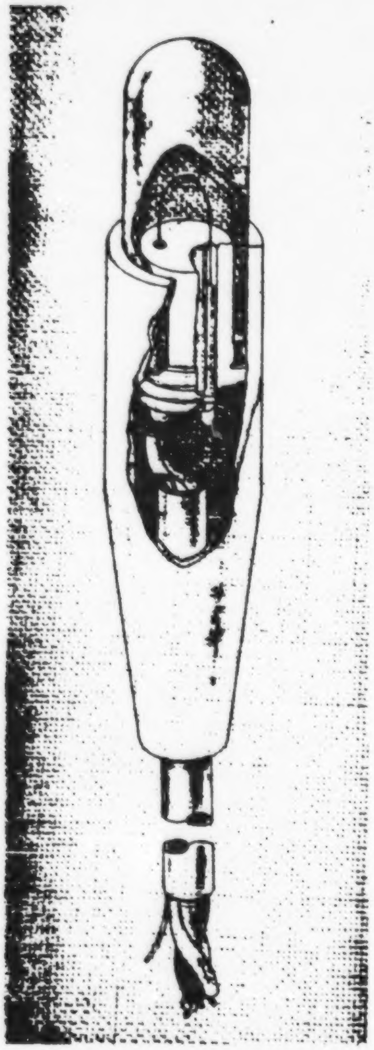

BREAKTHROUGH !

PROTECTED WITH [illegible] GUARD™ Thermocouple [illegible] the greatest nemesis of soil [illegible] has been eliminated! The [illegible] protects the psychrometer [illegible] from corrosion even in hostile soil environments (patent pending)

This proven transducer is used in research programs throughout the world. It may be employed in either wet bulb or dew point mode of operation.

Porous ceramic shields or exclusive Dutch weave stainless steel screen shields are available. The stainless steel screen has larger pore size and faster equilibration. The porous ceramic has thermal conductivity similar to most soils.

FEATURES

- Removable thermocouple shields for easy cleaning
- Controlled junction size and chamber geometry for consistent performance
- Internal connections gold plated for low corrosion
- High sensitivity
- Tested individually for cooling coefficient (π_v), leaks, cleanliness, and sensitivity
- Individual psychrometric calibration curve provided with each unit
- *SUREFAST*™ connector option available

SPECIFICATIONS

PSYCHROMETER OUTPUT: typically 4.7 microvolts/MPa at 25°C

HYGROMETER OUTPUT: typically 7.5 microvolts/MPa at 25°C
π_v 40 microvolts minimum (8 mA, 25°C)

RANGE π_y -7.5 MPa at 25°C (-7.3 MPa with π_v = 55 microvolts)

TYPE DESIGNATION

Specify type PCT-55 (ceramic shield) or type PST-55 (exclusive Dutch weave stainless steel screen) and 1.5 or 3 meter lead length by dash number.

Example PCT-55—15 (1.5 meters)
PCT-55—30 (3.0 meters)

Specify *SUREFAST*™ connector option by adding —SF.
Example: PCT-55-15—SF

PR-55

Psychrometer Microvoltmeter For Water Potential Measurement by the Wet Bulb Method

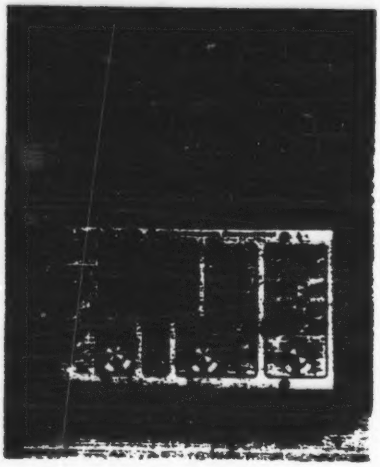

The PR-55 is designed to be used with thermocouple psychrometers to measure water potential. Cooling current and cooling time are automatically controlled. Inputs are provided for 10 thermocouple psychrometers. The microvolt output at the plateau is held on the digital display until manually released.

FEATURES

- Low noise, low drift, chopper-stablized microvoltmeter
- Automatic or manual control of cooling time
- Cooling current selection by thumbwheel switch
- Digital display with sample hold
- Digital temperature readout in degrees Celsius
- Rechargeable lead-acid (gel-type) battery with charger
- Low battery indicator
- Convenient sensor connection with SUREFAST™ connectors

SPECIFICATIONS

RANGES: 100 and 1000 microvolts

ACCURACY: ± 1% of full scale

ZERO DRIFT: Less than 0.1 microvolts per 24 hours. Less than 0.5 microvolts per °C

NOISE: 0.1 microvolts peak-to-peak

RISE TIME: 2 seconds

ZERO SUPPRESSION: ± 100 microvolts

RECORDER OUTPUT: 100 millivolts full scale

CONNECTORS: *SUREFAST*™ receptacles

BATTERY OPERATING TIME: 300 hours per charge (nominal), may be operated from line power with battery charger connected

WEIGHT: 5.0 kg

SIZE: 28 cm x 25 cm x 18 cm

REFERENCE JUNCTION: Copper-Constantan ± 0.3°C (0°C to 45°C)

CONTROLS	LIMITS	INCREMENT
Cooling Current	1-9 mA	1mA
Cooling Time	1-99 sec	1 sec
Delay Time	1-9 sec	1 sec

APPENDIX E

The Rotameter

HIGH ACCURACY ROTAMETERS

Unshielded–101-102-103-104-105
Shielded – 111-112-113-114-115

UNSHIELDED

Models: FL-101, FL-102, FL-103, FL-104, FL-105

Calibrated & Correlated

Conversion charts supplied with air and water flows for all floats versus glass with corresponding pressure drops.

- Individually calibrated with air to establish physical constants of meter and yield high precision.
- New correlation based on Stokes' law permits calculation of calibration curve for any fluid for which only the density and viscosity are required.
- Each meter serialized and supplied with calibration curve for air and water. Special coordinates convert this curve into a straight line.
- Specially designed Teflon® stops allow standard taper joints with precision bore ends to be attached to meter. O-ring seal makes this connection vacuum tight.
- Permanent ceramic scale and white background makes reading of black glass ball easy and accurate.
- Fluid comes in contact only with glass, Viton and Teflon — Ideal for corrosive fluids.

These OMEGA® High Accuracy Rotameters are manufactured to ultimate tolerances which give maximum precision for spherical float flowmeters. They are available in five sizes to cover the full range of flows normally encountered with spherical floats. The first three sizes are plain taper tubes while the last two sizes are beaded tubes to give stability where needed.

The new theory of correlation based on a dimensionless combination of Stokes' law and flow coefficients makes it relatively simple to precisely calculate the calibration for any fluid. Only the density and viscosity of the fluid at the conditions of flow are required. Because each meter is individually calibrated and plotted with coordinates to give a straight line, highest precision is possible at reasonable price. Each serialized meter comes with its own calibration curve giving flows for air and water directly without any calculation.

Precision-bore ends of each meter combined with special Teflon stops makes it a simple job to disassemble and clean.

Standard taper joints with special precision-bore ends can be purchased separately at any time and simply added to the plain tube ends whenever desired.

Statistical method of sampling controls accuracy to within ±2% or ±1 scale division (whichever is the greater).

MODEL NO.	AIR	WATER	FLOAT DIAM.	TUBE O.D.	TUBE LENGTH
FL-101	1-280	.01-4.0	.0625	5/16"	7½"
FL-102	10-1900	0.2-36	.125	5/16"	7½"
FL-103	200-14,000	3-300	.250	7/16"	7½"
FL-104	1000-36,000	10-850	.375	12/16"	9"
FL-105	3000-77,000	30-1900	.500	15/16"	9"

Each meter is supplied with complete directions and correlation chart for calculating the calibration curve for any fluid whose density and viscosity are known. Also included is a S.S. Float.

Flow ranges stated above may be extended by factors of from 2 to 3 by using heavier floats. See Accessories.

Taper Joint Sets available. Set consists of one inner and outer joint plus two O-rings.

Part No.	For Use With	Taper
FL-J1	FL-101	10/30
FL-J2	FL-102	12/30
FL-J3	FL-103	14/35
FL-J4	FL-104	19/38
FL-J5	FL-105	24/40

NOTE: Extremely dry gases, at low flows, may cause erratic readings due to electrostatic charge build-up.

Approximate Multiplying Factor for Floats

Gases	Water	For Float Types	(ρ_f)
1	1	Glass	2.53
1.78	2.14	316 S.S.	8.02
2.56	3.19	Tantalum	16.6
2.43	3.01	Tungsten C	14.9

DIRECTIONS

The individual calibration chart supplied with each meter is a plot of the percentage change in diameter ratio, R, against the scale reading of the meter, which is a straight line. On the left side of the chart is a direct reading scale of the equivalent flow of air at standard conditions, and a similar scale for water is on the right side.

When cleaning the meter, great care should be exercised not to lose the glass ball. It is possible to replace the glass ball; however, the calibration will not be as accurate, although deviations will only be minor.

Accuracy is ±2% of reading or ±1 division, whichever is the greater.

The dimensionless correlation chart of flow coefficient, C_R, against Stokes number, S_t, for different values of R may be used to calculate the calibration curve for any fluid whose density and viscosity are known at conditions of flow, by the following steps:

1. Select a suitable value of R and read the corresponding scale reading from the individual calibration curve supplied.
2. Obtain the values of weight of float in grams, W_f, and the density of float, ρ in gram/ml. from the calibration chart. Let ρ = density of fluid in grams/ml. and μ = viscosity of fluid in centipoises at conditions of flow.
3. Calculate the Stokes number from the following

$$S_t = 1.042 \frac{W_f(\rho_f - \rho)\rho}{\mu^2 \rho_f} R^3 \qquad R = \frac{Dt - Df}{Df} \times 100$$

Dt = Diam. of tube, Df = Diam. of float

4. From the correlation chart read off the corresponding value of C_R for the calculated value of S_t and the selected value or R.
5. Obtain the value of diameter of float in inches, D_f, from the calibration chart, and calculate the volumetric rate of flow in ml/min, q, from the following equation:

$$q = 59.8\, D_f\, C_R \sqrt{\frac{W_f(\rho_f - \mu)}{\rho_f\, \rho}}\, R \left[\frac{R}{100} + 2\right] K_f$$

K_f = 1 in most cases except as follows:

Fluid	Model	K_f
Gas (air)	FL-101	$1 + (R/10)^2$
Liq. (water)	FL-101	$1 - (R/100)$
Liq. (water)	FL-102	$1 - (R/250)$
Gas (air)	FL-103	$1 + (R/70)^2$

6. The volumetric rate of fluid flowing and measured at the conditions of flow may be converted into mass rate of flow by multiplying by the density.

7. To obtain a complete calibration curve several values of R may be selected. Gases may be plotted against the standard air scale and liquids against the standard water scale on the calibration chart to give very nearly straight lines.

SAMPLE CALCULATION

Flowmeter, No. FL-101, std. water at R = 25

1. From individual calibration chart, scale reading is 100 at R = 25.
2. W_t = .00530 grams, ρ_f = 2.53 grams/ml. For std. water: ρ = 1.0 grams/ml and μ = 1.0 cp
3. $$S_t = \frac{1.042 \times .00530 \times 1.53 \times 1.00}{1.0 \times 2.53} \times 15{,}625 = 52.2$$
4. From correlation chart, C_R = .450
5. D_t = .0625 inches and
$$q = 59.8 \times .0625 \times .450 \sqrt{\frac{.00530 \times 1.53}{2.53 \times 1.0}} \times 25(2.25) \times (.75)$$
$$= 4.02 \text{ ml/min.}$$
6. Mass flow: 4.02 x 1.0 = 4.02 grams/min.

JOINT SETS: When used with joint sets, it is recommended that short lengths of flexible tubing (such as tygon or Teflon) be used on each end to hold the joint securely to the flowmeter.

SHIELDED ROTAMETERS

Models: FL-111, FL-112, FL-113, FL-114, FL-115

These calibrated and correlated rotameters are available with all-plastic shields that confine fluid contact to the Viton® or Teflon® O-Rings, Teflon® inserts, and the glass tube. The polycarbonate shield makes it possible to use the rotameter under pressurized systems or in conditions where glass cannot be exposed.

- Outer protection tube made of polycarbonate with excellent optical properties
- Bushings made of corrosion resistant polypropylene, with Teflon® inserts.
- Bushings made with standard pipe thread on ends and Teflon® insert will also take flexible hose.
- O-Ring seals assure gas tight connection.

ACCESSORIES

Part No.	For Model No.	Description
FL-11	FL-111	6 pack of Teflon® O-Rings. Used to replace standard O-Rings when Viton® is not acceptable.*
FL-12	FL-112	
FL-13	FL-113	
FL-14	FL-114	
FL-15	FL-115	

* Viton cannot be used with: Ammonia, Amyl Acetate, Ethyl Acetate, Ethylene Oxide, Fluorine, Freon, Hydrogen Sulphide, Hydrogen Fluoride, Ketones, Potassium Hydroxide. When in doubt, use Teflon.

Model No.	Float Dia.	Pipe Thread	Outside Diam.	Length
FL-111	.0625	¼"	1"	10"
FL-112	.125	¼"	1"	10"
FL-113	.250	¼"	1"	10"
FL-114	.375	½"	1½"	12½"
FL-115	.500	½"	1½"	12½"

Also included is a S.S. Float.

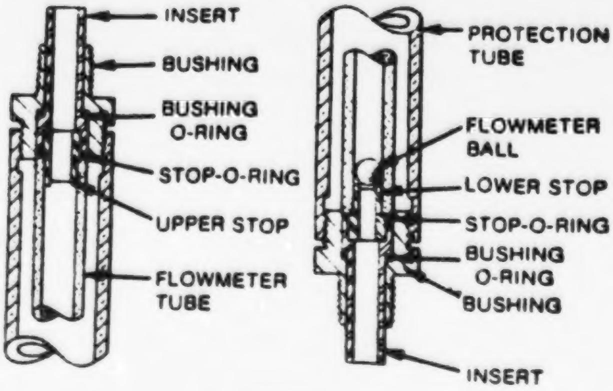

DIRECTIONS

ASSEMBLY — The shielded flowmeters are delivered completely assembled and ready for use. Note that the Teflon stops fit snugly into the Teflon inserts which are contained in the polypropylene bushings. The O-Rings should be in position inside the Teflon inserts before assembly.

CONNECTIONS TO SYSTEM — The ends of the bushings are provided with standard pipe threads for easy installation into piped system. However, enough of the smooth Teflon insert protrudes from the bushing so that flexible hose may also be used in connection to the system. For pressure systems, the flexible hose must be clamped in position. Although the use of glass under pressure is always subject to danger, hence the need for protective tubes, the following safe working pressures are recommended for each size:

Model No.	Pipe Thread	Instrument O.D.	Length	Insert O.D.	I.D.	Max Working* Pressure PSIG
FL-111	¼"	1"	10"	⅜"	¼"	500
FL-112	¼"	1"	10"	⅜"	¼"	400
FL-113	¼"	1"	10"	⅜"	¼"	350
FL-114	½"	1½"	12½"	⅝"	⅜"	300
FL-115	½"	1½"	12½"	⅝"	⅜"	250

* Special connections are recommended when working at maximum pressures.

The O-rings not only assure a pressure tight connection, but also allow for a certain amount of flexibility. Nevertheless, care should be taken in pressure installations that no undue strain is placed on the glass flowmeter tube.

CALIBRATION OF METERS — A calibration curve is supplied with each meter for air and water at standard conditions. For other fluids and other conditions, the correlation chart supplied with the meter is recommended for calculating the desired calibration curve. Where high precision is not required, the usual methods for correction of flowmeter readings under pressure may be used. However, for very low flows, especially with the FL-111 size meter, the usual corrections are too much in error and the correlation chart must be used.

Accuracy is ±2.0% of reading or ±1 division, whichever is the greater.

CLEANING — When disassembling the unit for cleaning, care should be taken not to lose the glass ball. When unscrewing the plastic tube, the stops may remain in the Teflon inserts (especially with the smaller sizes). These are easily removed by pushing out with a rod. In the case of the FL-115 meter, an internal chamfer is provided to facilitate the removal of a stop should it remain in the insert.

Normal methods of cleaning are recommended for each part. The flowmeter parts may be cleaned with strong solutions, such as chromic acid cleaning solution if necessary. The shield parts may be cleaned with detergents, but care should be taken not to scratch the plastic tube or clean it with organic solvents that may dissolve it.

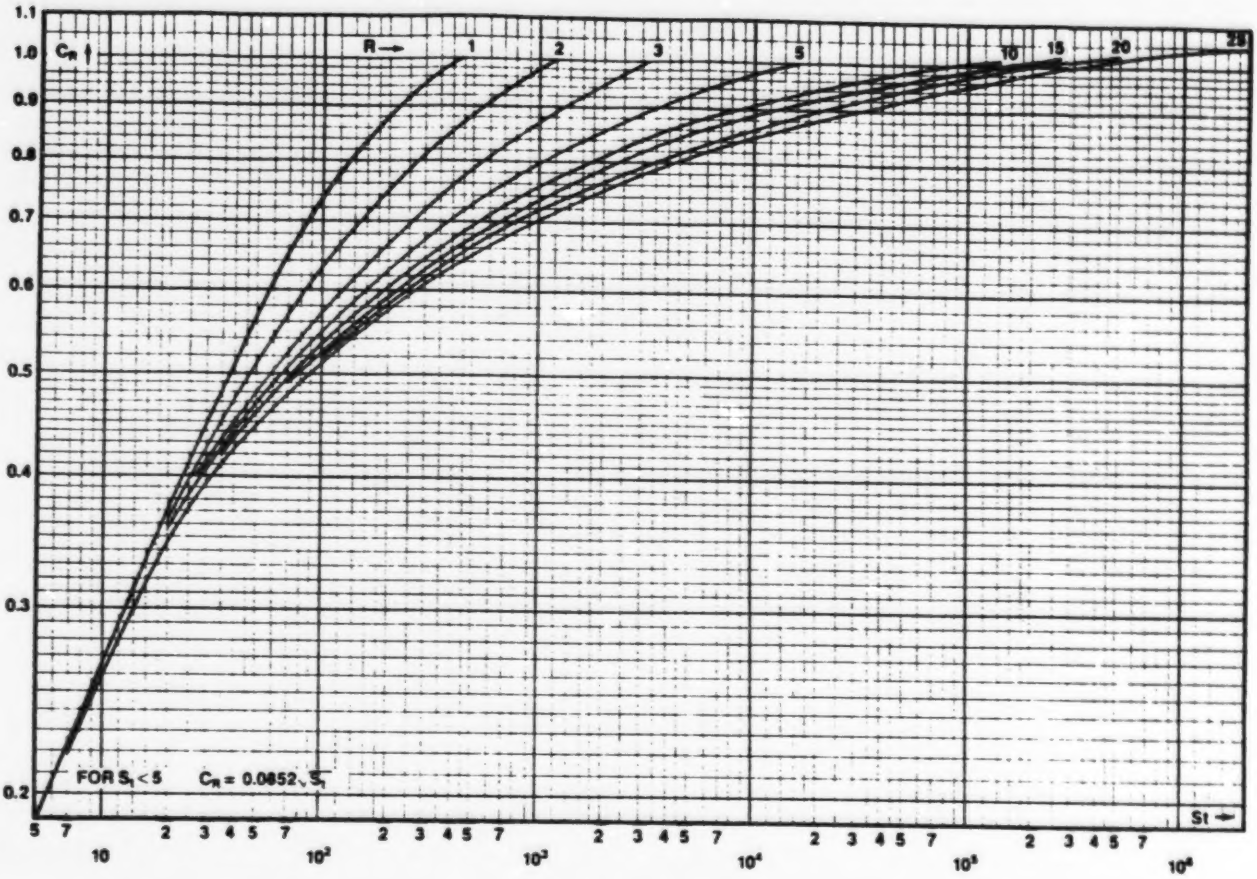

ANALYTICAL EQUATION FOR C_R vs St & R

The flow coefficient C_R may be calculated within an error of ±2% to ±5% (depending on the variables) by using the analytical function (common logs):

$$C_R = \frac{\sqrt{b^2 + 4ac} - b}{2a} \text{ where}$$

$a = 3.08 \log R - 1.25$
$b = 3.83 - 1.17 \log R$
$c = \log St - .111 \log R$

Example of calculation; interpolating the dimensionless chart of C_R vs St & R for value of R and St with:

$R = 12.8$ and $St = 39.6$, then
$\log R = 1.108$ and $\log St = 1.598$
$a = 3.41 - 1.25 = 2.16$
$b = 3.83 - 1.30 = 2.53$
$c = 1.598 - .123 = 1.475$

$$C_R = \frac{\sqrt{6.41 + 12.78} - 2.53}{2 \times 2.16}$$

$$= \frac{1.85}{4.32} = .428$$

C_R (From Chart) = .43

To use the Stokes number and volumetric flow rate equations for gases, ρ and μ at 70°F & 1 atm. must be known.

ρ for any gas may be approximated by using the molecular weight in the equation: $\rho^\circ = .0414 \times \text{mol. wgt.} \times 10^{-3}$ g/ml. Temp & Press. corrections to 70°F & 1 atm can be made from:

$$\rho' = \rho^\circ \times \frac{P}{760} \times \frac{530}{T}$$

with P in Torr and T in °R.
Example: to find ρ for O_2 at 70°F & 1 atm $\rho^\circ = .0414 \times 32 \times 10^{-3} = .00132$ g/ml.

Since μ cannot be determined readily, μ for commonly used gases are listed below in Table 1.

TABLE I

GAS	μ in cp	GAS	μ in cp
Air	.0181	H_2S	.0126
Ar	.0221	CH_4	.0109
CO_2	.0148	CH_3Cl	.011
CO	.0174	Ne	.031
Cl_2	.0133	NO	.0188
C_2H_4	.0101	N_2	.0175
He	.0194	N_2O	.0144
H_2	.0087	O_2	.020
HCl	.0144	SO_2	.0125
HI	.0166	Xe	.0226

Density & Viscosity of Liquids at 70°F & 1 atm are listed in Table II:

TABLE II

LIQUID	ρ in g/ml	μ in cp
Acetic Acid	1.049	1.221
Acetone	.790	.32
Aniline	1.022	4.40
Benzene	.879	.652
Butyl Acetate	.883	.732
n-butanol	.810	2.948
CCl_4	1.594	.969
Chlorobenzene	1.106	.799
Chloroform	1.483	.58
Diethyl Ether	.714	.233
Ethyl Acetate	.900	.455
Ethanol	.789	1.20
Ethylene Br	1.480	1.72
Ethylene Cl	.866	.79
Ethylene Glycol	1.109	19.90
Fluorobenzene	1.023	.598
Heptane	.684	.409
Methyl Acetate	.933	.381
Methanol	.791	.597
Nitrobenzene	1.204	2.03
n-octane	.703	.542
Propanol	.804	2.256
Toluene	.867	.590
o-xylene	.880	.810
m-xylene	.864	.620
p-xylene	.861	.648
Aqueous Solutions (% by weight)		
10% HCl	1.048	1.159
30% HCl	1.149	1.702
10% HNO_3	1.054	1.042
40% HNO_3	1.247	1.558
10% H_2SO_4	1.066	1.228
60% H_2SO_4	1.498	5.606

SPECIFICATIONS

METERING TUBE: Borosilicate glass
O-RINGS: Viton (optional Teflon available for shielded models)
FLOATS: 316SS and glass
FLOAT STOPS: Teflon
ACCURACY: ±2% reading, or ±1 scale division
REPEATABILITY: ±½% reading, or ±¼ scale division

SHIELDED MODELS ONLY

SHIELD: High-clarity polycarbonate
TUBING INSERT: Teflon
BUSHING: Polypropylene

RECOMMENDED INSTALLATION PRACTICES

Water hammer and surges can be damaging to any flowmeter and must *always* be avoided.

Water hammer occurs when a liquid flow is suddenly stopped as with quick closing and solenoid operated valves. Surges occur when flow is suddenly begun, as when a pump is turned on at full power or a valve is quickly opened.

Liquid surges are particularly damaging to flowmeters if the pipe is originally empty. To avoid damaging surges, fluid lines should remain full (if possible) and pumps should be brought up to power slowly and valves opened slowly. In addition, to avoid both water hammer and surges, a surge chamber should be installed.

WARRANTY

OMEGA warrants this unit to be free of defects in materials and workmanship and to give satisfactory service for a period of one (1) year from date of purchase. If the unit should malfunction, it must be returned to the factory for evaluation. Our Customer Service Department will issue an Authorized Return (AR) number immediately upon phone or written request. Upon examination by OMEGA, if the unit is found to be defective it will be repaired or replaced at no charge. However, this WARRANTY is VOID if the unit shows evidence of having been tampered with or shows evidence of being damaged as a result of excessive current, heat, moisture, vibration, or misuse. Components which wear or which are damaged by misuse are not warranted. These include contact points, fuses, and triacs.

THERE ARE NO WARRANTIES EXCEPT AS STATED HEREIN. THERE ARE NO OTHER WARRANTIES, EXPRESSED OR IMPLIED, INCLUDING BUT NOT LIMITED TO THE IMPLIED WARRANTIES OF MERCHANTABILITY AND OF FITNESS FOR A PARTICULAR PURPOSE. IN NO EVENT SHALL OMEGA ENGINEERING, INC. BE LIABLE FOR CONSEQUENTIAL, INCIDENTAL OR SPECIAL DAMAGES. THE BUYER'S SOLE REMEDY FOR ANY BREACH OF THIS AGREEMENT BY OMEGA ENGINEERING, INC. OR ANY BREACH OF ANY WARRANTY BY OMEGA ENGINEERING, INC. SHALL NOT EXCEED THE PURCHASE PRICE PAID BY THE PURCHASER TO OMEGA ENGINEERING, INC. FOR THE UNIT OR UNITS OR EQUIPMENT DIRECTLY AFFECTED BY SUCH BREACH.

Return Requests/Inquiries

Direct all warranty and repair requests/inquiries to OMEGA Customer Service Department, telephone number (203) 359-1660. Before returning any instrument, please contact the OMEGA Customer Service Department to obtain an authorized return (AR) number. The designated AR number should then be marked on the outside of the return package.

To avoid processing delays, also please be sure to include:

1. Returnee's name, address, and phone number.
2. Model and Serial numbers.
3. Repair instructions.

OMEGA
ENGINEERING, INC.

One Omega Drive, Box 4047
Stamford, Connecticut 06907-0047
(203) 359-1660 Telex: 996404 Cable: OMEGA FAX: (203) 359-7700

OMEGA® is a registered trademark of OMEGA ENGINEERING, INC.

© Copyright 1985 OMEGA ENGINEERING, INC. All rights reserved including illustrations. Nothing in this manual may be reproduced in any manner, either wholly or in part for any purpose whatsoever without written permission from OMEGA ENGINEERING, INC.

Printed in U.S.A.